

ANALYZING MURINE PRIMARY MESOTHELIAL CELL PROTEOMICS TO IDENTIFY  
CANDIDATE PROTEINS CONTRIBUTING TO GENDER DIFFERENCES IN  
COLORECTAL CANCER PERITONEAL METASTATIC RECEPTIVITY WITH AGING

A Dissertation

Submitted to the Graduate School  
of the University of Notre Dame  
in Partial Fulfillment of the Requirements  
for the Degree of

Doctor of Philosophy

by

Zhikun Wang

---

M. Sharon Stack, Director

Graduate Program in Chemistry and Biochemistry

Notre Dame, Indiana

October 2024

© Copyright 2024

Zhikun Wang

ANALYZING MURINE PRIMARY MESOTHELIAL CELL PROTEOMICS TO IDENTIFY  
CANDIDATE PROTEINS CONTRIBUTING TO GENDER DIFFERENCES IN  
COLORECTAL CANCER PERITONEAL METASTATIC RECEPTIVITY WITH AGING

Abstract

by

Zhikun Wang

Cancer is a disease that predominantly affects older individuals. While age remains one of the most significant risk factors for cancer and metastasis, the biological sex of the host also plays a crucial role in influencing metastasis and survival outcomes. Specifically in colorectal cancer (CRC), both cancer incidence and deaths from metastatic disease are higher in males relative to females. The study hypothesizes that gender- and/or age-related differences in peritoneal mesothelial cells impact the interaction between tumor and mesothelial cells (MC) early in metastatic dissemination, influencing CRC metastasis success.

In a comparative analysis using female or male young mice (3-6 months, equivalent to human 20-30 years old, FY and MY) and aged mice (20-23 months, equivalent to human 60-67 years old, FA and MA) in an intra-peritoneal (ip) metastasis model, results show that aged males exhibit the highest metastatic tumor burden which aligns with human epidem-

iological data. The results also show CRC selectively targets adipose tissues covered by visceral peritoneum. Additionally, the omentum shows gender-specific differences in aged groups.

To further explore these gender and age effects, the study investigates the proteome of murine primary peritoneal mesothelial cells (MPPMCs) isolated from young and aged male and female mice. In each cohort, ~2000 proteins and ~1000 protein groups were identified. Proteomic analysis revealed differences in protein expression based on gender and age, providing baseline data for future studies on how these factors regulate MC homeostasis and influence the initiation of peritoneal diseases.

One of the candidate proteins identified, protein tyrosine phosphatase type IVA 1 (Prl-1), has been characterized in its function in CRC metastasis. Prl-1, expressed exclusively in aged male mice, is found to promote CRC metastasis by aiding initial adhesion of tumor cells to mesothelial cells. The study identifies key signaling pathways, including RhoA-GTPase and src-FAK/p130cas, that are activated by Prl-1. A Prl-1 inhibitor, CMPD-43, shows promise in reducing cell adhesion and migration. The findings suggest that targeting Prl-1 could offer new therapeutic avenues to impede CRC progression and metastasis.

## CONTENTS

Figures.....	v
Acknowledgements .....	xii
Chapter 1. Introduction .....	1
1.1 What is Colorectal Cancer?.....	1
1.2 Colorectal Cancer Subtypes .....	11
1.3 CRC Disparities among Demographic Groups.....	14
1.3.1 CRC Disparities by Age .....	16
1.3.2 CRC Disparities by Gender .....	18
1.4 Peritoneum and Mesothelium.....	21
Chapter 2. In Vivo Cohort Study Using Allograft Model to Measure Cancer Metastasis .....	30
2.1 Abstract.....	30
2.2 Materials and Methods.....	32
2.2.1 Materials.....	32
2.2.2 Animal and cell line.....	32
2.2.3 RFP tagging of MC-38 cells.....	32
2.2.4 Assessing Tumor Burden in Allograft Model of CRC Metastasis .....	33
2.3 Results and Discussion.....	33
2.4 Conclusion .....	37
Chapter 3. Isolation and Proteomics Analysis of Murine Primary Peritoneal Mesothelial Cells Identifies Candidate Proteins Potentially Affecting CRC Peritoneal Metastasis Success .....	39
3.1 Abstract.....	39
3.2 Materials and Methods.....	40
3.2.1 Materials: .....	40
3.2.2 Animals: .....	41
3.2.3 Murine Primary Peritoneal Mesothelial Cell (MPPMC) Isolation, Culture, and Lysis: .....	42
3.2.4 Western Blots and Immunofluorescence: .....	43
3.2.5 MPPMC Proteomic Analysis.....	47
3.2.6 Database Analysis .....	48
3.3 Results and Discussion.....	48

3.3.1 Primary Cell Culture.....	48
3.3.2 MPPMC Proteomics Overview.....	49
3.3.3 MPPMC proteomics revealed protein of interests which potentially regulate CRC peritoneal metastatic success.....	57
3.4 Conclusion .....	62
3.5 Associated data .....	63
Chapter 4. Comprehensive analysis of prl-1 in colorectal cancer metastasis using <i>in vitro</i> and <i>ex vivo</i> model .....	64
4.1 Abstract.....	64
4.2 Prl-1 and CMPD-43, a prl-1 inhibitor.....	66
4.2.1 Prl-1 related pathways.....	67
4.3 Methods and materials .....	71
4.3.1 Materials.....	71
4.3.2 Animals .....	72
4.3.3 Cell Viability Assay.....	72
4.3.4 In vitro and ex vivo adhesion assays.....	73
4.3.5 Western blots.....	73
4.3.6 RhoA activity assay .....	74
4.4 Results and Discussion.....	75
4.4.1 General characterization of CMPD-43 on MC-38 and LP9 cells.....	75
4.4.2 MC-38 ex vivo adhesion assay onto murine peritoneum and omentum explants .....	78
4.4.3 Prl-1 function assays regarding the Prl1-RhoA-Ncad pathway .....	80
4.4.4 The effect of Prl-1 inhibition on the level of active FAK, p130cas, and ERK1/2.....	82
4.4.5 Limitations and Future directions.....	85
4.5 Conclusion .....	87
Chapter 5. Project summary .....	89
5.1 Introduction .....	89
5.2 Gender and Age Effect on CRC Intraperitoneal Metastasis Success .....	91
5.3 MPPMC Proteomics Revealed Protein Targets Potentially Mediating CRC Intraperitoneal Metastasis Success in Aged Males.....	92
5.4 Comprehensive Analysis of Prl-1 in Colorectal Cancer Metastasis .....	93
5.5 Future Directions.....	98
5.6 Conclusion .....	101

Bibliography.....	102
-------------------	-----

## FIGURES

Figure 1.1. a) Explanation of CRC development; 1) APC mutation happens first, followed by COX-2 overexpression which leads to hyperproliferation in the normal epithelium and the formation of aberrant crypt foci lead to the development of small adenomas; 2) Then a K-ras mutation promotes the growth of these adenomas into larger polyps; 3) Finally, the combination of a p53 mutation and the loss of 18q results in the emergence of malignant cells, culminating in colon carcinoma. b) Anatomical subtypes of colorectal cancer (CRC) and their associations with tumor molecular features and other factors. MSI: microsatellite instability, CIMP: CpG island methylator phenotype, HNPCC: hereditary non-polyposis colorectal cancer, CIN: chromosomal instability.....3

Figure 1.2. Colorectal cancer peritoneal metastasis from precancerous polyp to secondary tumors; 1) CRC starts as precancerous polyps; 2) CRC progress and form a primary tumor in the colorectal lumen; 3) Cancer cells start to migrate through the colon wall into the circulatory system or the peritoneal cavity; 4) Cancer cells float inside the peritoneal cavity as intraperitoneal free cancer cells (IFCCs); 5) IFCCs land and adhere on peritoneal mesothelial cells; 6) Adhered CRC cells start to invade into the sub-mesothelial matrix and form a secondary tumor.....5

Figure 1.3. Colorectal cancer metastasis patterns change over the past 2 decades. The incidence of localized-stage disease has sharply declined, decreasing by approximately 4% annually from 2006 to 2019 overall. However, there has been an increase in advanced-stage disease, particularly among those under 65 years old. Since around 2010, rates of regional- and distant-stage disease have risen by about 3% per year in people under 50 years old, and by 2% and 0.5% per year, respectively, in individuals aged 50-64. In contrast, these rates have stabilized in those aged 65 and older since about 2015. Consequently, there has been a shift in the incidence patterns, with regional-stage disease now being the most common



diagnosis among those over 50, as well as in younger adults, surpassing localized-stage disease.....8

Figure 1.4. 2023 Estimate of colorectal cancer cases and deaths; Numbers summarized from ACS statistical reports. The data reveal a clear increase in the number of cases and deaths with advancing age, with the highest incidence occurring in individuals aged 65 and older. There is a total of 8990, 19400, 42770 female CRC cases and 10560, 28810, 42490 male CRC cases for age groups 0-49, 50-64, 65+ years respectively (Bars, left y-axis). The number at the middle of each bar represents the # of colon cancer cases (without rectal). There is a total of 1600, 5130, 17350 female CRC deaths and 2150, 8030, 18290 male CRC deaths for age groups 0-49, 50-64, 65+ years respectively (Lines, right y-axis). Males overall have higher mortality than females. Although the risk of colorectal cancer is higher in men than in women, the number of new cases in people ages 65 years and older is similar.....17

Figure 1.5. Sagittal section of the peritoneal cavity (female adult). Peritoneal peritoneum (parietal and visceral, dark pink curves) is one of the major structures lining the majority of the inner surface area of the abdominal cavity. It also folds to form omentum, mesentery and mesosigmoid. These features make the peritoneum the front line facing metastatic cancer cells.....22

Figure 1.6. a) and b) Apical surface of mouse peritoneal mesothelium c) and d) Metastatic colorectal cancer growing on the peritoneal surface of mouse.....25

Figure 2.1. Work flow for assessing tumor burden in allograft model of CRC metastasis; MC-38-RFP cells ( $1 \times 10^5$ ) were injected intraperitoneally (i.p.) into 4 separate cohorts of FA, FY, MA, MY mice, 10 mice from each cohort. To monitor tumor growth, tumor burden was monitored by longitudinal live imaging of the RFP signal for 4 weeks. Mice were then sacrificed. Fluorescent images were taken *in situ* with abdominal cavity exposed. Peritoneal organs were collected individually for *ex vivo* fluorescent images. Fluorescent signals were quantitatively analyzed using ImageJ. F: Female; M: Male; A: Aged; Y: Young.....34

Figure 2.2. MC-38-RFP cells ( $1 \times 10^5$ ) were injected intraperitoneally (i.p.) into 4 separate cohorts of FA, FY, MA, MY mice, 10 mice from each cohort. To monitor tumor growth, tumor burden was monitored by longitudinal live imaging of the RFP signal for 4 weeks. a) *In vivo* live imaging at week 4; b) quantitative analysis of *in vivo* fluorescent images of the mice; Mice were then sacrificed. Fluorescent images were taken *in situ* with abdominal cavity exposed. Peritoneal organs were collected individually for *ex vivo* fluorescent images; c) *in situ* imaging of the peritoneal cavity; d) quantitative analysis of *in situ* fluorescent images of the abdominal organs F: Female; M: Male; A: Aged; Y: Young.....35

Figure 2.3. Follow-up comparisons of MA and MY cohorts. MC-38-RFP cells ( $1 \times 10^5$ ) were injected intraperitoneally (i.p.) into cohorts of MA, MY mice, 5 mice from each cohort. To monitor tumor growth, tumor burden was monitored by longitudinal live imaging of the RFP signal for 4 weeks. Left: *In Vivo* imaging of MA vs. MY mouse abdominal tumor burden at week 4 post injection; Right: Quantitative analysis of MA vs. MY mouse abdominal tumor burden. MA bears significantly higher tumor RFP signal than MY. M: Male; A: Aged; Y: Young.....36

Figure 2.4. Characterization of organ-specific tumor burden from the cohort study in Figure 2.2. Left: 6 out of 12 peritoneal organs collected are shown: liver, omentum, mesentery, peritoneal adipose on the left and right side, colon, genitalia. Right: Quantitative analysis of organ specific fluorescent images. Only significant differences are shown. F: Female; M: Male; A: Aged; Y: Young; \*:  $p < 0.05$ ; \*\*:  $p < 0.01$ ; \*\*\*:  $p < 0.001$ ; \*\*\*\*:  $p < 0.0001$ .....38

Figure 3.1. Validation of murine primary peritoneal mesothelial cells (MPPMC). (A) Representative morphology of MPPMC cultures collected from young (top panels) or aged (lower panels) mice shown at day 1, 2, and 4, as indicated (100X magnification). (B) Immuno-fluorescent staining of MPPMCs using anti-vimentin antibody (1:100 dilution) in 3% BSA for 1h at 37°C, followed by Alexa-Fluor conjugated secondary antibody (1:300) for 30 minutes at 37°C. Slides were mounted with VECTASHIELD Mounting Media with DAPI. (C) Immunofluorescent staining of MPPMC using anti-cytokeratin-18 antibody (1:100 dilution) in 3% BSA for 1h at 37°C, followed by processing as in (B). (DandE) Western blots of MPPMC and LP9 (human mesothelial cell line) cell lysates (10 ug protein). Lysates were electrophoresed on 9% SDS-PAGE and electroblotted to Immobilon membranes. After blocking with 5% milk/TBST, blots were probed with antibodies directed against (D) vimentin (1:1000 dilution) or (E) cytokeratin-18 (1:500 dilution), washed and incubated with horseradish peroxidase-conjugated secondary antibodies (1:4000) for 1 hour at room temperature. Blots were

developed using Super Signal West Dura Extended Duration Substrate (Thermo) and visualized using ChemiDoc™ Imaging.....45

Figure 3.2. Overview of proteomic data. (A) A Venn diagram showing common/unique protein groups between cohorts FA, FY, MA, and MY, having 150, 17, 66, 137 protein groups unique to their individual group, respectively. (B) An upset plot (UpSetR Shiny App) comparing the protein groups identified from the 4 cohorts.....51

Figure 3.3. Gene Ontology Enrichment (GOE) analysis on proteins exclusively to each cohort showing their corresponding biological processes. Results show histograms listing biological processes that proteins unique to (A) FA, aged female; (B) FY, young female; (C) MA, aged male; (D) MY, young male; are involved. The number of genes involved in each process is shown on the x-axis. Fold enrichment increases from top to bottom.  $-\log_{10}(\text{FDR})$  increases from yellow to blue.....53

Figure 3.4. Pairwise comparisons between gender- and age-cohorts. (A) FA vs. FY, (B) FA vs. MA, (C) MA vs. MY, (D) FY vs. MY. (Left Panels) Common and unique proteins are shown as Venn diagrams. (Right Panels) Volcano plots present proteins significantly ( $-\log_{10}(\text{p-value}) > 13$ ) up-/down- regulated ( $\log_2(\text{fold change}) > 1$ ). Proteins up-regulated when compared to the “base” are in blue, while those down-regulated are in yellow. The gene names for proteins with high significance and fold change are annotated.....56

Figure 3.5. Secondary comparisons between the pairwise (primary) comparisons from Figure 3.4. Comparisons use only proteins with high significance ( $-\log_{10}(\text{p-value}) > 13$ ) and fold change ( $\log_2(\text{fold change}) > 1$ ) as shown in Figure 3.4. Gene Ontology Enrichment analysis was performed on each of the 4 primary comparisons. The results are shown as histograms. Each character on the x-axis represents one biological process. The y-axis indicates  $\log_2(\text{Fold Enrichment})$ . (A) Comparison ①, FA vs. MA (blue) is compared to FY vs. MY (yellow); (B) Comparison ②, FA vs. FY (blue) is compared to MA vs. MY (yellow). Any character that has both a blue and yellow bin represents a common biological process shared by the 2 groups.....58

Figure 4.1. Prl-1 is involved in complex cellular signaling pathways which could potentially affect cancerous:mesothelial cell interactions. Prl-1 binds to the src homology 3 (SH3) domain of p115 Rho GTPase-activating protein (GAP). p115 RhoGAP directly binds Prl-1 *in vitro* and in cells via its SH3 domain, competitively prevents the canonical binding between the SH3 domain of p115 RhoGAP to RhoA and MEKK1, leading to their activation. The extracellular domains of N-cadherin

monomers engage in trans and cis interactions with partner monomers, facilitated by p120-catenin (p120), resulting in a lattice-like arrangement. Activation of RhoA keeps the  $\beta$ -catenin ( $\beta$ -cat) in place and leads to the accumulation of  $\alpha$ -catenin ( $\alpha$ -cat) at the N-cadherin intracellular domain. This promotes the anchorage of the N-cadherin-catenin complex to the actin cytoskeleton through actin-binding proteins, thereby stabilizing cell-cell contacts. Active MEKK1 further activates ERK1/2 which promotes the expression of matrix metalloproteases (MMPs). Additionally, Prl-1 stabilizes Snail2 by activating ubiquitin specific peptidase 36 (USP36). Snail2 activates the expression of multiple proteins including N-cadherin. Moreover, Prl1 activates the Src kinase through increased Tyr416 phosphorylation. Src selectively phosphorylate and activates focal adhesion kinase (FAK). Src and FAK also phosphorylate and activate p130cas (Crk-associated substrate). Both p-FAK and p-p130cas promote focal adhesion.....68

Figure 4.2. Cell viability tests of LP9 and MC-38 upon CMPD-43 treatments. LP9 and MC38 cells were cultured in 96-well plates until they reached confluency. Both cell types were treated with 10  $\mu$ M CMPD-43 for a duration of 6 hours. Following treatment, the cells were washed three times with PBS at room temperature for treatment termination. Subsequently, 20  $\mu$ L of the reagent mixture was added to each well containing 100  $\mu$ L of complete media. The plates were incubated at 37°C for one hour. The absorbance was measured at 490 nm. a) Cell viability (MTS) assay of LP9 and MC-38 cells after 6-hour treatment with CMPD-43; b) Cell viability (MTS) assay of LP9 cells after 6-hour treatment with CMPD-43; the culture continued until 48 hours.....76

Figure 4.3. a) Work flow of MC-38 cells adhesion assay onto LP9 cells; LP9 cells were grown in 24-well plate until confluency; LP9 or MC-38 or both were treated with CMPD-43 for a duration of 6 hours; MC-38-RFP cells ( $5 \times 10^5$ ) were added to each well, followed by a 45-minute incubation period; Adhesion was terminated by PBS wash, 3 min 3 times. b) % MC-38 adhesion onto LP9 cells. LP9 or MC-38 or both were treated with CMPD-43. Percentages are normalized on average adhesion of the controls.....77

Figure 4.4. a) Workflow of an ex vivo adhesion assay; Aged male mice were sacrificed via isoflurane; Peritoneum and omentum tissue explants were collected and pinned in silicone coated dishes; they were then treated with 10  $\mu$ M CMPD-43 for 6 hours; MC-38-RFP cells ( $5 \times 10^5$ ) were added each well, followed by a 45-minute incubation period; Adhesion was terminated by PBS wash, 3 min 3 times. b) Violin plots of % MC-38 adhesion onto CMPD-43 treated peritoneum and omentum. Percentages are normalized on average adhesion of the controls.....79

Figure 4.5 a) MC-38 adhesion onto LP9 with N-cad function blocking antibody (GC-4, 120 µg/mL, 1 hour incubation); MC-38-RFP cells ( $5 \times 10^5$ ) were added each well, followed by a 45-minute incubation period; Adhesion was terminated by PBS wash, 3 min 3 times; Treatment combinations includes: 1) Both cells treated with Control IgG; 2) LP9 treated with control IgG + MC-38 treated with GC-4; 3) MC-38 treated with Control IgG + LP9 treated with Anti-N-Cad; 4) Both cells treated with GC-4; b) Western blots for CMPD-43 treated LP9 cell lysates against N-cad. LP9 cells were grown to confluence before being treated with 10 µM CMPD-43 in complete media at various time points: 0, 3h, 6h, 12h, and 24h. At the 6-hour mark, treatments were stopped with two washes of PBS, followed by the replacement of complete media. Equal amounts of protein (30µg per lane) were separated by electrophoresis on 9% SDS-polyacrylamide gels and transferred onto methanol-activated polyvinylidene fluoride (PVDF) membranes. Membranes were blocked with 5% milk in TBST (150mM NaCl, 25mM Tris, 0.05% Tween 20) for one hour at room temperature to prevent non-specific binding. Primary antibodies against N-cad (1:500 in 5% BSA) and incubated with the membranes overnight at 4°C. After thorough washing, membranes were incubated with horseradish peroxidase-conjugated secondary antibodies at a 1: 2000 dilution for one hour at room temperature. The resulting signals were visualized using chemiluminescence with the ChemiDoc™ Imaging system.....81

Figure 4.6 a) RhoA activity in LP9 cells treated with/without CMPD-43; LP9 cells were cultured to confluence and treated with 10 µM CMPD-43 in complete media for 6 hours. Treatments were terminated by washing the cells twice with PBS. The RhoA G-LISA Activation Assay Kit was used for RhoA activity. Lysates were standardized to equivalent protein concentrations before being frozen and stored. Cell lysates were combined with binding buffer and loaded into 96-well binding strips, shaken at 200 rpm for 30 minutes at 4°C. This was followed by incubation with Antigen presenting buffer (2 minutes at room temperature), then with anti-RhoA primary antibody diluted 1/250 (200 rpm shaking for 45 minutes at room temperature), and finally with secondary HRP-labeled antibody diluted 1/62.5 (200 rpm shaking for 45 minutes at room temperature). The HRP detection reagent was added (50 µL each well, 15 min at 37 °C), and the reaction was terminated with the HRP Stop Buffer. Absorbance was measured at 490 nm. b) Western blots for CMPD-43 treated LP9 cell lysates against FAK, p-FAK, p130cas, p-p130cas, and N-cad. LP9 cells were grown to confluence before being treated with 10 µM CMPD-43 in complete media at various time points: 0, 3h, 6h, 12h, and 24h. At the 6-hour mark, treatments were stopped with two washes of PBS, followed by the replacement of complete media. Equal amounts of protein (30µg per lane) were separated by electrophoresis on 9% SDS-polyacrylamide gels and transferred onto methanol-activated polyvinylidene fluoride (PVDF) membranes. Membranes were blocked with 5% milk in TBST (150mM NaCl, 25mM Tris, 0.05% Tween 20) for one hour at room temperature to prevent non-specific binding. Primary antibodies against N-cad, p130cas, phospho-p130cas (p-p130cas), FAK, and phospho-FAK

(p-FAK) were diluted to 1:500 in 5% BSA/TBST and incubated with the membranes overnight at 4°C. After thorough washing, membranes were incubated with horseradish peroxidase-conjugated secondary antibodies at a 1: 2000 dilution for one hour at room temperature. The resulting signals were visualized using chemiluminescence with the ChemiDoc™ Imaging system.....84

Figure 5.1 Graphical Abstract. This project starts with statistical data of colorectal cancer (CRC) patients from different gender and age groups. Using murine models, the study progressed in 2 ways; one is using mouse allograph model to study CRC intra-peritoneal metastasis; the other in the proteomics analysis of isolated tumor naïve murine primary peritoneal mesothelial cells (MPPMCs). The observation from the tumor study, namely that, aged males present the highest tumor burden, was used as a guideline in analyzing the proteomics. Protein candidates potentially contributing to the gender/age differences in CRC metastatic success were identified, followed by protein function analysis. The characterized proteins can then be investigated in animal models and drug discovery for more personalized of CRC metastasis in the aged host.....90

## ACKNOWLEDGEMENTS

I would like to express my deepest gratitude to the following individuals and groups for their invaluable support and contributions to this work.

First and foremost, I am profoundly grateful to my advisor, Dr. Sharon Stack, for everything. Her unwavering guidance, insightful advice, and continuous encouragement have been instrumental in shaping my research journey. Dr. Stack's dedication, knowledge, and patience have not only contributed significantly to this work but also inspired me to grow as a researcher and a person.

I extend my heartfelt thanks to Yueying Liu, our former lab manager, and Jing Yang, our current lab manager, for teaching me everything I needed in the lab. Their support, skills, and willingness to share their knowledge have been invaluable in navigating the complexities of lab work and experimental procedures.

I would also like to acknowledge all the members of the Stack lab for their help with experiments and their collaborative spirit. Their camaraderie, intellectual discussions, and support have greatly enriched my research experience and made the lab a stimulating and enjoyable environment.

I am deeply thankful to my committee members, Dr. Matthew Champion and Dr. Laurie Littlepage, for their guidance, constructive feedback, and support throughout this process. Their insights and suggestions have been crucial in refining this work.

Special thanks to Dr. William Boggess at the ND Mass Spectrometry Core for patiently guiding me through the most difficult part of my research during the COVID-19 pandemic. His assistance and support were critical in overcoming significant challenges and ensuring the success of this project.

This study was supported in part by the Patterson Endowment for Excellence (Z.W.), the Walther Cancer Foundation Cancer Cure Ventures grant (R.S.), research grants RO1CA109545 and UO1CA236979 from the National Institutes of Health/National Cancer Institute (M.S.S.), and the Samuel Waxman Cancer Research Foundation (M.S.S.). Mass spectrometry experiments were performed in the University of Notre Dame Mass Spectrometry and Proteomics Facility. Also thanks Bio-Render for helping us creating figures and illustrations.

Lastly, I am forever indebted to my family in China for their endless love and support, especially my grandma with Alzheimer's. Despite my long absence, her enduring love and memory of me have been a constant source of strength and motivation. Her unwavering presence in my life has been a beacon of hope and inspiration.

Thank you all for making this journey possible.



## CHAPTER 1.

### INTRODUCTION

#### **1.1 What is Colorectal Cancer?**

Colorectal cancer (CRC) is recognized as one of the most prevalent malignancies globally, holding the position of the third most commonly diagnosed cancer and the second leading cause of cancer-related deaths for both men and women in the United States and worldwide.<sup>1,2</sup> Each year, the United States witnesses approximately 153,020 new cases of CRC and 52,550 deaths, with a notable portion of these cases occurring in individuals younger than 50 years.<sup>3</sup> Over 75% of colon and rectal cancers occur to people with no known risk factors.<sup>3</sup> More than half of CRC cases and fatalities are attributed to modifiable risk factors such as smoking, unhealthy diets, high alcohol consumption, physical inactivity, and excess body weight.<sup>1</sup> The 5-year survival rates for CRC patients differ drastically depending on the stage at diagnosis. Over 90% of patients would live if diagnosed at an early stage, whereas only about 10% of those with late-stage CRC survive beyond five years.<sup>4,5</sup> Despite a decline in the incidence rate for localized-stage CRC, there has been an alarming increase in advanced-stage diagnoses. Older people are usually more prone to diagnosis with an advanced-stage CRC. However, it has been suggested that there is a demographic shift towards more patients under 65 years of age who are also diagnosed

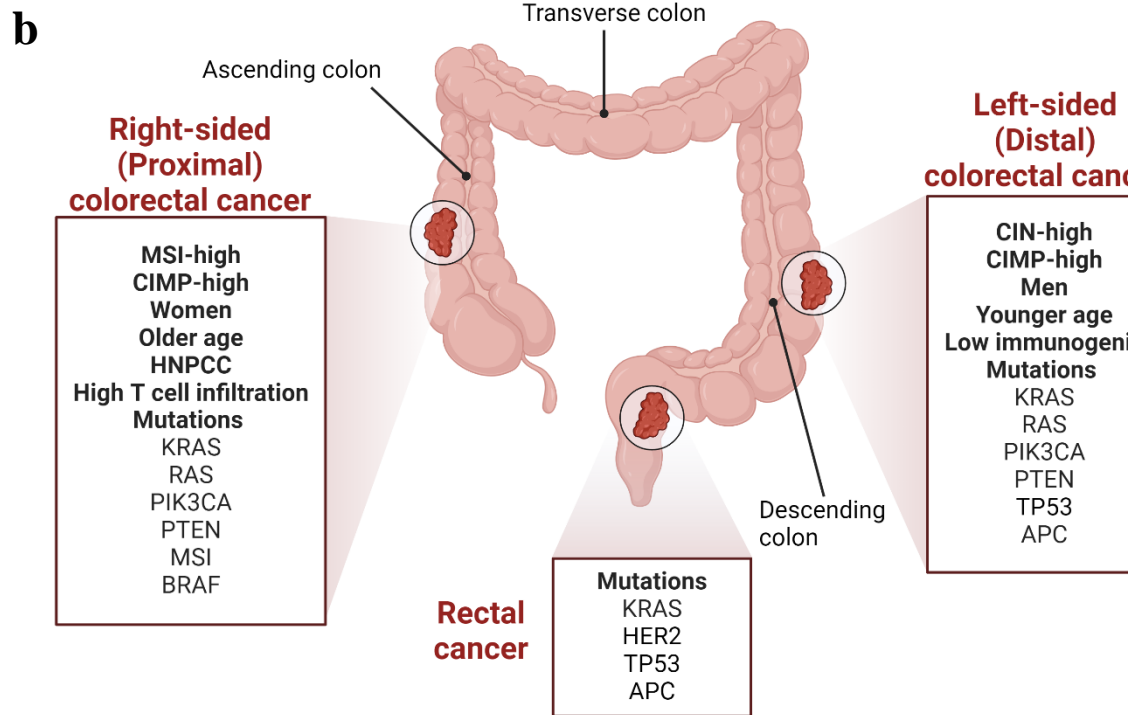
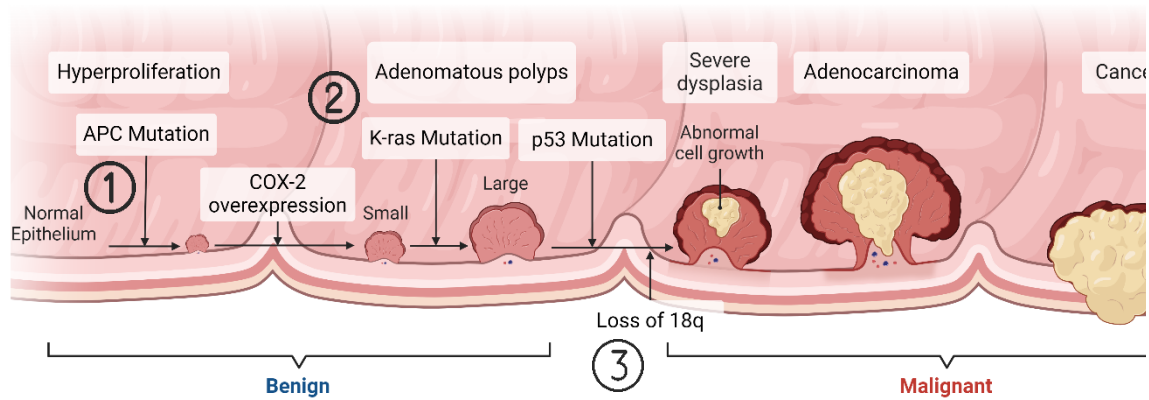
with an advanced-stage CRC.<sup>3</sup> This highlights a need to understand age related disparities for both old and young population.

Generally speaking, 50%–90% of all CRCs are sporadic and 10%–50% at hereditary or familial.<sup>6</sup> It is widely believed that somatic mutations in APC, K-ras, and p53 follow a sequential order [Figure 1.1a] during the progression from normal colonic mucosa to colon carcinoma.<sup>7</sup> Initial mutations in APC activates hyperproliferation in the normal epithelium and the formation of aberrant crypt foci lead to the development of small adenomas. Subsequently, a K- ras mutation promotes the growth of these adenomas into larger polyps. Finally, the combination of a p53 mutation and the loss of 18q result in the emergence of malignant cells, culminating in colon carcinoma.<sup>6</sup> While CRC typically originates as precancerous polyps in the epithelial mucosa of the colon or rectum, they can progress outward to potentially enter the circulatory system, forming distant metastases. It can also invade the lymphatic system or the peritoneal cavity via direct implantation, leading to regional metastases [Figure 1.2]. It is noted that around 20% of newly diagnosed CRC patients present with distant metastases, while roughly 50% of all colorectal cancer patients without initial metastases will eventually develop metastasis.<sup>2, 8, 9</sup>

Strikingly, researchers have suggested that unlike many other cancers, CRC may start developing into metastatic stage much earlier, as soon as the formation of the primary tumor. The exome-sequencing data from 118 biopsies from 23 CRC patients with metastases have shown that the genomic divergence between the primary tumor and metastasis is low and that canonical driver genes were acquired early. Analysis within a spatial tumor growth model and statistical inference framework indicates that early disseminated cells commonly (81%, 17 out of 21 evaluable patients) seed metastases while

**Figure 1.1. a) Explanation of CRC development; 1) APC mutation happens first, followed by COX-2 overexpression which leads to hyperproliferation in the normal epithelium and the formation of aberrant crypt foci lead to the development of small adenomas; 2) Then a K-ras mutation promotes the growth of these adenomas into larger polyps; 3) Finally, the combination of a p53 mutation and the loss of 18q results in the emergence of malignant cells, culminating in colon carcinoma. b) Anatomical subtypes of colorectal cancer (CRC) and their associations with tumor molecular features and other factors. MSI: microsatellite instability, CIMP: CpG island methylator phenotype, HNPCC: hereditary non-polyposis colorectal cancer, CIN: chromosomal instability.<sup>10, 11</sup>**

## a Sequential Progression of Colorectal Cancer



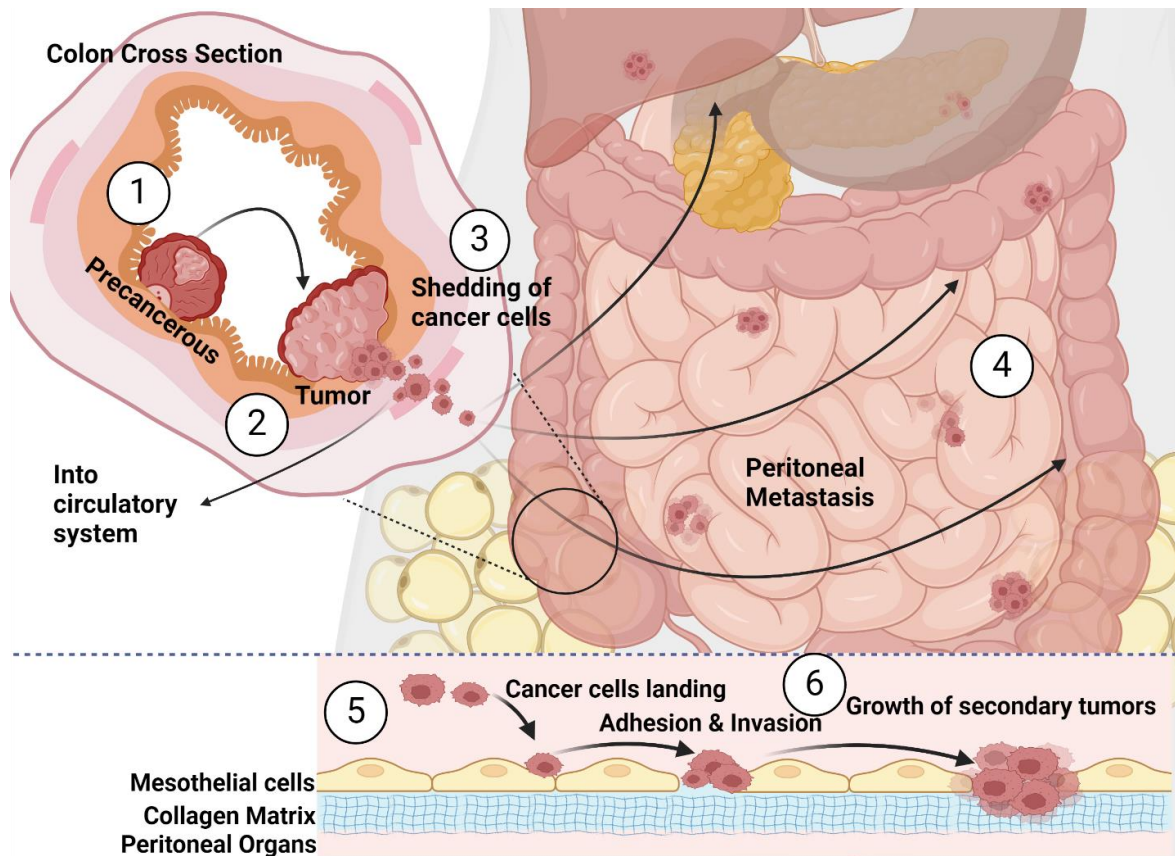


**Figure 1.2. Colorectal cancer peritoneal metastasis from precancerous polyp to secondary tumors; 1) CRC starts as precancerous polyps; 2) CRC progress and form a primary tumor in the colorectal lumen; 3) Cancer cells start to migrate through the colon wall into the circulatory system or the peritoneal cavity; 4) Cancer cells float inside the peritoneal cavity as intraperitoneal free cancer cells (IFCCs); 5) IFCCs land and adhere on peritoneal mesothelial cells; 6) Adhered CRC cells start to invade into the sub-mesothelial matrix and form a secondary tumor.**

the carcinoma is clinically undetectable (typically, less than 0.01 cm<sup>3</sup>).<sup>12</sup> And again, only about 10% of those with late-stage (Stage IV) CRC survive beyond five years.<sup>4, 5</sup>

The most frequent metastasis site is the liver (at least 25% of all CRC patients).<sup>12,</sup>

<sup>13</sup> As early as in 1889, Paget proposed the concept of “seed” and “soil” for “tumor cells” and “organs to be metastasized” in tumor metastasis.<sup>14</sup> CRC liver metastasis cascade follows exactly what he proposed, just in a much more complex way. Liver metastasis of CRC can happen both hematogenously (through the blood stream) as well as through

invasion into the peritoneal cavity or lymph nodes as an example of regional metastasis.<sup>15</sup>

<sup>16</sup> When the expression or function of intercellular adhesion molecules, like E-cadherin, is reduced, colorectal cancer (CRC) cells can detach from the primary tumor mass.<sup>17</sup> They migrate through the extracellular matrix (ECM), invade into the neighboring tissues, intra- and extra-vascularization if going through blood stream, survive in the circulation or peritoneal fluids, and finally, colonize to distant sites such as liver forming more aggressive secondary tumors.<sup>15</sup> CRCs as well commonly metastasize to the lung (distant metastasis) and peritoneum (regional). Pulmonary (lung) metastases occur in 15% of CRC patients, and the lung is the second site of metastases occurrence after the liver.<sup>18, 19</sup> Following that is the peritoneal metastasis (liver excluded) which accounts for 10-13% of all CRC patients.<sup>20, 21</sup> Various other metastatic sites have been identified such as bone, spleen, brain and distant lymph nodes.<sup>22</sup>

CRC intra-peritoneal (i.p.) metastasis can also be achieved via hematologic, lymph node, or direct extension. Cancer cells may enter the peritoneal cavity either as single cells or in clusters, transforming into intraperitoneal free cancer cells (IFCCs).<sup>17, 23</sup> The epithelial-mesenchymal transition (EMT) is crucial in endowing cancer cells with stem cell-like traits enabling them to survive matrix detachment, and increased motility, allowing them to migrate.<sup>24</sup> During EMT, cellular motility is heightened, the ECM and cell-cell adhesion are disrupted, apical-basal polarity is lost, and the cytoskeleton is reorganized. These changes, driven by actin contraction, enable cancer cells to break away from the primary tumor site, migrate, and invade surrounding tissues.<sup>17, 25</sup> The transformation of tumor cells at the invasive front into a mesenchymal-like state, as they shed their epithelial properties, enhances their aggressiveness.<sup>26</sup> This adaptation allows

tumor cells to mimic processes seen in normal embryonic development, aiding in their survival in different microenvironments and facilitating their spread.<sup>17</sup> Interestingly, it was suggested that the dissemination of IFCCs within the peritoneal cavity follows a specific pattern rather than occurring randomly. Factors such as respiratory movements, gravitational forces, and intestinal peristalsis influence this spread. These forces lead to changes in intra-abdominal pressure, which predispose certain regions, including the subdiaphragmatic area, the lesser sac, the mesentery, the diaphragm, and the paracolic sulcus, to a higher likelihood of metastasis.<sup>17, 27</sup>

Nevertheless, CRC peritoneal metastasis (PM) also differs from the more recognized hematogenous spread in multiple ways, particularly in the detachment, dissemination, and attachment of tumor cells. The development of peritoneal carcinomatosis involves five essential steps: (1) detachment of tumor cells from the primary tumor and acquisition of motility, (2) evasion of anoikis, (3) adherence to the peritoneal surface, (4) invasion into the peritoneum, and (5) proliferation and formation of peritoneal metastasis.<sup>28, 29</sup> The detachment of tumor cells from the primary tumor can occur through mechanisms such as spontaneous exfoliation of tumor cells in CRC growing through the serosa (T4 stage), spontaneous shedding of tumor cells into the lymphatics around the primary tumor due to increased interstitial fluid pressure, surgery-induced tumor spill from opening the tumor, transected lymphatics and blood vessels, or postoperative infections from anastomotic leakage, which has been associated with higher rates of tumor recurrence.<sup>28-31</sup> On a molecular level, the detachment of tumor cells and subsequent acquisition of motility result from the downregulation of cell-cell adhesion

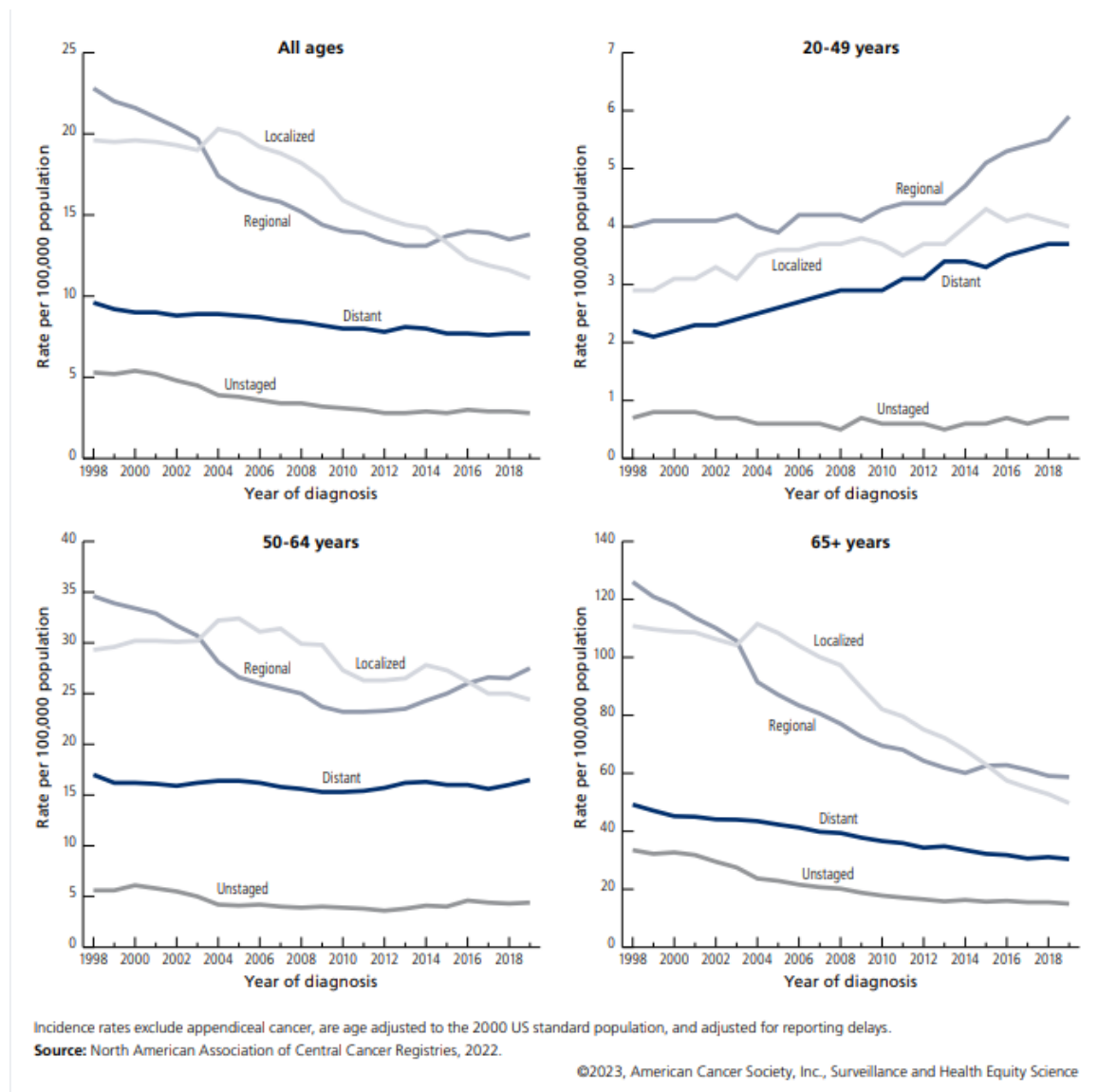


**Figure 1.3 Colorectal cancer metastasis patterns change over the past 2 decades. The incidence of localized-stage disease has sharply declined, decreasing by approximately 4% annually from 2006 to 2019 overall. However, there has been an increase in advanced-stage disease, particularly among those under 65 years old. Since around 2010, rates of regional- and distant-stage disease have risen by about 3% per year in people under 50 years old, and by 2% and 0.5% per year, respectively, in individuals aged 50-64. In contrast, these rates have stabilized in those aged 65 and older since about 2015. Consequently, there has been a shift in the incidence patterns, with regional-stage disease now being the most common diagnosis among those over 50, as well as in younger adults, surpassing localized-stage disease.<sup>3</sup>**



molecules (CAMs) as part of EMT and changes in the cytoskeleton. Importantly, CAMs include integrins, cadherins, and selectins. The EMT process also involves EGFR, c-MET, and, particularly in the context of peritoneal carcinomatosis, the EMT trigger TWIST.<sup>28, 32</sup>

Recently, attention has been focused on identifying the relevant adhesion molecules involved in peritoneal spread. Studies have shown that these molecules differ between hematogenous and peritoneal dissemination, suggesting distinct attachment processes. In hematogenous spread, primarily to the liver in CRC, adherence to the endothelium in the hepatic sinusoids requires CD44 binding to hyaluronan, blood group antigens sLeA and sLeX binding to selectins, and mucins binding to ECM components.<sup>28, 29</sup> In contrast, peritoneal carcinomatosis, important adhesion molecules include integrins (e.g.,  $\alpha 2 \beta 1$ ) and their ligands, proteoglycans (e.g., CD44), members of the immunoglobulin superfamily (e.g., ICAM1, VCAM1, L1CAM), mucins (e.g., MUC16), and the epithelial cell adhesion molecule (EPCAM). There is ongoing debate regarding the significance of each of these molecules concerning metastatic sites. Data suggest that blood group antigens are involved only in hematogenous spread, while L1CAM and proteoglycans are specific to peritoneal dissemination.<sup>28, 29</sup> Although the exact differences are still unclear, there is consensus on the critical role of adhesion molecules in metastatic spread, particularly since free-floating tumor cells in the peritoneal cavity do not necessarily result in peritoneal carcinomatosis.<sup>28, 29</sup> The invasion into the peritoneum requires proteolytic enzymes such as matrix metalloproteases (e.g., MMP2/7/9) secreted by tumor cells or surrounding stromal cells. After invasion, tumor cells must survive in the new environment and sustain proliferation, with IGF-1 and angiogenesis-promoting factors such as HIF1 $\alpha$  and VEGF playing crucial

roles. IGF-1 mRNA has been shown to be overexpressed in peritoneal spread compared to liver metastases.<sup>28, 32</sup>

Among individuals over 50 years old, it has been reported that regional metastasis, which metastasis into adjacent lymph nodes or the peritoneal cavity, has become more common, a trend also observed in younger adults.<sup>3</sup> Over the past decade, the incidence of localized-stage disease has decreased, but there has been an increase in regional-stage diagnoses, particularly among those under 65 years [Figure 1.3].<sup>3</sup> This stage of CRC presents unique treatment challenges and exhibits variations between men and women. Approximately 35-40% of all CRC patients experience peritoneal metastasis, which complicates treatment and necessitates specialized management strategies.<sup>3, 27, 33</sup> Compared to localized-stage or distant metastasis, peritoneal metastasis (PM) in CRC cases usually means that patients lose the possibility of conventional therapy and have a worse prognosis.<sup>17, 34, 35</sup>

Due to the nature of CRC, patients' and survivors' quality of life, including physical, social, sexual, and psychological well-being, could also be severely affected. One of major issue that many CRC survivors would face is a colostomy, a surgical operation, temporary or permanent, that involves making an opening, known as a stoma, in the large intestine (colon) and bringing it to the surface of the abdomen. The stoma enables bodily waste, including feces, to exit the body and be collected in a bag worn over the stoma.<sup>36</sup> An estimated 18%–35% of CRC survivors have received temporary or permanent intestinal ostomies as part of their cancer treatment.<sup>37</sup> Stoma issues such as leakage and skin irritation were frequently encountered by ostomates. Those without a stoma or with a reversed stoma often face long-term and unpredictable changes in bowel function. Survivors frequently

adjust their dietary habits, including the timing, quantity, and types of food they consume, to manage bowel function. Less frequent symptoms include fatigue, sleep disturbances, and anal pain.<sup>38</sup>

Fortunately, the diagnosis and treatment of CRC have seen significant advancements over the years. Since the mid-2000s, CRC incidence in the USA has decreased by 2–3% per year in both men and women.<sup>34</sup> New technologies such as targeted therapies and immunotherapy demonstrate superior quality of life benefits over traditional chemotherapies. Monotherapy with drugs like cetuximab has been associated with significant improvements compared to combination therapy.<sup>2</sup> Enhanced screening techniques, such as colonoscopy and fecal occult blood tests, have facilitated early detection and improved survival rates. The introduction of routine screenings in the late 20th century led to a shift in the stage at diagnosis, with more cases being identified at earlier, more treatable stages.<sup>1</sup> This contributed to a significant decline in the annual age-standardized CRC incidence rate from its peak in 1985, largely due to improved screening and prevention strategies.<sup>1</sup> Over the 10-year course, the 3-year survival rate for patients with metastatic rectal cancer has increased from 25% to 30%.<sup>2</sup> However, recent trends show a shift back to advanced-stage diagnoses, likely due to factors such as screening saturation and the aggressive nature of early-onset CRC.<sup>1</sup>

## **1.2 Colorectal Cancer Subtypes**

From a molecular perspective, colorectal cancer (CRC) is not a single disease but rather a collection of subtypes distinguished by specific genetic and morphological alterations. The most prevalent genetic alteration in CRC is chromosomal instability (CIN),

found in approximately 84% of all sporadic CRC cases. This subtype is characterized by numerous chromosomal changes, which contribute to tumorigenesis. Another significant subtype, present in about 13-16% of sporadic CRC cases, is hypermutated and exhibits microsatellite instability (MSI).<sup>39, 40</sup> MSI accounts for the inactivation of genes involved in the repair of base-base mismatches in DNA, defined as MMR genes such as hMSH2, hMLH1, hPMS1, hPMS2 or hMSH6.<sup>40</sup> Additionally, there are hereditary forms of CRC, such as Lynch syndrome and familial adenomatous polyposis, which, though less common, possess distinct genetic profiles and clinical implications.<sup>35</sup> In MMR deficiency, such inactivation can be inherited, as seen in hereditary non-polyposis colorectal cancer (HNPCC) (where approximately 95% of mutations involve hMSH2 or hMLH1), or acquired, as observed in tumors with methylation-associated silencing of a gene encoding an MMR protein. An example of this is the biallelic silencing of the MLH1 gene's promoter region through promoter methylation (13,30).<sup>40-42</sup> It has also been observed that germline deletions in the EpCAM (epithelial cell adhesion molecule) gene, also known as TACSTD1, have been found in some families with Lynch syndrome. These families lacked MMR gene mutations due to the uncommon hyper-methylation of the hMSH2 promoter.<sup>40, 43</sup>

CRC can be further categorized into several molecular subtypes, each exhibiting unique genetic and morphological traits. These consensus molecular subtypes (CMS) include CMS1 (MSI immune group), CMS2 (canonical subtype), CMS3 (metabolic subgroup), and CMS4 (mesenchymal type).<sup>44</sup> These subtypes correspond to different tumorigenesis pathways and have significant implications for both prognosis and treatment strategies. For example, CMS1 is frequently associated with microsatellite instability and immune cell infiltration, indicating a robust immune response towards the tumor. On the

other hand, CMS2 is characterized by chromosomal instability and the activation of WNT signaling pathways. CMS3 tumors frequently display mutations in *KRAS*, in line with an increase in metabolic pathways, and are generally CIMP low. TGF $\beta$  pathway is active in CMS4 tumors and serrated adenomas are predicted to progress to this cancer subtype. A large proportion of CMS1 and a subset of CMS4 tumors carry an activating mutation in *BRAF*.<sup>44</sup>

The development of CRC is influenced by the cell of origin and the initial genetic mutations, which determine the subtype and guide its progression along distinct developmental paths based on anatomical location and other factors. Right-sided CRC (proximal colon, RCRC) often features characteristics associated with CMS1, including microsatellite instability, CpG island methylator phenotype (CIMP), and the *BRAF*<sup>V600E</sup> mutation. In contrast, left-sided CRC (distal colon, LCRC) typically exhibits characteristics of CMS2, such as high chromosomal instability and common mutations in genes like *APC*, *KRAS*, and *TP53* [Figure 1.1b].<sup>10, 44, 45</sup> In a cohort study based on data from the SEER, the median survival of patients in the US was found to be 78 months for RCRC and 89 months for LCRC ( $P = 0.001$ ).<sup>11, 46, 47</sup> Interestingly, a comparison between stage III and IV RCRC and LCRC patients showed poorer overall survival for RCRC patients, while stage I and II RCRC patients exhibited better overall survival than those with LCRC.<sup>11, 46</sup> Generally speaking, women are more susceptible to right-sided colon cancer, which is linked to a more aggressive form of neoplasia compared to left-sided colon cancer [Figure 1.1b].<sup>4</sup> Right-sided colon cancer has patients 48% in males and 52% in females, while left sided colon cancer has 61% male patients and 39% female patients.<sup>48</sup> Left and right sided CRC have also shown age disparities [Figure 1.1b].

The right-sided CRC incidence rates increase with age: 49% (65–74 years), 58.2% (75–84 years), and 65.9% ( $\geq 85$  years) ( $p < 0.001$ ).<sup>49</sup> In the meantime, for individuals aged  $< 50$ , most of these tumors were distal (rectum, left-sided colon, and right-sided colon were 49.8%, 28.8%, and 21.4%, respectively).<sup>50</sup> These variations underscore the biological diversity within CRC and highlight the importance of considering tumor location in both diagnosis and treatment planning.<sup>10, 11</sup>

### **1.3 CRC Disparities among Demographic Groups**

Significant disparities exist in CRC incidence and outcomes across different demographic groups. A comprehensive study examined somatic mutation patterns by race/ethnicity and sex among 5,856 non-Hispanic White (NHW), 535 non-Hispanic Black (NHB), and 512 Asian/Pacific Islander (API) CRC patients, including 2,016 early-onset cases (diagnosed before the age of 50). Disparities were noted in the impact of mutations in genes like APC and FBXW7 between early-onset and late-onset non-hypermuted CRC. APC mutation rates in those patients across racial/ethnic groups are 59% of API individuals, 76% of NHB individuals, and 75% of NHW individuals. 21% of tumors from young non-Hispanic Asian individuals had FBXW7 mutations versus 15% of young NHW or 11.7% of young NHB patients.<sup>51</sup> Similarly, FLT4, RNF43, LRP1B, PIK3CA, and ATRX are also shown to get significantly differed across racial/ethnic groups for early-onset non-hypermuted tumors.<sup>51</sup>

Another study showed that of incidences per 100,000 population, African Americans are 41.9 while that of European Americans are 37.0 in 2021.<sup>52</sup> The newest

SEER data are consistent with the finding [Table 1],<sup>54</sup> with American Indian/Alaska native people having the highest incidences, 58.6, followed by NHB (43.6) and NHW (37.7). At diagnosis, African Americans and European Americans present at a similar ratio for Stage I and II patients, 37% vs. 38%. Only 32% of African Americans present with regional/less fatal disease as compared to 36% of European Americans. However, 26% of African Americans present with metastatic CRC as compared to only 22% of European Americans.<sup>52</sup> Overall 5-year CRC survival rates for African Americans have been consistently 6-12% below that of European Americans, with African American overall survival rates at 61% and European American survival rates at 67% in 2017.<sup>52</sup>

TABLE 1.1

SEER U.S. AGE-ADJUSTED COLORECTAL CANCER INCIDENCES PER  
100,000, 2021

Race	Hispanic (any race)	Non-Hispanic			
		American Indian Alaska Native	Asian Pacific Islander	Black	White
<b>Overall</b>	35.3	58.6	31.3	43.6	37.7
<b>Female</b>	30.9	52.4	27.4	38.8	33.1
<b>Male</b>	40.4	65.9	36	50.3	42.8

### 1.3.1 CRC Disparities by Age

It is increasingly recognized that cancer is fundamentally a disease associated with aging. Our lab has also demonstrated that the peritoneal metastatic tumor burden from ovarian cancer increases with age.<sup>53</sup> Similarly, age is one of the primary risk factors for colorectal cancer (CRC), with approximately 90% of patients being over 50 years old.<sup>54-57</sup>. At diagnosis, the median age of patients with colon cancer is 68 years for men and 72 years for women; the median age of patients with rectal cancer is 63 years for both genders.<sup>34</sup> Statistics from the American Cancer Society (ACS) and Surveillance, Epidemiology, and End Results Program (SEER) indicate that patients older than 65 have significantly higher incidence rates for all stages of CRC.<sup>3,47</sup> Additionally, a higher incidence of CRC has been observed in men compared to women across most age groups, especially under the age of 65 [Figure 1.4].<sup>54</sup>

A review of operative outcomes for colorectal cancer in the United States, utilizing data from the Nationwide Inpatient Sample between 2001 and 2010, revealed that among an estimated 1,043,108 CRC patients, 63.8% of surgeries were performed on those aged 65 and older, and 22.6% on patients aged 80 and older. Patients aged 80 and older were 1.7 times more likely to undergo urgent admission compared to those younger than 65. When compared to patients aged 45 to 64, the study found that risk-adjusted in-hospital mortality increased with advancing age: 65 to 69 years (odds ratio, 1.32; 95% CI, 1.18-1.49), 70 to 74 years (2.02; 1.82-2.24), 75 to 79 years (2.51; 2.28-2.76), 80 to 84 years (3.15; 2.86-3.46), and 85 years and older (4.72; 4.30-5.18) ( $P < .01$ ). Similarly, higher risk-adjusted morbidity was observed with increasing age: 65 to 69 years (odds ratio, 1.25; 95% CI, 1.21-



1.29), 70 to 74 years (1.40; 1.36-1.45), 75 to 79 years (1.54; 1.49-1.58), 80 to 84 years (1.68; 1.63-1.74), and 85 years and older (1.96; 1.89-2.03) ( $P < .01$ ).<sup>58</sup> Such comparison highlighted the need to improve and develop health care strategy to better help aged CRC patients.

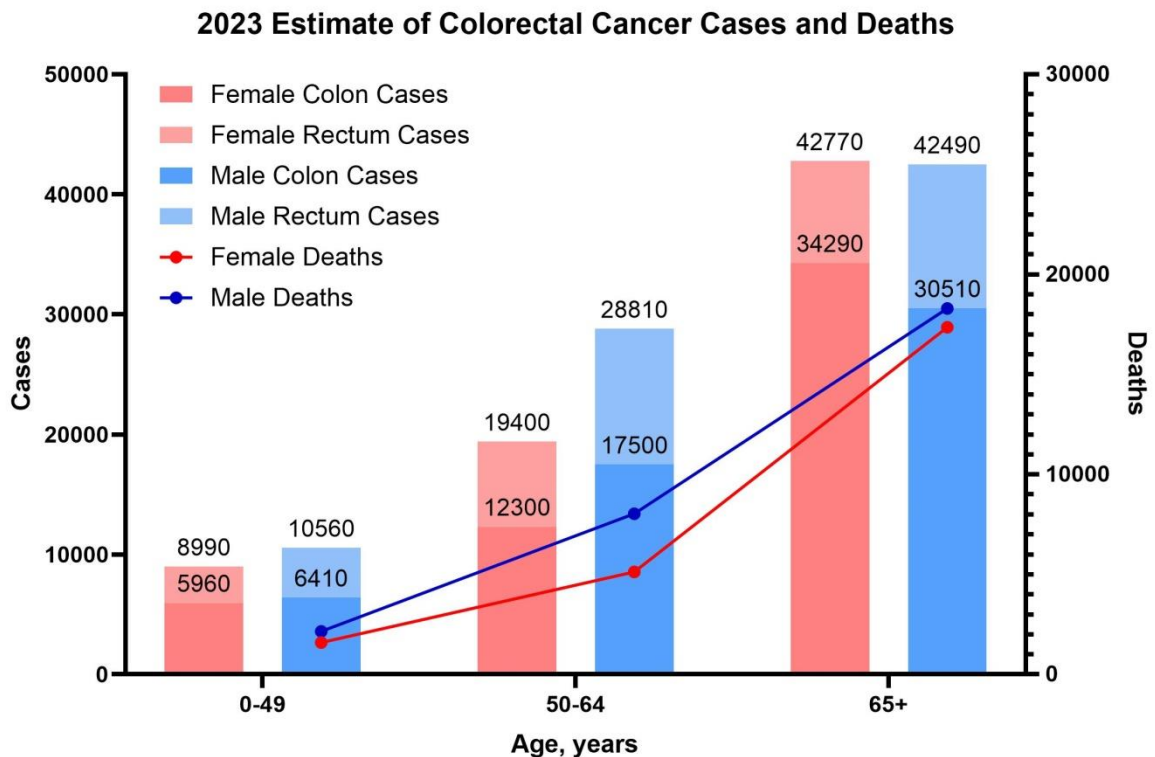


**Figure 1.4. 2023 Estimate of colorectal cancer cases and deaths; Numbers summarized from ACS statistical reports. The data reveal a clear increase in the number of cases and deaths with advancing age, with the highest incidence occurring in individuals aged 65 and older. There is a total of 8990, 19400, 42770 female CRC cases and 10560, 28810, 42490 male CRC cases for age groups 0-49, 50-64, 65+ years respectively (Bars, left y-axis). The number at the middle of each bar represents the # of colon cancer cases (without rectal). There is a total of 1600, 5130, 17350 female CRC deaths and 2150, 8030, 18290 male CRC deaths for age groups 0-49, 50-64, 65+ years respectively (Lines, right y-axis). Males overall have higher mortality than females. Although the risk of colorectal cancer is higher in men than in women, the number of new cases in people ages 65 years and older is similar.<sup>3</sup>**

The impact of age on CRC extends beyond the increased risk and mortality rates. Age-related factors also influence the biology and treatment response of CRC, further complicating management in older adults. Moreover, older patients often present with comorbid conditions, which can affect their ability to tolerate and respond to treatment. These age-related variations underscore the need for tailored approaches in the prevention, diagnosis, treatment, and longterm survivorship of CRC among older adults. Overall, the intersection of aging and CRC highlights the importance of continued research and intervention strategies aimed at improving outcomes for this more vulnerable population. By addressing the unique characteristics posed by age, researchers and healthcare providers can better support older adults in managing CRC and enhancing their quality of life.

### **1.3.2 CRC Disparities by Gender**

While age is one of the major risk factors for cancer and metastasis, biological sex also significantly impacts metastasis and survival rates. In numerous cancer types (pan-cancer), the incidence and survival rates both are lower in males compared to females.<sup>59</sup> For instance, studies on 164,996 colorectal cancer patients in Germany demonstrated that biological gender affects survival rates, with women showing significantly higher long-term survival rates. However, this advantage diminishes after the age of 65 [Figure 1.4].<sup>60</sup> A recent study involving over 14 million patients found that while males have a lower cancer incidence (Incidence Rate Ratio 0.958; 95% CI 0.957–0.959;  $P < 0.001$ ), they experience worse survival outcomes (Hazard Ratio 1.568; 95% CI 1.564–1.573;  $P < 0.001$ ) compared to females.<sup>59</sup> Furthermore, cancer incidence is higher in females compared to

males in the age range of 15 to 39 and those 65 and older, whereas it is higher in males compared to females aged 0 to 14 and 40 to 64.<sup>59</sup>

In another review, the Global Cancer Observatory evaluated the age-standardized incidence rates (ASIR) and showed that globally in every 100,000 population each year, incidences in males (23.6 per 100,000 person-years) was 45% higher compared to females (16.3 per 100,000 person-years).<sup>10, 61</sup> Additionally, males have a 50% higher cumulative risk (CR) of developing CRC than females (CR 2.75 vs. 1.83).<sup>10, 62</sup> In Korea, cancer statistics from 2017 showed an ASIR of 30.8 per 100,000 persons, with rates of 39.9 in males and 23.0 in females.<sup>10, 63</sup> The sex disparity in younger patients is not clear since the incidence of CRC in females under 50 years old is very low. The tendency for CRC to occur more frequently in males than in females becomes apparent from ages 45–50 in the USA, UK, and China.<sup>10</sup>

Several factors potentially contribute to these disparities including sex hormones, biases in coding and noncoding cancer drivers, mutation prevalence and signatures, and reproductive stages.<sup>64-66</sup> Data from the American Cancer Society (ACS) confirm that men have a higher overall risk of developing CRC compared to women, though the number of new cases in older age groups, more than 65 years old, is similar between genders.<sup>3</sup> Women generally have a survival advantage over men, particularly under the age of 65.<sup>3</sup> Additionally, the incidence of CRC in younger adults is on the rise, presenting unique challenges for diagnosis and treatment.<sup>1</sup> Females and males have also shown disparities in the rate of developing left and right sided CRC, which has been described in Chapter 1.2.

Screening uptake also varies by gender. In a study in the UK, women under 69 years were more likely to present as emergency cases, while men are more often diagnosed through screening and two-week-wait referrals, a system that allows a patient with cancer related symptoms to be seen as quickly as possible.<sup>67</sup> Similar gender-specific differences have been observed in Korea, China, and England.<sup>68-70</sup> There are growing calls for gender- and age-based screening and treatment protocols for CRC.<sup>68, 71</sup> However, common gender differences such as sex hormones exhibit age-dependent changes in their abundance, which do not always correspond to the magnitude of sex differences in cancer incidence and severity.<sup>72</sup>

It has been suggested that this disparity may also be due to behavioral and social differences: men typically consume more red or processed meat, have higher alcohol consumption, smoke more, and tend to accumulate more abdominal visceral fat. Notably, although racial disparities greatly influence CRC incidence, in the US males presented with higher CRC incidences in all racial groups [Table 1.1]. All these factors are linked to an increased risk of CRC. However, some studies have indicated that even when these modifiable factors are controlled for, differences in CRC incidence between men and women remain.<sup>54, 55, 67, 73, 74</sup> These findings suggest that while the fundamental biology of sex differences impacts cancer, the influence of host biological sex on cancer peritoneal metastasis remains largely unknown. Unfortunately, the understanding of how gender and age affect CRC progression and metastasis remains either lacking or conflicting.<sup>65</sup> Such complexity highlights the necessity for further research to unravel the interplay between gender, age, and CRC, which could lead to more tailored and effective screening and treatment strategies.

## 1.4 Peritoneum and Mesothelium

As mentioned in Chapter 1.1, metastatic CRC (Stage IV), can be either distant or regional. Regional metastasis of CRC has become more common;<sup>3</sup> thus, it is important to examine the peritoneal cavity where the colon and rectum sits. The peritoneal cavity, which houses numerous vital organs, provides an environment conducive to the progression of late-stage cancer progression known as intraperitoneal metastasis. One of the primary components of this cavity is the peritoneum [Figure 1.5], consisting of two main compartments separated by a thin basement membrane (BM): the mesothelium and supporting connective tissues.<sup>75-77</sup> This expansive, translucent serous membrane lines the inner walls of the abdominal cavity and the external surfaces of the visceral organs, known respectively as the parietal (18%) and visceral (82%) peritoneum.<sup>53, 75, 76, 78-81</sup> The peritoneum's continuous surface area is approximately 1 to 2 square meters, nearly equivalent to that of the skin.<sup>53, 75, 76</sup> Surprisingly, almost all peritoneal organs, including stomach, liver, and spleen, are not originally located within the peritoneal cavity itself which normally only contains peritoneal fluid. Instead, during embryological development, intraperitoneal organs invaginate and are completely or almost completely covered by the visceral layer of peritoneum.<sup>82</sup> In addition to covering the visceral organs, the peritoneum folds on itself to form structures such as the mesentery and the omentum [Figure 1.5], which are significant sites for peritoneal metastasis.<sup>53, 83</sup>

The mesothelium, an elastic monolayer of mesothelial cells (MC) with a collagen I-rich sub-mesothelial matrix [Figure 1.2], lines the surface of the peritoneum. The sub-mesothelial matrix comprises extracellular matrix (ECM) proteins, capillaries, fibroblasts,

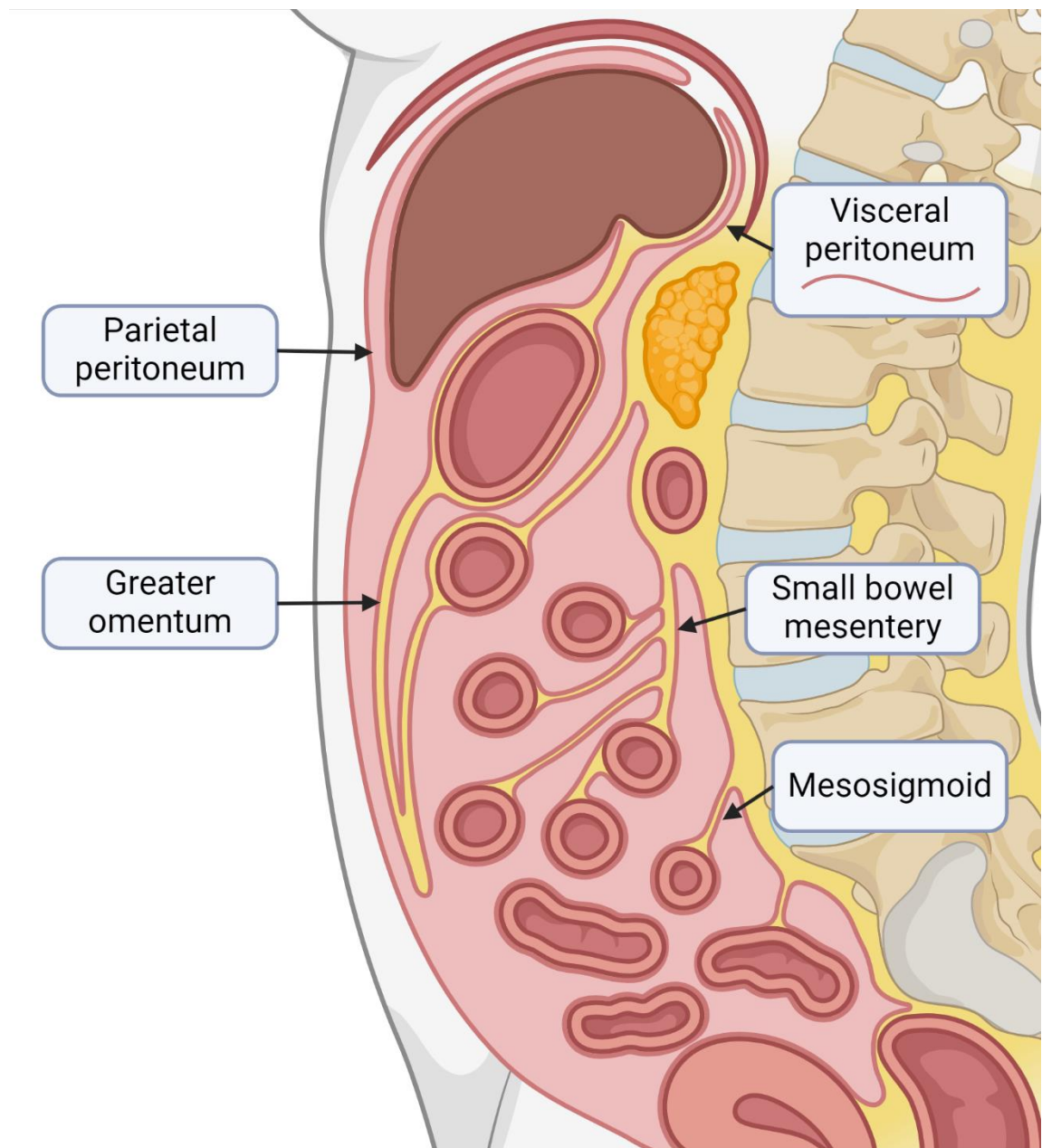


**Figure 1.5. Sagittal section of the peritoneal cavity (female adult). Peritoneal peritoneum (parietal and visceral, dark pink curves) is one of the major structures lining the majority of the inner surface area of the abdominal cavity. It also folds to form omentum, mesentery and mesosigmoid. These features make the peritoneum the front line facing metastatic cancer cells.**

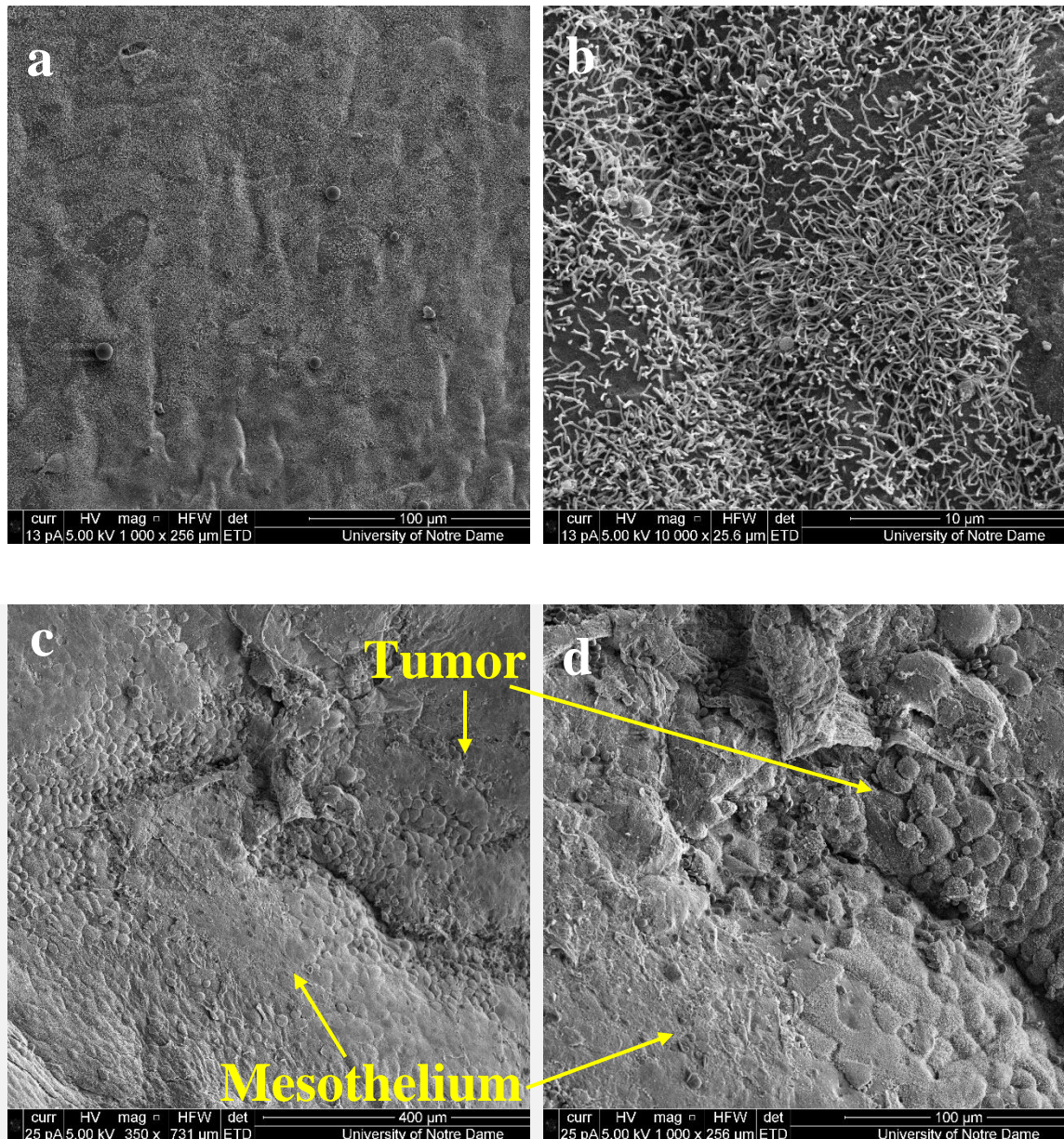
and various types of innate immune cells, such as natural killer (NK) cells, mast cells, and macrophages.<sup>75</sup> The ECM acts as a scaffold and transmits biochemical and biomechanical signals to cells.<sup>84</sup> The mesothelium functions to protect and reduce friction between abdominal organs, acts as a dialyzing membrane, and participates in host defense and regeneration, thus contributing to the homeostasis of the peritoneal cavity.<sup>77</sup> This anatomical structure is crucial in the context of peritoneal metastasis in colorectal cancer (CRC). During the process of CRC peritoneal metastasis, cancer cells detached from the primary tumor must first adhere to the surface of adjacent organs in order to colonize a new metastasis site. As a result, the mesothelium, more specifically the mesothelial cells, will be the first in contact. Mesothelial cells are specialized epithelial cells that originate from the mesoderm during development.<sup>85</sup> They possess unique mesenchymal characteristics, expressing vimentin and cytokeratin 18, which distinguishes them from other epithelial cells.<sup>86-91</sup>

Figure 1.6a and 1.6b show scanning electron microscopy (SEM) images revealing the apical surface of the mouse peritoneal mesothelium. The monolayer is covered with numerous long and thin microvilli, which are less densely packed than those in the epithelium lining the lumen of the intestine or kidney, where nutrient transport occurs.<sup>92</sup> Mesothelial cells are arranged in a mosaic or polygonal pattern, with microvilli often being most dense at the borders.<sup>93</sup> Figure 1.6c and 1.6d illustrates the junction between the host mesothelium and a secondary colorectal cancer tumor growing on the surface of this peritoneum.

A critical early event for successful metastasis onto peritoneal organs is the interaction of cancer cells with these peritoneal mesothelial cells. Only after a successful

adhesion of the cancer cell onto the mesothelial cell can a cancer cell begin its next steps including invasion into the sub-mesothelial collagen matrix and proliferate. As a result, it will be necessary to investigate the activities of cell adhesion proteins such as N-cadherin and E-cadherin, as well as matrix modifying proteins such as matrix metalloproteases (MMPs). It is also reported that free CRC cells release a range of pro-inflammatory cytokines, such as tumor necrosis factor (TNF)- $\alpha$ , interleukin (IL)-1 $\beta$ , IL-6, and interferon (IFN)- $\gamma$ . These cytokines stimulate healthy cells, especially peritoneal MCs to upregulate the expression of intercellular adhesion molecules such (ICAM), platelet endothelial cell adhesion molecule (PECAM), vascular cell adhesion molecule (VCAM), and other immunoglobulin superfamily cell adhesion molecules (IgCAMs). This response leads to mesothelial cells contracting and becoming more rounded, exposing the basement membrane. Concurrently, IFCCs adhere to MCs through the specific interaction between CD43 (sialophorin) on the cancer cells and the IgCAMs on HPMCs.<sup>17, 94</sup> Following this, mesothelial cells produce lysophosphatidic acid, which further enhances the adhesion of cancer cells, creating a positive feedback loop. Additionally, IFCCs express CD44, a cell surface glycoprotein that binds to hyaluronic acid secreted by mesothelial cells, promoting tumor cell adhesion to the mesothelium.<sup>95</sup> A small number of tumor cells then invade the mesothelial layer, inducing apoptosis in HPMCs via the FasL/Fas pathway, thereby breaching the peritoneal barrier and infiltrating the sub peritoneal space.<sup>17, 96</sup> Such process also involves the action of matrix metalloproteinases (MMPs), which are released by cells such as mesothelial cells, fibroblasts, inflammatory cells, and macrophages when tumor cells invade the sub-peritoneal space. These MMPs degrade the extracellular matrix (ECM), facilitating the spread of cancer.<sup>17</sup> Additionally, the urokinase-type plasminogen activation





**Figure 1.6. a) and b) Apical surface of mouse peritoneal mesothelium c) and d) Metastatic colorectal cancer growing on the peritoneal surface of mouse.**

system contributes by activating pro-MMPs and further breaking down ECM components.<sup>97-99</sup> This degradation allows tumor and stromal cells to secrete various growth factors, including the epidermal growth factor receptor (EGFR) and insulin-like growth factor 1 (IGF-1), through autocrine and paracrine signaling, promoting the continuous

proliferation of cancer cells.<sup>17, 100</sup> This interaction is hypothesized to be differentially impacted by both gender- and age-related differences in peritoneal mesothelial cells, thereby influencing the success of CRC metastasis. Understanding these interactions and the role of mesothelial cells can provide insights into the mechanisms of peritoneal metastasis and help develop targeted therapies to prevent or treat metastatic spread in CRC patients.

### **1.5 Study Objective**

The primary objective of the proposed study is to deepen our understanding of how gender and age differences influence peritoneal metastasis in colorectal cancer (CRC) through the use of proteomic approaches. Previous research has indicated that approximately 35-40% of CRC patients develop peritoneal metastasis, a severe condition that can ultimately lead to death.<sup>3, 27, 33</sup> The metastasis process may begin as early as the formation of the primary tumor, suggesting that any patient diagnosed with CRC has a significant risk of developing metastasis in the future.<sup>12</sup> While early-stage CRC can often be treated successfully with surgery, metastatic CRC is much more challenging to eliminate and is frequently fatal. Among the estimated 150,000 CRC cases, approximately 50,000 deaths occur, with many attributed to metastasis, particularly among older individuals and males.

The overarching goal of this study is to identify and investigate therapeutic targets that are unique to for different gender and age groups, with the aim of preventing or treating CRC metastasis in these populations. To achieve this goal, the study is structured around three main aims.

The first aim focuses on the hypothesis that different gender and age groups exhibit distinct patterns or extent of CRC metastasis. This aim will be addressed by examining the functional impact of gender- and age-related changes in peritoneal tissues on tumor-host interactions in CRC metastasis. Using an allograft model, the study will compare metastatic seeding in cohorts of young and aged male and female mice, which will be injected intraperitoneally (i.p.). Both *in vivo* and *ex vivo* fluorescent imaging techniques will be employed to qualify CRC metastasis patterns across these different groups.

The second aim explores the hypothesis that the group with the most significant tumor burden will have a unique host proteome compared to others, with specific proteins driving these differences. This aim will involve conducting a proteomic characterization of gender- and age-related differences in tumor-naïve murine primary peritoneal mesothelium. The study includes the development of techniques to isolate and culture murine primary peritoneal mesothelial cells (MPPMC), enabling an analysis of proteomic differences in non-cancerous cells across different gender and age groups. This analysis will help identify unique proteins in the most tumor-rich group identified in the first aim.

The third aim of the study seeks to characterize and validate the proteins identified in the second aim through *in vitro* and *ex vivo* protein function assays. The underlying hypothesis here is that treating healthy cells with inhibitors targeting the proteins identified in the second aim will reduce the impact of age and gender differences observed in the first aim, particularly in cancer cell adhesion models that are involved in early metastatic seeding. By doing so, the study aims to explore how these proteins contribute to CRC metastasis and their potential as therapeutic targets.

In summary, Aim 1 will first investigate the gender and age effects on CRC peritoneal metastasis. Aim 2 will then identify proteins that are differentially expressed in these groups through proteomic analysis. Finally, Aim3 will validate the role of these protein(s) in mediating CRC metastasis, with the ultimate goal of identifying therapeutic targets that can be used to prevent metastasis in different gender and age groups.

Unlike most studies that focus on the cancer itself, this study is concentrating on the hosts. While the incidence of cancer may be unpredictable and challenging to prevent, it is possible to explore potential methods tailored to the needs of different genders and age groups to prevent primary or recurrent colorectal cancer from metastasizing, which accounts for the majority of fatalities. Our innovative approach seeks to provide molecular-level insights by identifying proteins specific to each gender and age group. The long-term goal is to understand how these proteins contribute to intra-peritoneal metastatic seeding and to identify new targets for preventing metastatic spread. One of the significant findings from this study is the identification of Prl-1 (Chapter 4), Phosphatase of regenerating liver 1, as a target that enhances the success of CRC peritoneal metastasis. Prl-1 is found exclusively expressed in the MPPMCs from Aged Male mice which has shown the most tumor burden in the *in vivo* study. The pro-metastatic effects of Prl-1 have been validated through the inhibition of Prl-1 and its downstream targets in both *in vitro* and *ex vivo* assays.

By focusing on the proteomic differences associated with gender and age, this study aims to uncover specific proteins that play critical roles in the metastatic process. Understanding these differences could lead to the development of more effective, targeted

therapies that consider the patient's age and gender, thereby improving treatment outcomes and survival rates for CRC patients with peritoneal metastasis.

## CHAPTER 2.

### IN VIVO COHORT STUDY USING ALLOGRAFT MODEL TO MEASURE CANCER METASTASIS

#### **2.1 Abstract**

Cancer is a disease that predominantly affects older individuals. Our laboratory has recently demonstrated an increase in peritoneal metastatic tumor burden from ovarian cancer with advancing age.<sup>53</sup> While age remains one of the most significant risk factors for cancer and metastasis, the biological sex of the host also plays a crucial role in influencing metastasis and survival outcomes. Notably, in a pan cancer research, the survival rates tend to be lower in males compared to females, while the incidence rates for males are equal or less than females.<sup>59</sup> It indicates that males are overall more prone to cancer related death, especially given that there is a similar number of patients diagnosed with cancer in both genders. Specifically in colorectal cancer (CRC), both cancer incidence and deaths are higher in males, especially under the age of 65, highlighting the serious mortality concerns for male CRC patients. Chapter 1 has explored published data on gender and age disparities, highlighting their substantial impact on CRC prognosis and survival. The findings suggest that fundamental biological differences between sexes influence cancer progression, yet the specific effects of biological sex on cancer peritoneal metastasis remain unclear.

This study seeks to enhance our understanding of the influence of gender and age on peritoneal metastasis in colorectal cancer (CRC). It is hypothesized that gender- and age-related differences in peritoneal mesothelial cells will differentially affect the interaction between tumor cells and mesothelial cells, thereby influencing the success of CRC metastasis. The initial objective is to evaluate the effects of gender and age on CRC intra-peritoneal (i.p.) metastasis. A comparative analysis of metastatic seeding has been conducted in cohorts of young and aged, male and female mice injected intra-peritoneally, utilizing both *in vivo* and *ex vivo* fluorescent imaging techniques. Our results indicate that aged male mice exhibit the highest tumor burden which aligns with epidemiological data. Additionally, CRC appears to selectively target adipose tissues which are heavily covered by visceral peritoneum during i.p. metastasis. Males, in particular, show a greater number of tumors in abdominal adipose tissue compared to females, with tumor intensity increasing with age. Notably, the omentum exhibits gender-specific differences predominantly in aged groups, rather than in young groups.

These findings provide valuable insight into the biological mechanisms that may promote CRC i.p. metastasis, particularly in aged males. By focusing on the proteins potentially involved in this process, as will be further explored in Chapter 3, we aim to identify new targets for therapeutic intervention to prevent metastatic dissemination.

## **2.2 Materials and Methods**

### **2.2.1 Materials**

The cell culture media used is composed of Dulbecco's Modification of Eagle's Medium (DMEM, Corning, Midland, MI), supplemented with 1% penicillin-streptomycin solution (Corning), 10% fetal bovine serum (FBS, Gibco, Carlsbad, CA), 1% Non-essential amino acids (Sigma-Aldrich, St. Louis, MO), 1% GlutaMAX (Gibco), 1% HEPES buffer (Corning), and 1% Sodium pyruvate (Gibco).

### **2.2.2 Animal and cell line.**

C57Bl/6 male and female mice were purchased from Jackson Laboratory at 2 age points: mature young (3-6 months old) mice (equivalent to human 20-30 years old) and aged (20-23 months old) mice (equivalent to human 60-67 years old).<sup>53, 101</sup> Cohorts (10 mice per cohort) were defined as Female Young (FY), Female Aged (FA), Male Young (MY) and Male Aged (MA). All animal procedures were carried out according to the regulations of the Institutional Animal Care and Use Committee (IACUC) at the University of Notre Dame. The murine colon adenocarcinoma cell line MC-38, syngeneic with C57Bl/6, was purchased from Kerafast, MA.

### **2.2.3 RFP tagging of MC-38 cells**

MC-38 was seeded on 24 well plates, 3000 cells/well until 80% confluency. Lentivirus encoding red fluorescent protein (RFP) was added to each well in a Multiplicity of Infection (MOI) gradient from 0.5 to 20 and incubated for 24 hours. Cells which survived were first screened under fluorescent microscope for RFP signal. Cells with MOI



= 10 were selected and sent to IUSM-SB Core Facility for cell sorting, generating new culture of MC-38-RFP cells [Figure 2.1].

#### **2.2.4 Assessing Tumor Burden in Allograft Model of CRC Metastasis**

To establish an allograft model of i.p. metastasis [Figure 2.1], MC-38-RFP cells ( $1 \times 10^5$ ) were injected intraperitoneally (i.p.) into 4 separate cohorts of FA, FY, MA, MY mice, 10 mice from each cohort. Mice were monitored 3 times per week for disease condition and *in vivo* live imaging was taken each week to monitor tumor growth. Mice abdominal hair was removed weekly before imaging under anesthesia. Mice were anesthetized with 2.5% isoflurane, then placed on a sterile heating pad during imaging and hair removal. A nose cone was used to deliver 2.5% isoflurane during procedures. Tumor burden was monitored by longitudinal live imaging of the RFP signal for 4 weeks. Mice were then sacrificed. Fluorescent images were taken *in situ* with abdominal cavity exposed. Peritoneal organs were collected individually for *ex vivo* fluorescent images. Fluorescent signals were quantitatively analyzed using ImageJ. Tumor burden in the abdominal and organ images was analyzed by calculating the tumor area and the intensity of the RFP signal in that area (Raw Integrated Density). The threshold was set to 5500-65535 for *in vivo* pictures and 10000-65535 for *ex vivo* and *in situ* pictures. The quantitative data is analyzed with standard two-way ANOVA.

### **2.3 Results and Discussion**

In this cohort study, visual inspection of the tumor burden in live mice indicated that the Male Aged cohort displayed the greatest tumor growth, as observed through *in vivo* imaging [Figure 2.2a]. Both aged female and male demonstrated more tumor burden than

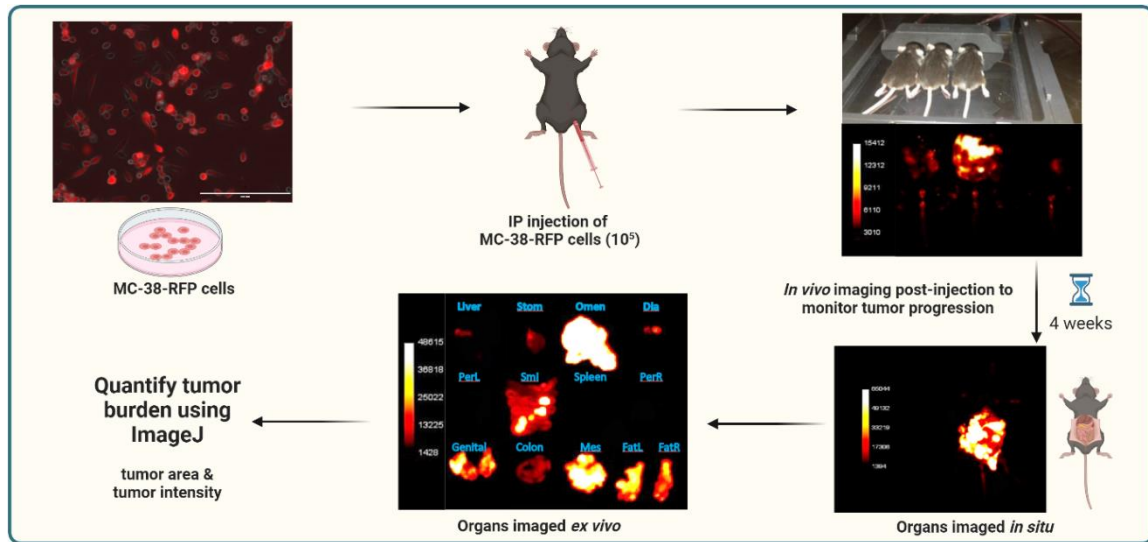


**Figure 2.1 Work flow for assessing tumor burden in allograft model of CRC metastasis; MC-38-RFP cells ( $1 \times 10^5$ ) were injected intraperitoneally (i.p.) into 4 separate cohorts of FA, FY, MA, MY mice, 10 mice from each cohort. To monitor tumor growth, tumor burden was monitored by longitudinal live imaging of the RFP signal for 4 weeks. Mice were then sacrificed. Fluorescent images were taken in situ with abdominal cavity exposed. Peritoneal organs were collected individually for ex vivo fluorescent images. Fluorescent signals were quantitatively analyzed using ImageJ. F: Female; M: Male; A: Aged; Y: Young**

the young groups [Figure 2.2b]. To obtain a more precise measure of tumor burden, we utilized *in situ* fluorescent imaging of the exposed abdominal cavity post-sacrifice [Figure 2.2c], with the mean tumor burden quantified in Figure 2.2d. Overall, aged male mice had the highest tumor burden, significantly exceeding that of the FA and FY groups. This observation aligns with clinical data indicating increased CRC incidence and mortality with aging.<sup>3, 47, 58</sup> Similarly, epidemiological studies reveal that men generally experience higher CRC incidence and poorer survival rates compared to women.<sup>10, 61, 102</sup> While it is reasonable to hypothesize that aged males would exhibit the highest tumor burden, data show that females tend to have worse survival outcomes beginning after age 65, suggesting

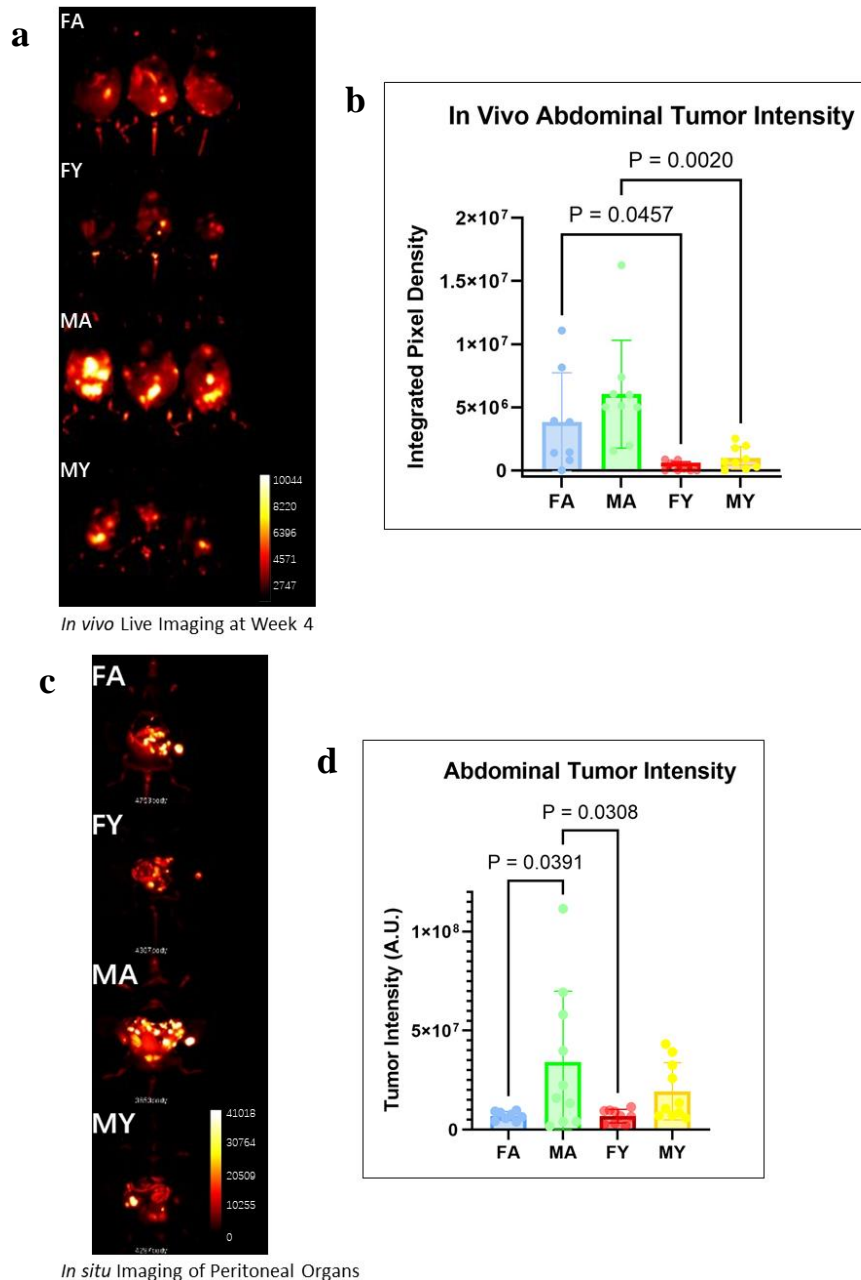


**Figure 2.2** MC-38-RFP cells ( $1 \times 10^5$ ) were injected intraperitoneally (i.p.) into 4 separate cohorts of FA, FY, MA, MY mice, 10 mice from each cohort. To monitor tumor growth, tumor burden was monitored by longitudinal live imaging of the RFP signal for 4 weeks. a) *In vivo* live imaging at week 4; b) quantitative analysis of *in vivo* fluorescent images of the mice; Mice were then sacrificed. Fluorescent images were taken *in situ* with abdominal cavity exposed. Peritoneal organs were collected individually for *ex vivo* fluorescent images; c) *in situ* imaging of the peritoneal cavity; d) quantitative analysis of *in situ* fluorescent images of the abdominal organs F: Female; M: Male; A: Aged; Y: Young

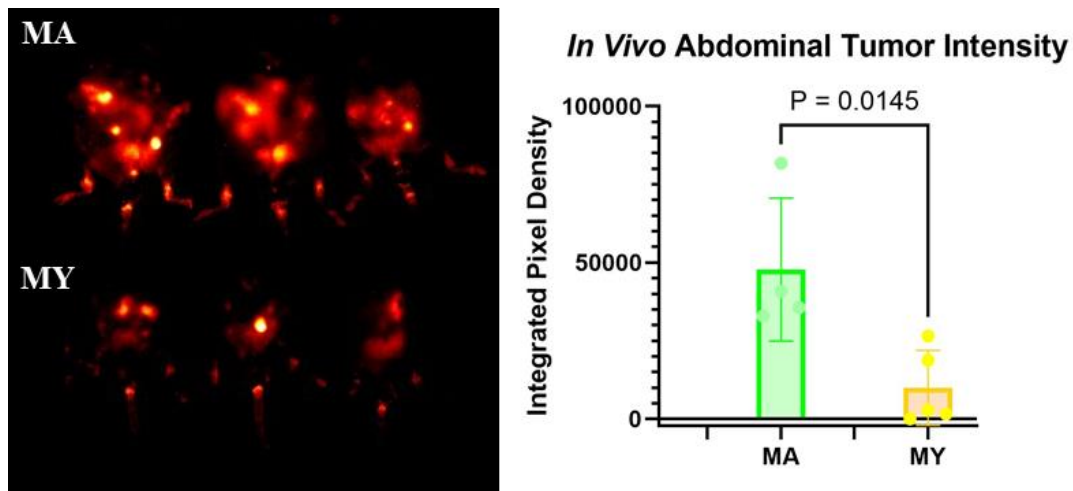


**Figure 2.3** Follow-up comparisons of MA and MY cohorts. MC-38-RFP cells ( $1 \times 10^5$ ) were injected intraperitoneally (i.p.) into cohorts of MA, MY mice, 5 mice from each cohort. To monitor tumor growth, tumor burden was monitored by longitudinal live imaging of the RFP signal for 4 weeks. Left: *In Vivo* imaging of MA vs. MY mouse abdominal tumor burden at week 4 post injection; Right: Quantitative analysis of MA vs. MY mouse abdominal tumor burden. MA bears significantly higher tumor RFP signal than MY. M: Male; A: Aged; Y: Young.

that the tumor burden in aged females could be comparable to that in aged males.<sup>3, 54</sup> This discrepancy may arise from differences in the physiological aging process between humans and mice. Furthermore, *in vivo* imaging [Figure 2.2a and b] and *in situ* imaging [Figure 2.2c and d] gave somewhat different results, with respect to statistical significance. *In vivo* imaging showed significant differences when comparing MA to MY and FA to FY, while *in situ* imaging showed significant differences when comparing FA to MA and FY to MA. These results highlight the inherent challenges in quantifying widely disseminated i.p. metastasis. Overall, the MA cohort displayed the greatest overall tumor burden. In a follow-up experiment using only the MA and MY cohorts ( $n = 5$ ), *in situ* imaging showed a statistically significant differences comparing MA to MY [Figure 2.3]. Organ-specific

analysis of tumor burden is presented in Figure 2.4, offering a more nuanced interpretation of CRC i.p. metastasis. Of the 12 peritoneal organs collected, data for six selected organs are shown: liver, genitalia, colon (origin site of CRC), omentum, mesentery, and peritoneal adipose tissue. Other organs, including the intestine, stomach, diaphragm, parietal peritoneum, and spleen, are not shown due to the absence of RFP signal. Notably, CRC cells demonstrate a strong preference during i.p. metastasis, favoring the omentum, mesentery, and peritoneal adipose tissues. These are all visceral adipose tissues originated from the folding of the visceral peritoneum,<sup>53, 83</sup> overlaid with a monolayer of visceral mesothelial cells that have been reported to contribute to inflammation, fibrosis, and adipocyte development.<sup>103</sup> However, their interaction with CRC requires further investigation. Gender differences were particularly pronounced in organ-specific analysis. Regardless of age, males exhibited a greater tumor burden in abdominal adipose tissue compared to females, with tumor intensity increasing with age in males. Additionally, gender-specific differences were evident in the omentum of aged groups, but not in the younger cohorts. This analysis underscores the importance of considering both gender and age in determining CRC metastatic patterns. To identify proteins on peritoneal MC that contribute to i.p. metastatic seeding, proteomic profiles will be analyzed in Chapter 3. Ultimately, this research aims to discover new therapeutic targets to prevent metastatic spread, particularly in high-risk populations such as older males.

## **2.4 Conclusion**

Aim 1 of this study elucidates the role of age and gender in peritoneal metastasis of colorectal cancer (CRC) using a murine model. Our findings demonstrate increased *in vivo* tumor burden with age in both male and female. Male aged mice exhibit the highest tumor

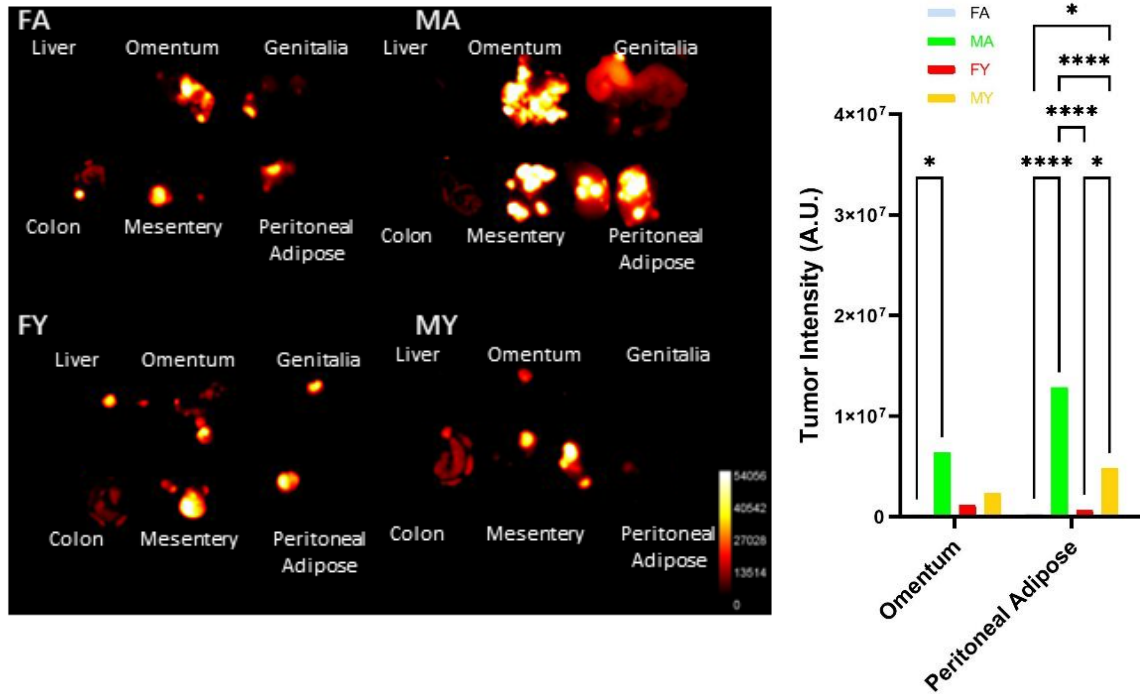


**Figure 2.4 Characterization of organ-specific tumor burden from the cohort study in Figure 2.2. Left: 6 out of 12 peritoneal organs collected are shown: liver, omentum, mesentery, peritoneal adipose on the left & right side, colon, genitalia. Right: Quantitative analysis of organ specific fluorescent images. Only significant differences are shown. F: Female; M: Male; A: Aged; Y: Young; \*:  $p < 0.05$ ; \*\*:  $p < 0.01$ ; \*\*\*:  $p < 0.001$ ; \*\*\*\*:  $p < 0.0001$ .**

burden, particularly in adipose organs formed by the folding of visceral peritoneum, consistent with epidemiological data suggesting higher CRC incidence and mortality in males. The study also highlights the gender-specific differences in tumor burden are more pronounced in aged mice, particularly in the omentum and peritoneal adipose. These observations suggest that biological sex and age significantly influence CRC metastatic patterns, potentially via sex-specific proteins. Future proteomic analyses, as outlined in Chapter 3, will aim to identify these proteins and explore their roles in promoting peritoneal metastasis.

CHAPTER 3.

ISOLATION AND PROTEOMICS ANALYSIS OF MURINE PRIMARY  
PERITONEAL MESOTHELIAL CELLS IDENTIFIES CANDIDATE PROTEINS  
POTENTIALLY AFFECTING CRC PERITONEAL METASTASIS SUCCESS

### **3.1 Abstract**

A major abdominal organ is the peritoneum, a vast serous membrane that lines the inner walls of the abdominal cavity and the outside of the visceral organs with a continuous surface area of 1-2 m<sup>2</sup>, nearly equal to that of the skin.<sup>76, 79, 80, 104</sup> The peritoneum consists of two compartments separated by a basement membrane: the mesothelium and supporting loose connective tissue.<sup>76, 77, 104</sup> The mesothelium, a monolayer of mesothelial cells (MC), functions to reduce friction between abdominal organs, supports the homeostasis of the peritoneal cavity, and acts as a protective barrier to the collagen I-rich submesothelial matrix<sup>77, 105</sup> and the underlying abdominal organs. As a result, many peritoneal diseases, including peritonitis, primary cancer (mesothelioma), and metastatic cancer including ovarian, pancreatic and colorectal cancer, initiate from interactions with the mesothelium.

The mouse cohort study in Aim 1 demonstrated that the male aged cohort exhibited the most tumor burden; however, the impact of gender and age on the peritoneal MC has not been evaluated. To address this knowledge gap, the objective of this study was to identify and characterize gender- and age-related differences in the proteome of murine

primary peritoneal MC. Primary peritoneal MC were isolated from female or male young mice (3-6 months, FY and MY) and aged mice (20-23 months, FA and MA), lysed, trypsin digested using a S-Traps, then subjected to bottom-up proteomics using an nLC-Orbitrap mass spectrometer. In each cohort, ~2000 proteins and ~1000 protein groups were identified. Proteins were categorized using Gene Ontology Enrichment and pairwise comparisons between gender and age cohorts were conducted. This study establishes baseline information for future studies on peritoneal mesothelial cells in health and disease at two important physiologic age and gender points. Segregation of the data by both gender and age could reveal novel contributory factors to specific disease states involving the peritoneal cavity. This highly accessible *in vitro* primary cell model may have utility for future studies to examine the interaction between the mesothelium and foreign materials. The resulting data identify sex- and age-related differences that may regulate MC homeostasis in the healthy peritoneum and influence the initiation and progression of peritoneal diseases.

### **3.2 Materials and Methods**

Raw and processed data are available through the MassIVE data exchange and cross-posted to ProteomeExchange. MSV000092134  
<ftp://MSV000092134@massive.ucsd.edu> (For Review) Password: MouseAge2302\*  
<https://massive.ucsd.edu/ProteoSAFe/static/massive.jsp>

#### **3.2.1 Materials:**

Rat tail collagen type I and trypsin were purchased from Corning. MPPMC culture media compositions include Dulbecco's Modification of Eagle's Medium (DMEM,



Corning, Midland, MI), Ham's F12 (Corning), 1% penicillin streptomycin solution (Corning), 15% fetal bovine serum (FBS, Gibco, Carlsbad, CA), 10ng/mL epidermal growth factor (EGF, Gibco), 400 ng/mL hydrocortisone (Corning), 1% GlutaMAX (Gibco), 1% HEPES buffer (Corning), 1% ITS (ITS+1 Liquid Media Supplement, Sigma-Aldrich, St. Louis, MO). Primary antibodies used are vimentin (Sigma-Aldrich, catalog #: V5255), cytokeratin 18 (catalog #: ab668, Abcam, Cambridge, MA). Anti-mouse IgG peroxidase-conjugated secondary antibodies were from Sigma-Aldrich. Peroxidase detection reagents, SuperSignal West Dura, and Halt™ Protease Inhibitor were obtained from ThermoFisher (Rockford, IL). Ammonium-Chloride-Potassium (ACK) Lysing Buffer was purchased from Gibco. LP9 cell culture media compositions include Medium 199 (Sigma-Aldrich), F12 medium (Gibco), supplemented with 15% FBS, 10 ng/mL EGF, 400 ng/mL Hydrocortisone, 1% Penicillin/Streptomycin (Pen/Strep; Lonza), 1% L-GlutMAX (Thermo Fisher Scientific) and 1% HEPES. All methods were carried out in accordance with the University of Notre Dame Institutional Review Board (IRB) and Institutional Biosafety Committee (IBC) guidelines and regulations. Experimental protocols were approved by the IBC committee (protocol 23-04-7798, expiration 06/14/26).

### **3.2.2 Animals:**

C57Bl/6 male and female mice were purchased from Jackson Laboratory and housed at Freimann Life Science Center at 2 age points: mature young (3-6 months old) mice (equivalent to human 20-30 years old) and aged (20-23 months old) mice (equivalent to human 60-67 years old).<sup>53, 101</sup> Cohorts (6 mice per cohort) were defined as Female Young (FY), Female Aged (FA), Male Young (MY) and Male Aged (MA). All animal procedures

were carried out according to the regulations of the Institutional Animal Care and Use Committee (IACUC) at the University of Notre Dame.

### **3.2.3 Murine Primary Peritoneal Mesothelial Cell (MPPMC) Isolation, Culture, and**

#### **Lysis:**

Mice were sacrificed via isoflurane overdose in accordance with IACUC guidelines. To isolate primary MCs, immediately after sacrifice, mice were injected intra-peritoneally (i.p.) with 3 mL of 0.125% trypsin. Mice were maintained at 37°C for 20 minutes, during which they were gently rotated to mix the peritoneal fluid every 2-3 minutes. After incubation, 6 mL of isolation media (DMEM/F12 1:1, 10% FBS, 1% Pen/Strep) were injected i.p. into each mouse to neutralize the trypsin and the peritoneal fluid was collected. The abdominal cavity was further washed with 3 mL of isolation media and the collected mixture was centrifuged at 180xg at 4°C. Each cell pellet was re-suspended in 2 mL ACK lysing buffer for 2 minutes on ice to remove blood cells followed by mixing with 6 mL of PBS to terminate the reaction. After centrifugation (180xg, 4 °C), pellets were washed with 6 mL isolation media, followed by another centrifugation (180xg, 4 °C). Cells were re-suspended in culture media (DMEM/F12 1:1, 15% FBS, EGF 10 ng/mL, hydrocortisone 400 ng/mL, 1% Pen/Strep, 1 % L-glutamax, 10 mM HEPES, ITS 1:100) and plated onto tissue culture dishes coated with rat tail collagen type I (10 µg/ml in coating buffer 0.1 M Na<sub>2</sub>CO<sub>3</sub>, pH9.6) or chamber slides as previously described.<sup>106</sup>

In each cohort, 6 mice were sacrificed for MPPMCs and cells from each mouse were plated into individual wells of 24-well collagen-coated plates. Adherent cells were washed with warm PBS at 24 hours after being plated to remove non-adherent and/or dead

cells, then cultured for an additional three days prior to changing to serum free medium for 24 hours to remove serum protein contaminants. For proteomic analysis, after washing three times with PBS, cells were lysed by adding 100  $\mu$ L modified RIPA (mRIPA) buffer (150mM NaCl; 50mM Tris, pH 7.5; 20mM NaF; 10mM Na<sub>2</sub>P<sub>2</sub>O<sub>7</sub>; 5mM EDTA; 1% Triton X-100; 0.1% SDS) containing protease inhibitors to each well for 10 minutes at 4°C. Preliminary analyses showed that the mass balance of these proteins was predominately media and murine blood-associated proteins. Therefore, lysates from each cohort were pooled prior to analysis in order to increase the depth coverage of the proteome and to minimize the impact of individual subjects. It should be noted that, as a primary cell, MPPMC do not maintain indefinite viability and can be maintained for a very limited number of passages (1-2 for cells from A mice, x-y for cells from Y mice, *data not shown*), thus limiting the number of cells available from each subject. Pooled lysates, 100  $\mu$ g each cohort, were concentrated and trypsin digested using the S-Trap protocol (Protifi).<sup>107</sup>

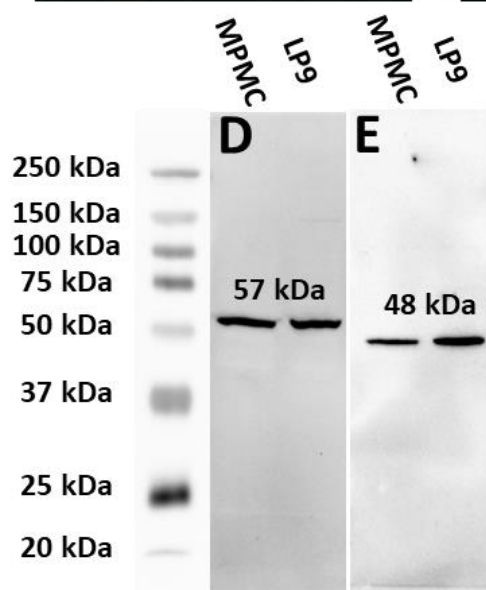
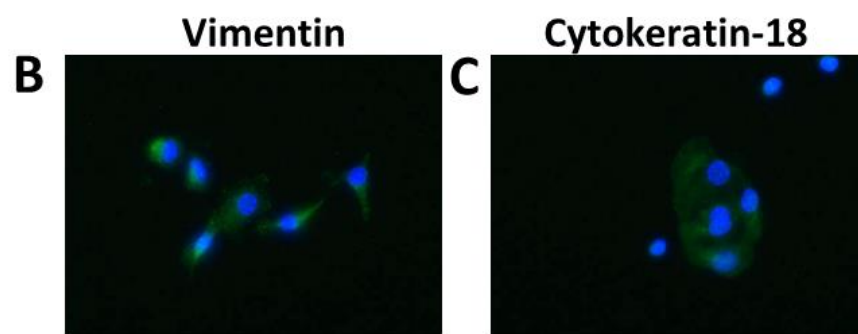
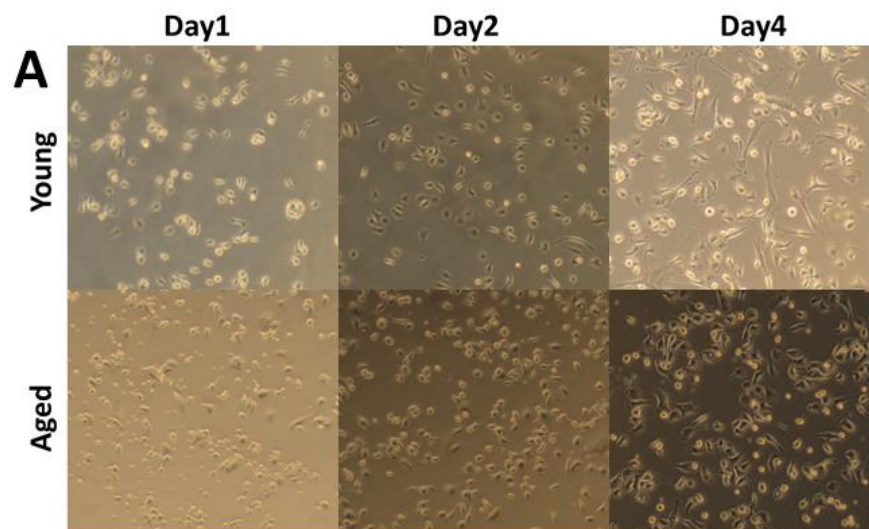
### **3.2.4 Western Blots and Immunofluorescence:**

MC are unique among normal cells in that they display both epithelial and mesenchymal characteristics, a property usually limited to regenerating or neoplastic cells. To validate the epithelial and mesenchymal properties, isolated MPPMCs were evaluated by western blotting and immunofluorescence staining for expression vimentin (mesenchymal marker) and cytokeratin 18 (epithelial marker).<sup>88-91</sup> For immunofluorescence experiments, freshly isolated MPPMCs were cultured on 22mm<sup>2</sup> glass coverslips (coated with rat tail collagen type I), washed twice with ice-cold PBS, and fixed with 4% paraformaldehyde in 0.12M sucrose in PBS for 20 minutes at room

temperature. Cells were blocked with 3% Bovine Serum Albumin (BSA) in PBS for 1 hour at room temperature, incubated with primary antibody (1:100) in 3% BSA for 1h at 37°C, rinsed thrice for 5 minutes with PBS, and incubated with appropriate Alexa-Fluor conjugated secondary antibody at a 1:300 dilution for 30 minutes at 37°C. After washing, cells were allowed to dry, mounted with VECTASHIELD Mounting Media with DAPI (Vector laboratories), and visualized on a Leica DM5500 B Fluorescence Microscope.<sup>108</sup> Images presented here were cropped from the full visual field. Brightness and contrast were adjusted equally across all images.

For western blots, protein concentration of cells lysed with mRIPA buffer containing protease and phosphatase inhibitor was measured using DC™ Protein Assay (Bio-Rad). Protein (20µg) was electrophoresed on 9% SDS-polyacrylamide gels and transferred to methanol-activated polyvinylidene membranes. After transfer, membranes were blocked with 5% milk in TBST (150mM NaCl, 25mM Tris, 0.05% Tween 20 for 1 hour at room temperature) to prevent non-specific binding. Primary antibodies, vimentin (Sigma-Aldrich, catalog #: V5255, 1:1000) and cytokeratin 18 (Abcam, catalog #: ab668, 1:500) were diluted as indicated in 5% milk/TBST and incubated overnight at 4°C. After washing, the membranes were incubated with horseradish peroxidase-conjugated secondary antibodies (1:4000 dilution) for 1 hour at room temperature, and then visualized with chemiluminescence using ChemiDoc™ Imaging.<sup>108, 109</sup> Gels presented here (**Figure 3.1**) were equally adjusted for brightness and contrast. Grouping of gels was performed, they are delineated with spacing as shown in **Figure 3.1**.

**Figure 3.1. Validation of murine primary peritoneal mesothelial cells (MPPMC). (A) Representative morphology of MPPMC cultures collected from young (top panels) or aged (lower panels) mice shown at day 1, 2, and 4, as indicated (100X magnification). (B) Immuno-fluorescent staining of MPPMCs using anti-vimentin antibody (1:100 dilution) in 3% BSA for 1h at 37°C, followed by Alexa-Fluor conjugated secondary antibody (1:300) for 30 minutes at 37°C. Slides were mounted with VECTASHIELD Mounting Media with DAPI. (C) Immunofluorescent staining of MPPMC using anti-cytokeratin-18 antibody (1:100 dilution) in 3% BSA for 1h at 37°C, followed by processing as in (B). (DandE) Western blots of MPPMC and LP9 (human mesothelial cell line) cell lysates (10 ug protein). Lysates were electrophoresed on 9% SDS-PAGE and electroblotted to Immobilon membranes. After blocking with 5% milk/TBST, blots were probed with antibodies directed against (D) vimentin (1:1000 dilution) or (E) cytokeratin-18 (1:500 dilution), washed and incubated with horseradish peroxidase-conjugated secondary antibodies (1:4000) for 1 hour at room temperature. Blots were developed using Super Signal West Dura Extended Duration Substrate (Thermo) and visualized using ChemiDoc™ Imaging.**



### 3.2.5 MPPMC Proteomic Analysis

For each cohort, pooled lysates were denatured, reduced and alkylated with iodoacetamide and digested using S-Traps following manufacturers recommendations.<sup>107</sup> Samples were analyzed in technical triplicate per pooled cohort for a total of 12 analyses. Digested samples were analyzed at the University of Notre Dame Mass Spectrometry core facility. Bottom-up proteomics experiments were conducted with a Thermo-Finnegan Q-Exactive (QEHF) mass spectrometer coupled to a Waters MClass ultrahigh pressure liquid chromatography system via a nanoelectrospray ionization source. Tryptic peptides were harvested from S-Trap columns and the solvent was removed by evaporation. The peptides were re-dissolved in solvent A (0.1% formic acid in water, Burdick and Jackson, MI). The volume was adjusted according to the original protein content to normalize the sample concentration. A sample containing tryptic peptides (1 µg/ul) was eluted from an Acquity BEH C18 column, 1.7-µm particle size, 300 Å (Waters) column (100 µm inner diameter × 100 mm long) using a 100-min gradient at a flow rate of 0.9 µL/min [4–33% organic solvent B (0.1% formic acid in acetonitrile), Burdick and Jackson] for 90 min, 33–80% B for 2 min, constant at 80% B for 6 min, and then 80–0% B for 2 min to re-equilibrate the column. Data were collected in positive ionization mode. Mass spectra were acquired in the Orbitrap using a TOP17 Data Dependent Acquisition (DDA) method with 60k resolving power and tandem mass spectra were then generated for the top seventeen most abundant ions with charge states  $z = 2-5$  inclusive. Fragmentation of selected peptide ions was achieved via higher energy collisional dissociation (HCD) at normalized collision energy of 28 eV in the HCD cell of the QEHF.

### 3.2.6 Database Analysis

PEAKS Online software (Bioinformatics Solutions Inc.) filtered to a 1% false discovery rate (FDR) was used to identify proteins present in each sample by matching tandem mass spectra with peptides expected for proteins from the Uniprot mus (mouse) database and common contaminants (Approximately 56,000 entries). Fixed modification of Carbamidomethylation (C) and variable modification of deamidation (NQ) phosphorylation (STY), oxidation (M) and pyroglutamic formation (QE) were considered as possible post-translational modifications. The study utilized the PEAKS Label Free Quantitation to make pairwise comparisons, “Female Young vs. Female Aged”, “Female Young vs. Male Young”, “Male Aged vs. Female Aged”, and “Male Young vs. Male Aged.” From each comparison, proteins differentially expressed (>2-fold) with high significance (ANOVA,  $-\log_{10} P \text{ value} > 10^{-1.3}$ , 95% CI) were selected. Venn diagrams were generated using the online tools from UGent Bioinformatics and Evolutionary Genomics.<sup>110</sup> Gene ontology enrichment analysis was performed on those proteins for their biological processes using the ShinyGO online software (FDR cutoff  $\alpha=0.05$ , Pathway size 2-2000).<sup>111</sup>

## 3.3 Results and Discussion

### 3.3.1 Primary Cell Culture

This study presents a reproducible method for isolation and short-term primary culture of peritoneal MC from young and aged mice [**Figure 3.1A**]. A unique aspect of



MC is that they display both epithelial and mesenchymal characteristics. Analysis of MPPMC using immunocytochemistry shows that all DAPI-positive nuclei are associated with positive staining for cytokeratin 18 and vimentin [**Figure 3.1B**], indicating the lack of potentially contaminating macrophages or fibroblasts (cytokeratin 18 negative).<sup>89</sup> Expression was confirmed by western blotting [**Figure 3.1C**].<sup>88-90</sup> One observation is that MPPMC from young mice generally grow and divide faster than those from old mice. Our results also show that young primary cells survive longer relative to cells obtained from old animals (> 1 month *vs* ~3 weeks, respectively, *data not shown*). As observed with many normal (i.e., non-malignant) primary cultures, cells at both ages proliferate better when in close cell:cell contact with neighboring cells. Little detachment, cell death, or crowding of the plate was observed in the first 3 weeks in culture. These primary cell cultures represent an *in vitro* model to enable examination of the impact of host sex and/or age on the interaction between the mesothelium and foreign materials such as asbestos fibers or other cell types including bacteria and metastatic cancer cells with less confounding factors relative to *in vivo* experiments.

### 3.3.2 MPPMC Proteomics Overview

MPPMC lysates from unpassaged day 4 primary cultures were concentrated and trypsin digested using S-Traps. Bottom-up proteomic analyses were then performed as described in order to compare expressed proteins in the four experimental groups: Female Young (FY), Female Aged (FA), Male Young (MY) and Male Aged (MA). Each cohort, FA, FY, MA, MY, contains a total of 2721, 1982, 2484, 2364 proteins and 899, 662, 816, 805 protein groups respectively. FA, FY, MA, MY, have 379, 58, 202, 423 proteins and

150, 17, 66, 137 protein groups [**Figure 3.2 and Table 3.1**] unique to their individual group, respectively. This represents proteins identified with at least one peptide-sequence-match with a false discovery rate of 1%. Detailed protein information is found in **Supplemental Tables 1-4** and has been uploaded to MassIVE as indicated in data availability. Gene Ontology enrichment analysis was performed separately on the highly significant proteins as determined by ANOVA in PEAKS, filtered to include those unique to each group [**Figure 3.3A-D**]. In the males, a majority of proteins specific to MA are involved in protein/large molecule transportation and localization. The rest of MA and a majority of MY proteins are involved in translation and a variety of metabolic processes. On the other hand, the proteins specific to FA are mostly involved in multiple metabolic pathways. The number of unique proteins in FY is too small for informative analysis.

For each pairwise comparison (primary comparisons), the PEAKS Label Free Quantitation uses one of the groups as the “base” and measures the fold change and significance ( $-10\log_{10}(p\text{-value})$ ) of each protein from another group as compared to the “base”. The results are collected in Venn diagrams and volcano plots [**Figure 3.4A-D**] representing proteins up- (blue) or down- (yellow) regulated as compared to the “base”. All proteins having 64-fold-change or more,

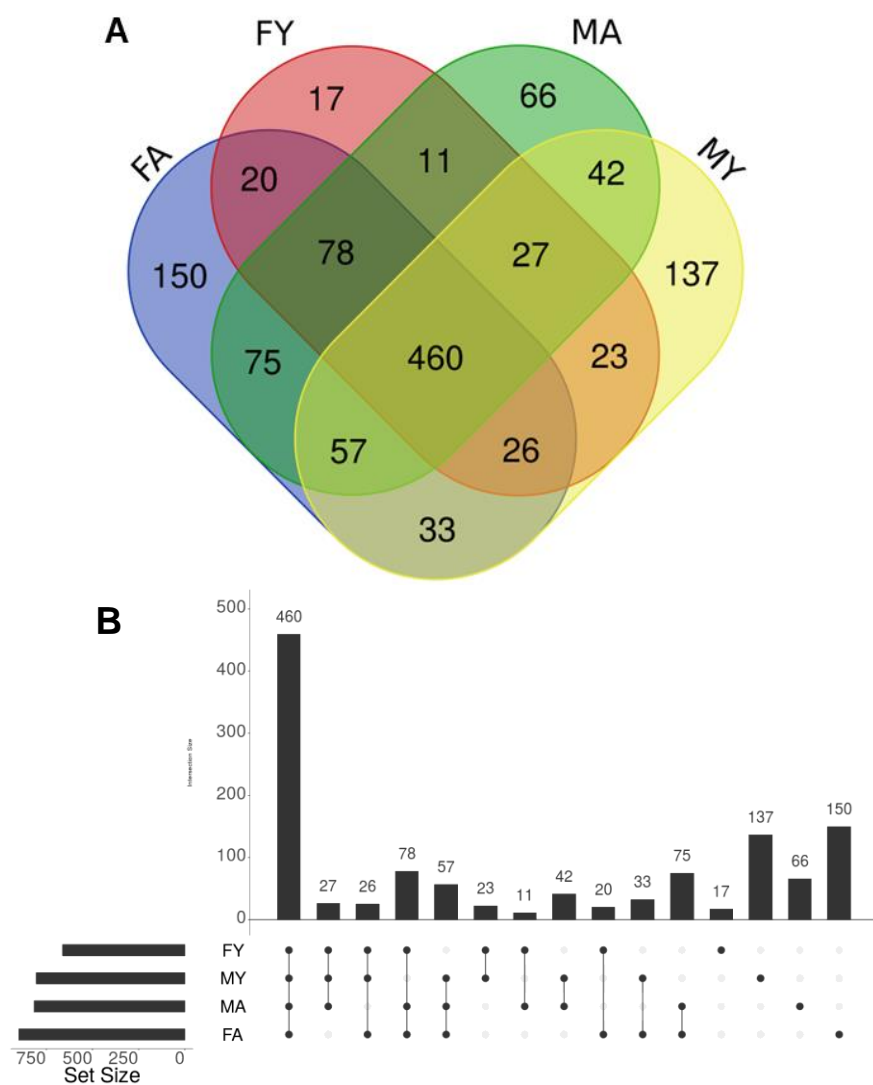


**Figure 3.2 Overview of proteomic data.** (A) A Venn diagram showing common/unique protein groups between cohorts FA, FY, MA, and MY, having 150, 17, 66, 137 protein groups unique to their individual group, respectively. (B) An upset plot (UpSetR Shiny App) comparing the protein groups identified from the 4 cohorts.<sup>112</sup>

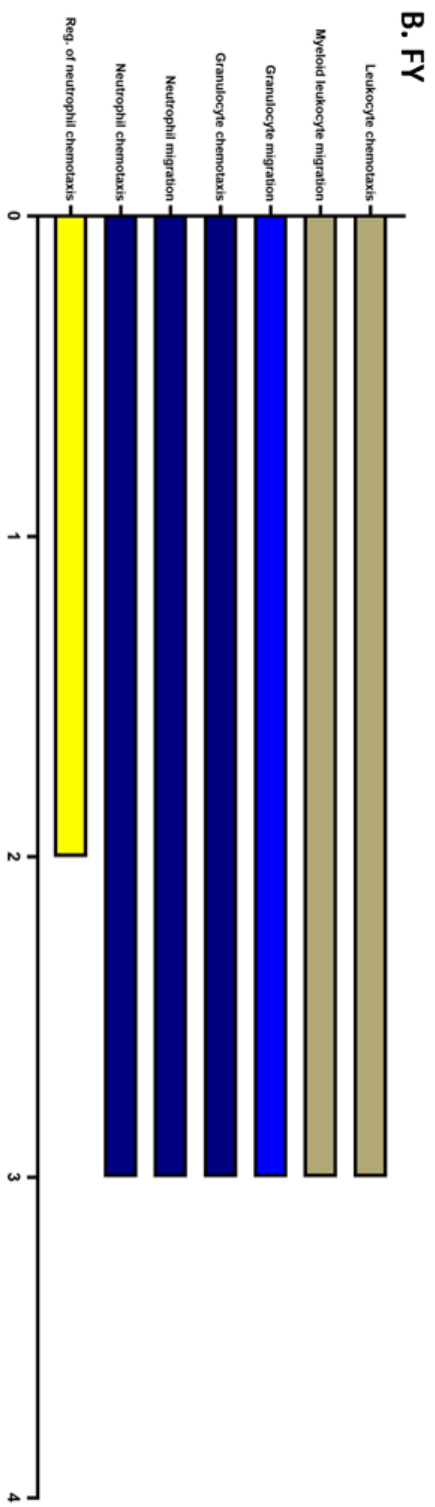
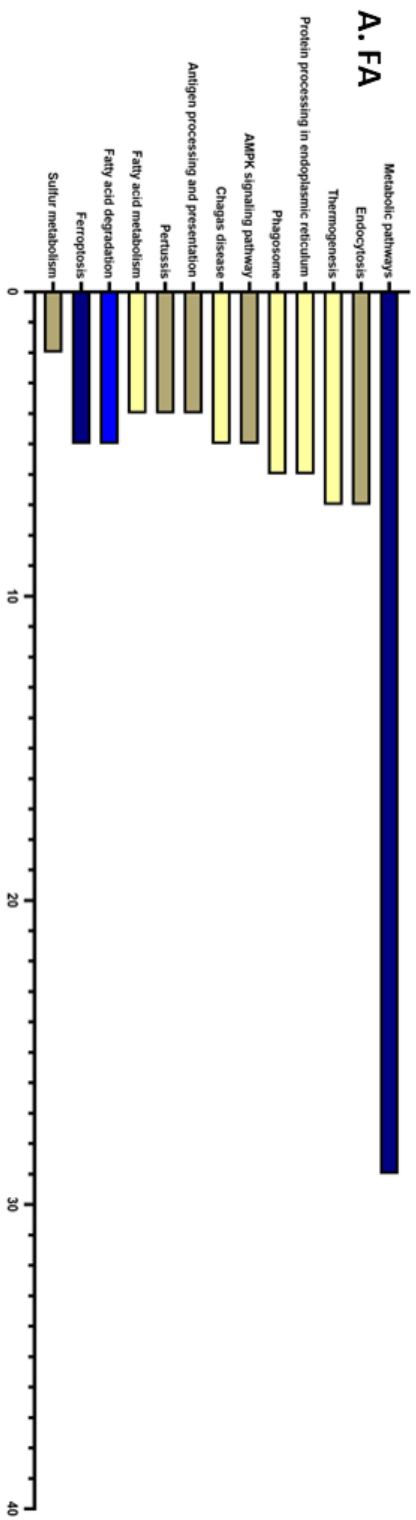
TABLE 3.1

## MS RESULTS FOR THE 4 COHORTS

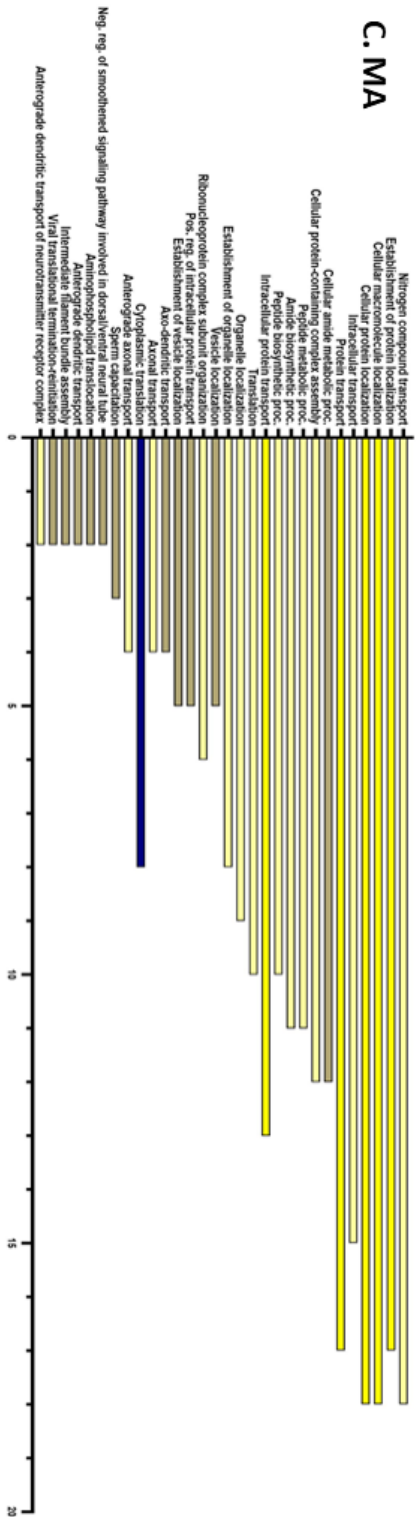
Sample Name	Run	MS1	MS2	PSM	Peptides	Proteins	Protein Groups
All (4 samples)	12	189219	184794	24531	5137	3697	1215
Female Aged (FA)	3	45878	49256	7278	3256	2721	899
Female Young (FY)	3	48673	42087	4681	2162	1982	662
Male Aged (MA)	3	45286	50454	7330	3233	2484	816
Male Young (MY)	3	49400	42997	5242	2594	2364	805

including ‘infinity’, are binned on the left and right margins of each plot. In each of the primary pairwise comparisons, the list of proteins with high fold-change and significance (blue and yellow) are extracted. Gene Ontology enrichment analysis showing the biological processes prevalent in each list of proteins was also performed [Figure 3.5]. The 4 lists of proteins/biological processes generated from primary comparisons were then subjected to 2 secondary comparisons. In comparison A [Figure 3.5A], “FA vs. MA”, gender specific differences in aged mice, was compared to “FY vs. MY”, gender specific differences in young mice. Their common biological processes indicate gender specific differences in all ages. In comparison B [Figure 3.5B], “FA vs. FY”, aging specific differences in female mice, is compared to “MA vs. MY”, aging specific differences in male mice. Their common biological processes indicate aging specific differences in all sexes. Comparison A shows that male and female MPPMCs are different in their protein translation and

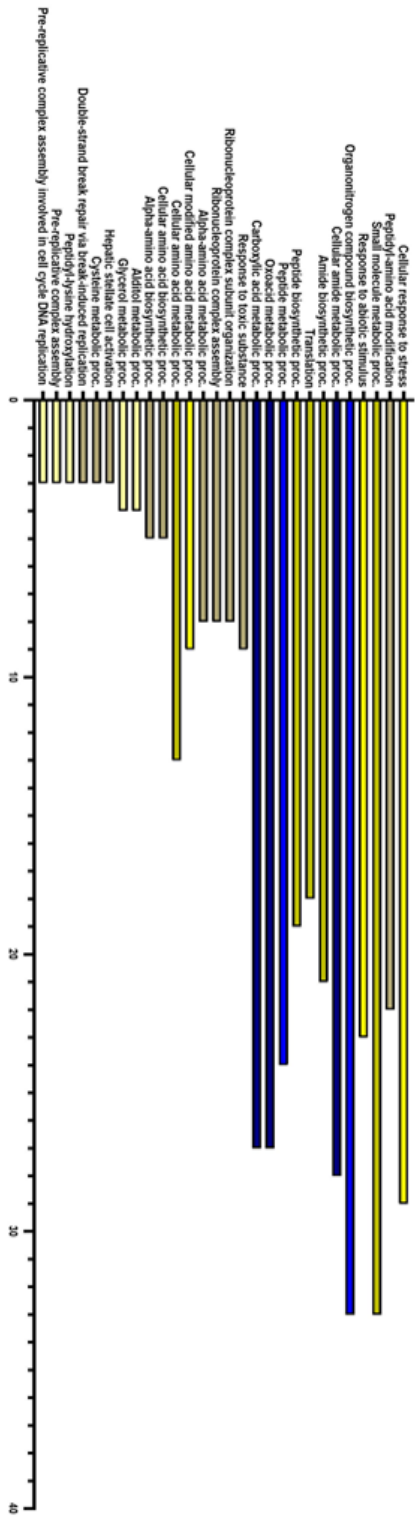
**Figure 3.3. Gene Ontology Enrichment (GOE) analysis on proteins exclusively to each cohort showing their corresponding biological processes. Results show histograms listing biological processes that proteins unique to (A) FA, aged female; (B) FY, young female; (C) MA, aged male; (D) MY, young male; are involved. The number of genes involved in each process is shown on the x-axis. Fold enrichment increases from top to bottom.  $-\log_{10}(\text{FDR})$  increases from yellow to blue.**



## C. MA



## D. MY



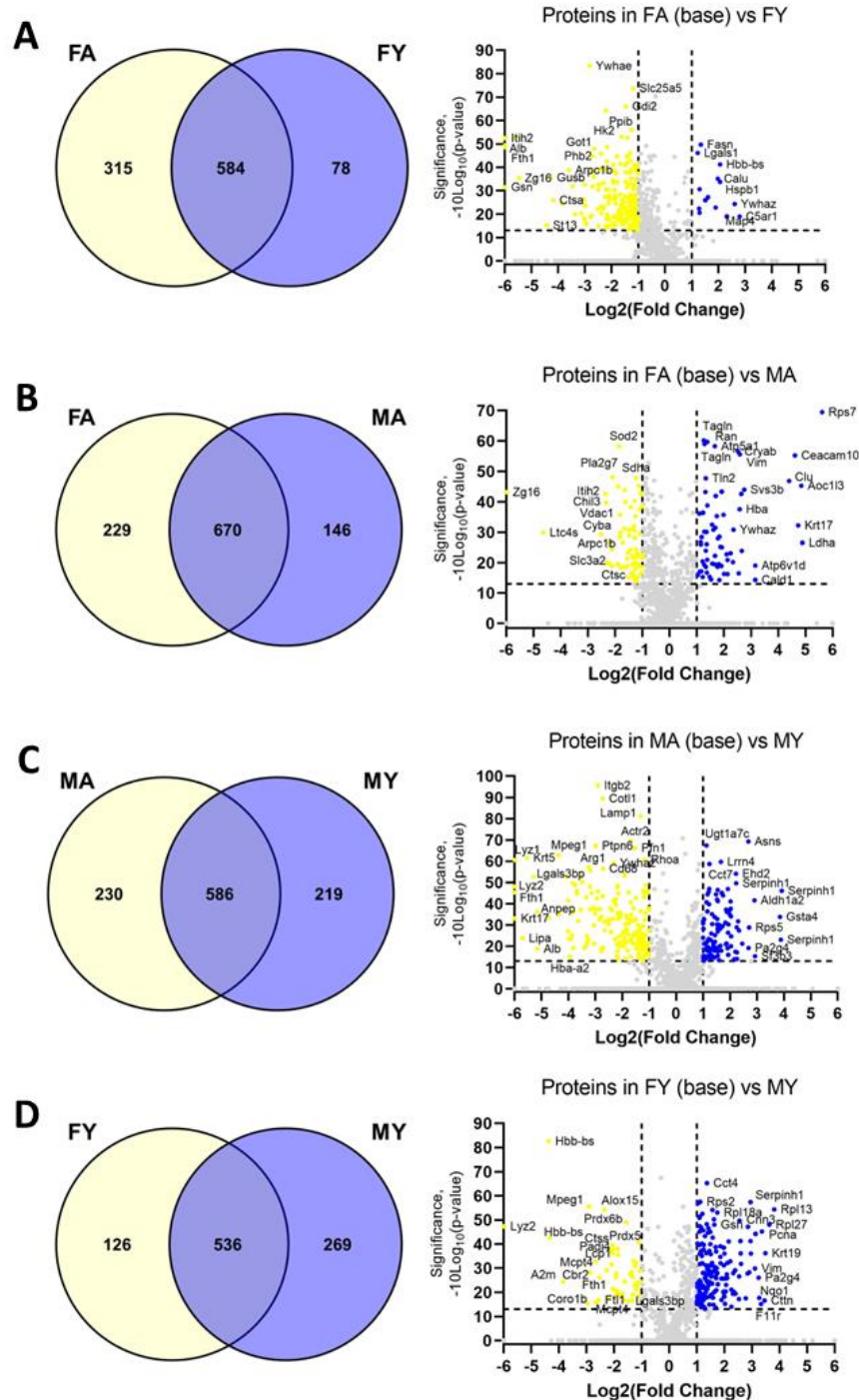


**Figure 3.4. Pairwise comparisons between gender- and age-cohorts. (A) FA vs. FY, (B) FA vs. MA, (C) MA vs. MY, (D) FY vs. MY. (Left Panels) Common and unique proteins are shown as Venn diagrams. (Right Panels) Volcano plots present proteins significantly ( $-10\log_{10}(p\text{-value}) > 13$ ) up-/down- regulated ( $\log_2(\text{fold change}) > 1$ ). Proteins up-regulated when compared to the “base” are in blue, while those down-regulated are in yellow. The gene names for proteins with high significance and fold change are annotated.**



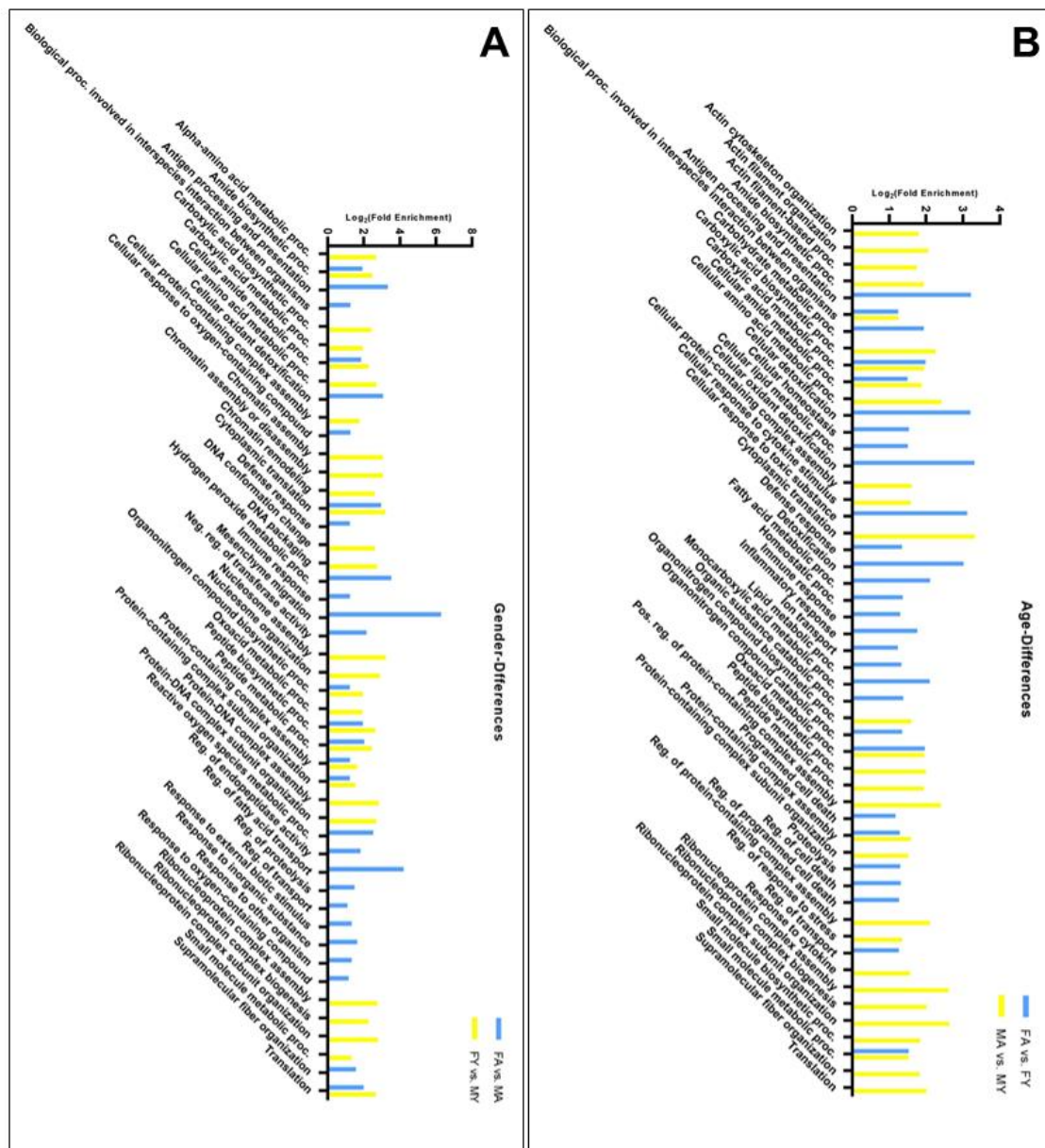
peptide metabolism pathways. Comparison B indicates that the aged and young mesothelial cells have distinct metabolic processes. Interestingly, such results have a good correlation to the gene ontology enrichment analysis on the unique proteins in each cohort [Figure 3.3].

### **3.3.3 MPPMC proteomics revealed protein of interests which potentially regulate CRC peritoneal metastatic success.**

Our results identified differentially expressed proteins previously associated with peritoneal diseases including YWHAZ (tyrosine 3-monooxygenase/tryptophan 5-monooxygenase activation protein zeta), GSN (gelsolin), VIM (vimentin), and LGALS3BP (galectin 3 binding protein). It has been demonstrated that mesothelial cells treated with the secretome from malignant mesothelioma cultures decrease expression of YWHAZ and increase LGALS3BP levels.<sup>113</sup> In another study, YWHAZ, GSN, VIM were enriched in the mesothelium in a rat model of chronic peritoneal dialysis.<sup>114</sup> YWHAZ affects many vital cellular processes, including but not limited to metabolism, signaling, apoptosis, and cell cycle regulation.<sup>115</sup> Newly characterized miRNAs, miR-1-3P and miR-22, have been identified to target YWHAZ and inhibit metastasis of colorectal cancer and hepatocellular carcinoma respectively.<sup>116, 117</sup> YWHAZ also modulates glycolysis and promotes ovarian cancer metastasis.<sup>115</sup> YWHAZ is up regulated in FY and MA when both compared to FA and in MA compared to MY. Future studies may address the role of YWHAZ in cancer peritoneal metastasis, particularly in the MA host.

GSN is a multifunctional actin-binding protein and a substrate for extracellular matrix modulating enzymes.<sup>118, 119</sup> Outside the cell, GSN also play a role in the presentation

**Figure 3.5. Secondary comparisons between the pairwise (primary) comparisons from Figure 3.4. Comparisons use only proteins with high significance ( $-10\log_{10}(p\text{-value}) > 13$ ) and fold change ( $\log_2(\text{fold change}) > 1$ ) as shown in Figure 3.4. Gene Ontology Enrichment analysis was performed on each of the 4 primary comparisons. The results are shown as histograms. Each character on the x-axis represents one biological process. The y-axis indicates  $\log_2(\text{Fold Enrichment})$ . (A) Comparison ①, FA vs. MA (blue) is compared to FY vs. MY (yellow); (B) Comparison ②, FA vs. FY (blue) is compared to MA vs. MY (yellow). Any character that has both a blue and yellow bin represents a common biological process shared by the 2 groups.**



of lysophosphatidic acid and other inflammatory mediators to their receptors.<sup>118, 119</sup> Many patients with renal diseases require constant automated peritoneal dialysis. It was discovered that their effluent after each peritoneal dialysis have simultaneous decrease in GSN levels, representing the presence of chronic inflammation. GSN interacts with MMP14 to enhance the activation of MMP2, thereby promoting the invasion and metastasis of hepatocellular carcinoma.<sup>15</sup> In contrast, GSN is also shown to have a tumor invasion suppressor role in colon cancer.<sup>120</sup> In this study, both FA and MY express more GSN than FY.

VIM is a mesenchymal protein and widely accepted as a biomarker for epithelial–mesenchymal transition.<sup>121</sup> It maintains cytoskeleton organization and focal adhesion stability.<sup>122, 123</sup> VIM is up regulated in MA and MY compared to FA and FY respectively, a clear gender difference that may account for many gender-specific phenotypes in cancer peritoneal metastasis. LGALS3BP is down regulated in MY when compared to MA and FY. LGALS3BP is a large oligomeric protein originally identified as a tumor-secreted antigen<sup>124, 125</sup> associated with inflammatory processes.<sup>126</sup> The majority of LGALS3BP proteins are heavily glycosylated and secreted to interact with the extracellular matrix.<sup>127</sup> It is associated with an IFN-induced signaling scaffold during viral infection, as well as certain bacterial proteins within infected cells.<sup>127-129</sup> Low expression of LGALS3BP implicates malignant progression and poor prognosis of colorectal cancer patients.<sup>130</sup> Similar results have been found in Ewing’s sarcoma. Patients with tumors expressing high levels of LGALS3BP display a lower risk of developing metastasis and dying.<sup>124</sup> Cancer cells overexpressing LGALS3BP were unable to form metastasis when injected into mice.<sup>124</sup>

Additional proteins identified as exclusively expressed in the MA cohort have not previously been associated with CRC peritoneal metastasis. The 202 proteins exclusively expressed in MA, the cohort with the most tumor burden (**Aim 1**), were examined for potential candidates that may contribute to metastasis success. Proteins were scored according to certain characteristics: 1) membrane proteins that regulate cell:cell adhesion or migration; 2) proteins that are involved in cell signaling; 3) proteins that have been shown to promote cell proliferation; 4) onco-proteins that have been reported as elevated in cancer tissue. From this analysis, three proteins of interests are: CD166, CLU, and Prl-1.

Activated leukocyte cell adhesion molecule (CD166) is a cell surface glycoprotein involved in homotypic and heterotypic cell adhesion.<sup>131</sup> Besides cell adhesion, other ALCAM functions have been described such as angiogenesis, transmigration of monocytes, leukocyte intravasation across blood brain barrier, T cell activation, hematopoiesis, neurite extension, osteogenesis, and embryonic implantation in the uterus.<sup>131-133</sup> CD166 has been reported to be increased in various cancers, such as those of the thyroid, head and neck, lungs, and liver.<sup>134</sup> It has been shown in both ovarian and colorectal cancer, CD166 is capable of mediating the binding and subsequent uptake of cancer derived extracellular vesicles (EV) through homophilic or heterophilic interactions. Interestingly, such interaction can happen no matter whether it's the cells or the EVs which are carrying CD166 on their surface.<sup>135</sup>

Clusterin (CLU) is a highly conserved glycoprotein participates in a series of biological processes, including cell adhesion and programmed cell death.<sup>136, 137</sup> It also exists in exosomes and helps cancer cells to metastasize.<sup>136, 138</sup> Clusterin levels are

positively correlated with the degree of invasiveness and Clusterin regulated EMT through modulating ERK signaling and slug expression.<sup>139</sup> Its overexpression has been observed in many cancer types including but not limited to gastric, ovarian, breast, and colorectal cancer.<sup>140</sup> However, other studies have suggested that CLU can also have tumor suppressor activity in prostate, lung, and oral cancers, and low expression of CLU may be associated with worse prognosis and genetic instability.<sup>141</sup>

Prl-1 is one of the members of the family phosphatases of regenerating liver. Prl-1 has been identified as a critical factor in various cancers, including lung, ovarian, and colon cancers. Prl-1 has 2 forms, one as nuclear protein and the other as membrane protein. Initially characterized as a nuclear protein regulating cell growth, Prl-1 is known to influence cell proliferation and differentiation in a tissue-specific manner. The protein undergoes prenylation, facilitating its transport to membrane structures and impacting cell growth and migration through pathways involving proteins such as extracellular signal-regulated kinase 1/2 (ERK1/2), proto-oncogene c-Src (src), and RhoA-GTPase activities, thereby regulating signal transduction pathways, cell proliferation, and actin dynamics.<sup>142</sup>

### **3.4 Conclusion**

To our knowledge, this represents the first sex- and age-based comparison of the primary murine mesothelial cell proteome. The study provides valuable baseline information for a wide range of future studies on the role and function of peritoneal mesothelial cells in health and disease at two important physiologic age points. The very next step would be to analyze the function of candidate proteins to unveil their roles in colorectal cancer peritoneal metastasis. These proteins are potential targets for specialized

or even personalized treatments to prevent CRC from entering late stages. Future studies could compare the current data using healthy MPPMC to cells obtained from disease-bearing models to facilitate the understanding of key mesothelial cell components in peritonitis, mesothelioma, and cancer intra-peritoneal metastasis. Importantly, segregation of the data by both sex and age could reveal novel contributory factors to specific disease states involving the peritoneal cavity.

A limitation of this study design is the lack of extracellular matrix and secreted proteins in the samples analyzed. In addition, the mesothelial microenvironment *in vivo* is not only comprised solely of mesothelial cells. The collagen coating on the culture dishes used for plating of primary cell cultures does not completely mimic the more complex collagen matrix in live animals. Moreover, our lab recently demonstrated changes in sub-mesothelial collagen ultrastructure in aged mice relative to young using second harmonic generation and scanning electron microscopy.<sup>106</sup> Fibroblasts and immune cells are also not represented in the primary culture system, but could impact the mesothelial cell proteome *in vivo* due to signaling induced by soluble factors or cell:cell interactions. Future studies incorporating other aspects of the *in vivo* mesothelial cell microenvironment will generate a more complete portrait of the mesothelial proteome.

### **3.5 Associated data**

Raw and processed data are available through the MassIVE data exchange and cross-posted to ProteomeExchange. MSV000092134  
<ftp://MSV000092134@massive.ucsd.edu> (For Review) Password: MouseAge2302\*  
<https://massive.ucsd.edu/ProteoSAFe/static/massive.jsp>

CHAPTER 4.

COMPREHENSIVE ANALYSIS OF PRL-1 IN COLORECTAL CANCER  
METASTASIS USING IN VITRO AND EX VIVO MODEL

**4.1 Abstract**

This study investigates the role of protein tyrosine phosphatase type IVA 1 (Prl-1) in colorectal cancer (CRC) intraperitoneal (i.p.) metastasis, specifically exploring whether Prl-1 expressed in mouse primary peritoneal mesothelial cells (MPPMCs) from aged male mice promotes CRC metastasis via aiding their initial adhesion. Furthermore, the research aims to elucidate the pathways and proteins involved in this process. Prl-1, a membrane-associated phosphatase, has been identified as a critical factor in various cancers, including lung, ovarian, and colon cancers. Initially characterized as a nuclear protein regulating cell growth, Prl-1 is known to influence cell proliferation and differentiation in a tissue-specific manner. The protein undergoes prenylation, facilitating its transport to membrane structures and impacting cell growth and migration through pathways involving proteins such as extracellular signal-regulated kinases 1/2 (ERK1/2), proto-oncogene c-Src (src), and RhoA-GTPase activities.

The study emphasizes the interactions between Prl-1 and various signaling pathways. Disruption of Prl-1 trimerization has been identified as a promising therapeutic



strategy, with Prl-1 inhibitors like CMPD-43 demonstrating potent anticancer activity by inhibiting Prl-1-induced cell adhesion and metastasis. Four pathways have been implicated in Prl-1 pro-metastatic functions: 1) Rho family GTPases and N-cadherin; 2) kinase activation of src and the focal adhesion complexes; 3) ERK1/2 and matrix metalloproteinase (MMPs); and 4) the stabilization of Snail2 through USP36, highlighting the complexity of the network of interactions mediated by Prl-1.

Key experimental approaches include cell viability assays using MTS, *in vitro* and *ex vivo* adhesion assays, and western blot analyses. These methods were employed to assess the cytotoxicity of CMPD-43, its effect on cell adhesion, and the expression and activation levels of signaling proteins such as FAK, p130cas, and RhoA. The results demonstrate that CMPD-43 exhibits selective cytotoxicity towards cancer cells, significantly reduces cell adhesion at higher concentrations, and decreases the levels of active signaling proteins involved in focal adhesion and cell migration. A decrease in RhoA activity supports the conclusion that Prl-1 facilitates cell-cell adhesion via the Prl1-RhoA-Ncad pathway. Notably, the study found that inhibiting Prl-1 also reduces the total levels of FAK and p130cas, suggesting an impact on cell-cell matrix adhesion.

The findings provide valuable insights into the role of Prl-1 in cancer metastasis, highlighting its potential as a therapeutic target. By disrupting key interactions and signaling pathways, Prl-1 inhibitors like CMPD-43 could impede the progression and metastatic spread of colorectal cancer, offering new avenues for treatments.

## 4.2 Prl-1 and CMPD-43, a prl-1 inhibitor

Prl-1, a membrane-associated protein tyrosine phosphatase, has been identified as a significant factor in various cancers, including lung, ovarian, and colon cancers.<sup>143</sup> It was first discovered as a nucleus protein which regulates cell growth and was shown overexpressed in a number of tumor cell lines.<sup>144</sup> Further investigation has suggested it regulates cell proliferation and differentiation in a tissue specific manner.<sup>145</sup> Interestingly, this protein can also undergo prenylation, which facilitates its transport to membranes structures such as the ER and the cell surface membrane.<sup>146, 147</sup> Initial studies indicated that Prl-1 is expressed at high levels in growing rat hepatic cells, rat intestinal epithelia, and some tumor cell lines, suggesting it could modulate cell growth or differentiation in a tissue-dependent manner.<sup>144-147</sup> Its expression is induced by the Egr-1 transcription factor during liver regeneration and in mitogen-activated cells.<sup>146, 148</sup> Prl-1 mRNA is widely expressed in normal adult human tissues, although levels vary among different tissues.<sup>146,</sup>

149

In colorectal cancer cells, GINS2 has been shown to promote the expression of Prl-1, a novel p53 target. GINS2 is a newly discovered oncogene that is overexpressed in several cancers. The Go-Ichi-Ni-San (GINS) family, including four subunits (GINS1–4), has a specific function in DNA replication and cell cycle, and plays a vital role in the development of chromosome and DNA replication forks.<sup>150-152</sup> Lowering GINS2 levels increases p53 protein levels, while overexpressing Prl-1 decreases them. Notably, Prl-1 overexpression can partially counteract the effects of GINS2 downregulation in colon cancer cells, indicating a complex interaction between these proteins.<sup>153</sup>

A significant development in targeting Prl-1 for cancer therapy involves disrupting its trimerization. Using structure-based virtual screening and medicinal chemistry, researchers have identified compounds such as Cmpd-43 that disrupt Prl-1 trimerization.<sup>154</sup> These compounds inhibit Prl-1-induced cell proliferation and migration by attenuating ERK1/2 and Akt activity. They have demonstrated potent anticancer activity in both *in vitro* and *in vivo* models, supporting the concept of trimerization inhibitors as potential treatments for Prl-driven cancers. CMPD-43 selectively suppressed the growth of MCF7 breast cancer cells while showing lower toxicity toward non-tumorigenic MCF10A cells, highlighting its potential as a therapeutic agent with minimal side effects on normal cells.<sup>154-156</sup> Thanks to Dr Bai's (Purdue University) generosity, we are able to receive from him a plentiful quantity of CMPD-43 for our research.

#### **4.2.1 Prl-1 related pathways**

Prl-1 plays a role in promoting cancer cell progression, migration, and metastasis by interacting with several cellular pathways [Figure 4.1]. It enhances cancer cell proliferation and epithelial-mesenchymal transition via the PI3K/AKT pathway.<sup>157, 158</sup> Additionally, Prl-1 regulates Rho family GTPases to promote invasion and motility, highlighting its role in cancer progression.<sup>159</sup> More specifically, it activates both the ERK1/2 and RhoA signaling pathways, contributing to cell growth and migration.<sup>155</sup> Recent research identified a Prl-1-binding peptide (Peptide 1) with high sequence identity to a conserved motif in the src homology 3 (SH3) domain of p115 Rho GTPase-activating protein (GAP). p115 RhoGAP directly binds Prl-1 *in vitro* and in cells via its SH3 domain.<sup>155</sup> Structural analyses of the Prl-1 Peptide 1 complex revealed a novel protein-

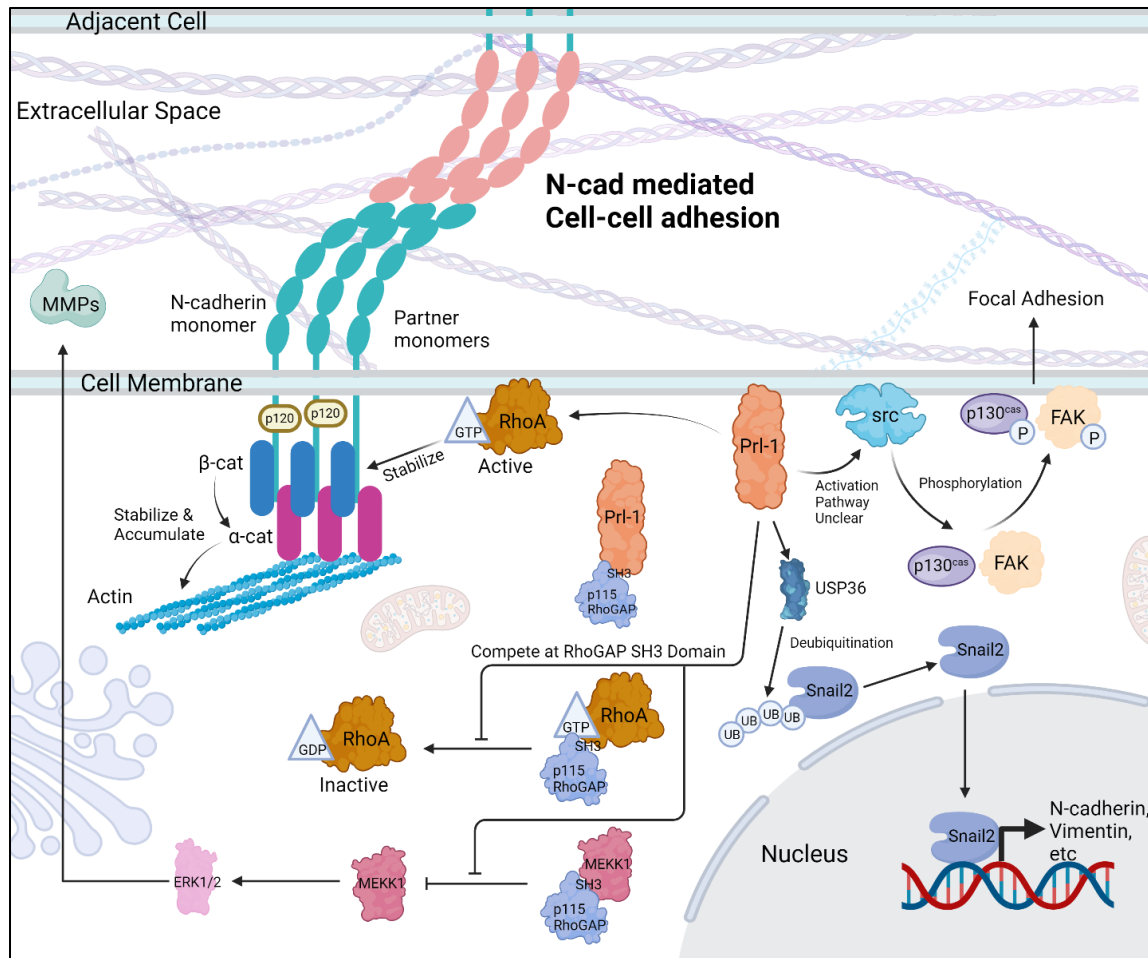


**Figure 4.1. Prl-1 is involved in complex cellular signaling pathways which could potentially affect cancerous:mesothelial cell interactions. Prl-1 binds to the src homology 3 (SH3) domain of p115 Rho GTPase-activating protein (GAP). p115 RhoGAP directly binds Prl-1 in vitro and in cells via its SH3 domain, competitively prevents the canonical binding between the SH3 domain of p115 RhoGAP to RhoA and MEKK1, leading to their activation. The extracellular domains of N-cadherin monomers engage in trans and cis interactions with partner monomers, facilitated by p120-catenin (p120), resulting in a lattice-like arrangement. Activation of RhoA keeps the β-catenin (β-cat) in place and leads to the accumulation of α-catenin (α-cat) at the N-cadherin intracellular domain. This promotes the anchorage of the N-cadherin-catenin complex to the actin cytoskeleton through actin-binding proteins, thereby stabilizing cell-cell contacts. Active MEKK1 further activates ERK1/2 which promotes the expression of matrix metalloproteases (MMPs). Additionally, Prl-1 stabilizes Snail2 by activating ubiquitin specific peptidase 36 (USP36). Snail2 activates the expression of multiple proteins including N-cadherin. Moreover, Prl1 activates the Src kinase through increased Tyr416 phosphorylation. Src selectively phosphorylates and activates focal adhesion kinase (FAK). Src and FAK also phosphorylate and activate p130cas (Crk-associated substrate). Both p-FAK and p-p130cas promote focal adhesion.**

protein interaction whereby a sequence motif within the PxxP ligand-binding site of the p115 RhoGAP SH3 domain occupies a folded groove within Prl-1.<sup>155</sup> This interaction prevents the canonical binding between the SH3 domain of p115 RhoGAP to RhoA and MEKK1, leading to the activation of RhoA and ERK1/2, respectively, signaling by inhibiting the catalytic activity of p115 RhoGAP.<sup>155</sup>

RhoA plays an important role in regulation of cell:cell junctional integrity [Figure 4.1]. The extracellular domains of N-cadherin monomers engage in trans and cis interactions with partner monomers, facilitated by p120-catenin (p120), resulting in a lattice-like arrangement. Activation of RhoA keeps the  $\beta$ -catenin ( $\beta$ -cat) in place and leads to the accumulation of  $\alpha$ -catenin ( $\alpha$ -cat) at the N-cadherin intracellular domain.<sup>160</sup> This promotes the anchorage of the N-cadherin-catenin complex to the actin cytoskeleton through actin-binding proteins, thereby stabilizing cell-cell contacts. Initial ligation of N-cadherin extracellular domains also triggers PI3K/Akt signaling.<sup>160</sup> Furthermore, Prl-1 also activates ERK1/2 which upregulates MMP2 and MMP9 through transcription factors AP1 and Sp1, providing a potential mechanism whereby Prl-1 may regulate tumor invasion.<sup>161</sup>

Additionally, Prl-1 stabilizes Snail2 by activating ubiquitin specific peptidase 36 (USP36), identifying snail family transcriptional repressor 2 (Snail2) as a crucial mediator of Prl-1's oncogenic effects in glioblastoma (GBM) pathogenesis [Figure 4.1]. Snail2 regulates the expression of multiple proteins including N-cadherin. This suggests that Prl-1 activates USP36-mediated Snail2 deubiquitination, providing a novel mechanism for Prl-1's role in cancer progression.<sup>162</sup> Moreover, Prl1 activates the Src kinase through increased Tyr416 phosphorylation.<sup>161</sup> Src selectively phosphorylate and activates Focal adhesion

kinase (FAK), regulates adhesion dynamics and survival signaling, thus potentially enhances cell migration and anchorage-independent growth.<sup>163</sup> Src and FAK also phosphorylate p130cas (Crk-associated substrate), a protein implicated in cell transformation, adhesion, migration, growth factor stimulation, and cytokine receptor engagement [Figure 4.1].<sup>164</sup>

In summary, Prl-1 is a critical factor in cancer progression and metastasis, affecting various signaling pathways and interacting with key regulatory proteins. Its role in promoting cancer cell growth, migration, and survival makes it a promising target for cancer therapy. The discovery of compounds that can inhibit Prl-1 activity offers new opportunities for therapeutic intervention in Prl-driven cancers. The study proposes further investigation into several signaling pathways potentially influenced by Prl-1, with plans to:

1. **N-cadherin Mediated Pathways:** Evaluate whether the adhesion of MC38 to LP9 cells is N-cadherin (N-cad) dependent using adhesion assays with anti-N-cad antibodies. Western blot analyses will measure changes in N-cadherin levels in response to CMPD-43 treatment. Finally, a RhoA activity assay will measure if CMPD-43 treatment alters the level of active RhoA, thereby regulating N-cad assembly via the Prl1-RhoA-Ncad pathway.
2. **Src-p130cas and FAK Pathway:** Assess the impact of CMPD-43 treated LP9 cells on the phosphorylation levels of p130cas, and FAK. The hypothesis suggests that inhibiting Prl-1 may reduce the phosphorylation levels of both, potentially inhibiting focal adhesion formation.
3. **Erk1/2-MMPs Pathway:** Investigate the total and phosphorylated ERK1/2 levels using western blots with/without CMPD-43 to understand Prl-1's role in extracellular matrix degradation or modification.
4. **USP36-Snail2-Ncad Pathway:** Examine the potential reduction in USP36 and Snail2 levels following CMPD-43 treatment, with a focus on N-cad expression modulation using western blots. A deubiquitination assay could be used to confirm if inhibiting Prl-1 in LP9 cells reduce Snail2 level via polyubiquitination.

## **4.3 Methods and materials**

### **4.3.1 Materials**

LP9 is a commercially available peritoneal mesothelial cell line commonly used to model mesothelial monolayer environments. These cells originate from a human female and have been immortalized for use in cell culture. Our preliminary studies have confirmed that LP9 cells express Prl-1 proteins (data not shown). The compound CMPD-43 was synthesized and generously provided by Dr. Bai from Purdue University. For experimental purposes, rat tail collagen type I and trypsin were procured from Corning. The primary antibodies used in this study include N-cad (Catalog #33-3900, ThermoFisher), p130cas (Catalog #610272, BD, Franklin Lakes, NJ), phospho-p130cas (Y410, Catalog #4011S, Cell Signaling, Danvers, MA), FAK (Catalog #06-543, Millipore, Burlington, MA), and phosphor-FAK (Y397, Catalog #05-1140, Millipore). Additionally, a function-blocking anti-N-cadherin antibody, clone GC-4, was obtained from Sigma-Aldrich, along with anti-mouse and anti-rabbit IgG peroxidase-conjugated secondary antibodies. Peroxidase detection reagents, including SuperSignal West Dura, and Halt™ Protease Inhibitor were sourced from ThermoFisher. The LP9 cell culture media were prepared using Medium 199 (Sigma-Aldrich) and F12 medium (Gibco), supplemented with 15% FBS, 10 ng/mL EGF, 400 ng/mL Hydrocortisone, 1% Penicillin/Streptomycin (Pen/Strep; Lonza), 1% L-GlutMAX (Thermo Fisher Scientific), and 1% HEPES. The CellTiter 96® AQueous Non-Radioactive Cell Proliferation Assay (MTS) was obtained from Promega, Madison, WI. The RhoA G-LISA Activation Assay Kit (Colorimetric format) was purchased from

Cytoskeleton, Denver, CO. MitoTracker™ dyes (red and green) were acquired from Thermo Fisher Scientific.

#### **4.3.2 Animals**

Male C57Bl/6 mice were used for the study, housed at the Freimann Life Science Center. All mice used belong to the male aged (MA) cohort (20-23 months old), equivalent to human ages of about 60-67 years.<sup>53, 101</sup> All procedures involving animals were performed following the ethical guidelines and regulations set by the Institutional Animal Care and Use Committee (IACUC) at the University of Notre Dame, ensuring compliance with institutional and national standards for animal welfare.

#### **4.3.3 Cell Viability Assay**

To evaluate the effects of CMPD-43 on cell viability, the MTS assay (CellTiter 96® AQueous Non-Radioactive Cell Proliferation Assay) was utilized. LP9 mesothelial cells and MC38 colorectal cancer cells were cultured in 96-well plates until they reached confluency. Both cell types were treated with 10  $\mu$ M CMPD-43 for a duration of 6 hours. Following treatment, the cells were washed three times with PBS at room temperature to terminate the exposure. Subsequently, 20  $\mu$ L of the reagent mixture was added to each well containing 100  $\mu$ L of complete media. The plates were incubated at 37°C for one hour to allow the cells to metabolize the compound and release fluorophores. The absorbance was measured at 490 nm using a standard microplate reader to determine cell viability. The assays were performed in biological triplicate. Data were analyzed via ANOVA using GraphPad Prism. Results were combined to one chart for presentation.



#### 4.3.4 In vitro and ex vivo adhesion assays

MC-38-RFP cells were pre-labeled with MitoTracker Red at a concentration of 1 nM for 30 minutes to enhance the fluorescent signal. Mice were euthanized via excessive inhalation of isoflurane. The parietal peritoneum and omentum were then harvested and pinned in a silicone gel-coated 6-well plate. These tissues were incubated with 10  $\mu$ M CMPD-43 in MPPMC culture media for 6 hours. Afterward, the explants were rinsed twice with cold PBS to halt the treatment. The adhesion assay involved seeding 500,000 MC-38-RFP cells per well, followed by a 45-minute incubation period. Adhesion was terminated by PBS wash, 3 min 3 times. The number of adhered cells was quantified under a fluorescent microscope. For the *in vitro* adhesion assay, a similar protocol was followed, using cultured LP9 cells instead of mouse tissue explants. Additionally, adhesion assays were conducted to assess whether the adhesion of MC38 to LP9 cells is dependent on N-cad. This was tested using anti-N-cad antibodies (GC-4) at a concentration of 120  $\mu$ g/mL, with treatment variations including: 1) Both cells treated with Control IgG; 2) LP9 treated with control IgG + MC-38 treated with GC-4; 3) MC-38 treated with Control IgG + LP9 treated with Anti-N-Cad; 4) Both cells treated with GC-4. All assays were performed in biological triplicate. Data were analyzed via t-tests using GraphPad Prism.

#### 4.3.5 Western blots

LP9 cells were grown to confluence before being treated with 10  $\mu$ M CMPD-43 in complete media at various time points: 0, 3h, 6h, 12h, and 24h. At the 6-hour mark, treatments were stopped with two washes of PBS, followed by the replacement of complete media. For Western blot analysis, protein concentrations in cells lysed with mRIPA buffer

containing protease and phosphatase inhibitors were measured using the DC™ Protein Assay (Bio-Rad). Equal amounts of protein (30µg) were separated by electrophoresis on 9% SDS-polyacrylamide gels and transferred onto methanol-activated polyvinylidene fluoride (PVDF) membranes. Membranes were blocked with 5% milk in TBST (150mM NaCl, 25mM Tris, 0.05% Tween 20) for one hour at room temperature to prevent non-specific binding. Primary antibodies against N-cad, p130cas, phospho-p130cas (p-p130cas), FAK, and phospho-FAK (p-FAK) were diluted to 1:500 in 5% BSA/TBST and incubated with the membranes overnight at 4°C. After thorough washing, membranes were incubated with horseradish peroxidase-conjugated secondary antibodies at a 1:2000 dilution for one hour at room temperature. The resulting signals were visualized using chemiluminescence with the ChemiDoc™ Imaging system. All gel images presented in Chapter 4 were adjusted uniformly for brightness and contrast to maintain consistency across experiments. The assays were performed in biological triplicate for confirmation.

#### **4.3.6 RhoA activity assay**

To assess RhoA activity, LP9 cells were cultured to confluence and treated with 10 µM CMPD-43 in complete media for 6 hours. Treatments were terminated by washing the cells twice with PBS. The RhoA G-LISA Activation Assay Kit was utilized for this purpose, with all necessary reagents provided by the kit, except for cell culture media and PBS. Cells were lysed using the lysis buffer supplied in the kit. Protein concentrations in the lysates were determined by mixing 20 µL of each lysate with 1 mL of Precision Red™ Advanced Protein Assay Reagent and measuring the absorbance at 600 nm. Lysates were standardized to equivalent protein concentrations before being frozen and stored. For the assay, cell

lysates were combined with binding buffer and loaded into 96-well binding strips, shaken at 200 rpm for 30 minutes at 4°C. This was followed by incubation with Antigen presenting buffer (2 minutes at room temperature), then with anti-RhoA primary antibody diluted 1/250 (200 rpm shaking for 45 minutes at room temperature), and finally with secondary HRP-labeled antibody diluted 1/62.5 (200 rpm shaking for 45 minutes at room temperature). The HRP detection reagent was added (50 µL each well, 15 min at 37 °C), and the reaction was terminated with the HRP Stop Buffer. Absorbance at 490 nm was measured as an indicator of RhoA activity, providing insights into the regulatory effects of CMPD-43 on the signaling pathway. The assays were performed in biological triplicate. Data were analyzed via t-tests using GraphPad Prism. Results were combined to one chart for presentation.

## **4.4 Results and Discussion**

### **4.4.1 General characterization of CMPD-43 on MC-38 and LP9 cells**

The MTS assay is a method used to assess cell viability and proliferation by measuring the metabolic activity of cells. Since Prl-1 is involved in regulating cell proliferation, inhibiting this protein may potentially halt the cell cycle and trigger apoptosis or even necrosis.<sup>144, 145</sup> Although previous studies by Dr. Bai and colleagues have demonstrated that CMPD-43 exhibits minimal cytotoxicity in normal cells compared to cancer cells, it remains essential to evaluate its effects specifically on MC-38 and LP9 cells.<sup>154, 165</sup> An MTS assay [Figure 4.2a] was conducted to determine the cytotoxic effects of CMPD-43 on these cell lines. The results indicated that CMPD-43 does exhibit a slight cytotoxic effect on both MC-38 and LP9 cells (90% and 85% viability of the controls,

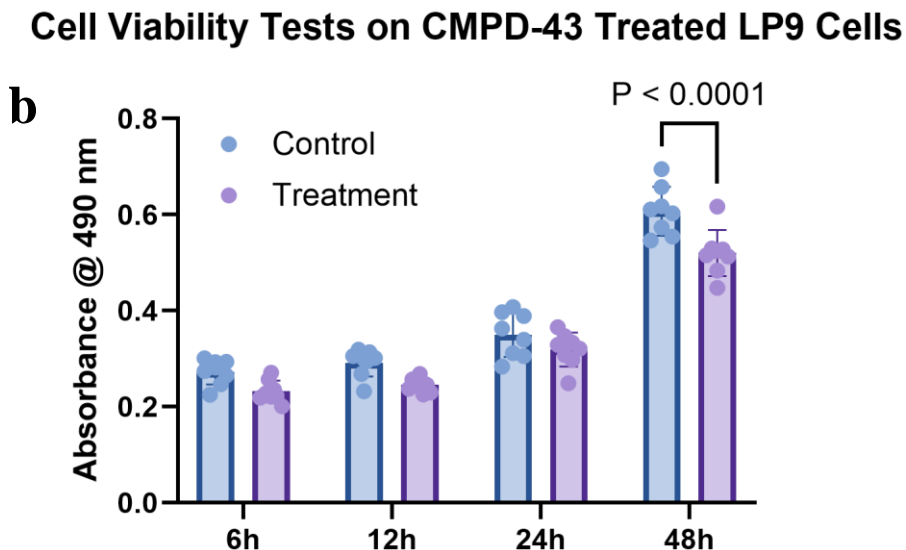
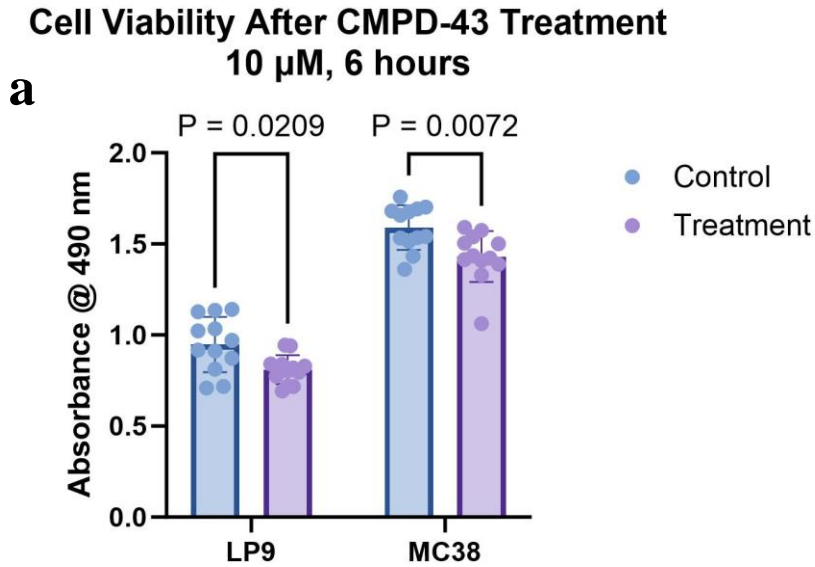
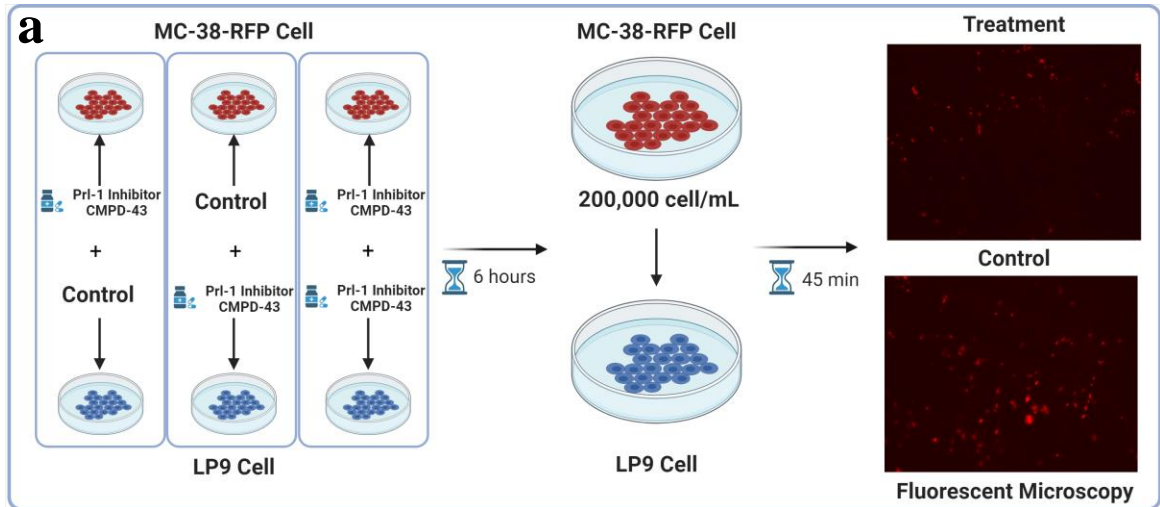


**Figure 4.2** Cell viability tests of LP9 and MC-38 upon CMPD-43 treatments. LP9 and MC38 cells were cultured in 96-well plates until they reached confluency. Both cell types were treated with 10  $\mu$ M CMPD-43 for a duration of 6 hours. Following treatment, the cells were washed three times with PBS at room temperature for treatment termination. Subsequently, 20  $\mu$ L of the reagent mixture was added to each well containing 100  $\mu$ L of complete media. The plates were incubated at 37°C for one hour. The absorbance was measured at 490 nm. a) Cell viability (MTS) assay of LP9 and MC-38 cells after 6-hour treatment with CMPD-43; b) Cell viability (MTS) assay of LP9 cells after 6-hour treatment with CMPD-43; the culture continued until 48 hours.



### % Adhesion of Cmpd-43 Treated Cells vs. Non-treated Control

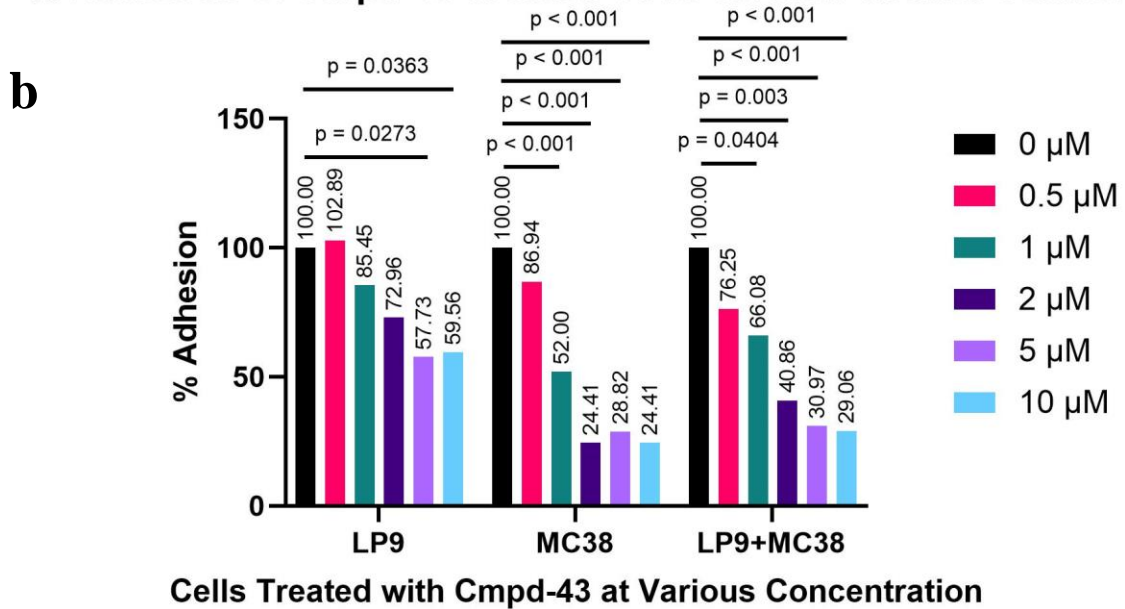


Figure 4.3 a) Work flow of MC-38 cells adhesion assay onto LP9 cells; LP9 cells were grown in 24-well plate until confluency; LP9 or MC-38 or both were treated with CMPD-43 for a duration of 6 hours; MC-38-RFP cells ( $5 \times 10^5$ ) were added to each well, followed by a 45-minute incubation period; Adhesion was terminated by PBS wash, 3 min 3 times. b) % MC-38 adhesion onto LP9 cells. LP9 or MC-38 or both were treated with CMPD-43. Percentages are normalized on average adhesion of the controls.

respectively). Another MTS test was conducted with LP9 cells treated with CMPD-43 for 6 hours and examination of cell viability at various time points between 6 to 48 hours. A slight but significant reduction (85% viability) was observed at 48 hours [Figure 4.2b]. These results indicate that although CMPD-43 has some effect on cell viability in both cell lines, the reduction in cell viability was not substantial enough to interfere with subsequent experimental procedures.

An *in vitro* adhesion assay was then performed to investigate the effects of CMPD-43 on the adhesion of MC-38 cells to LP9 cells at varying concentrations of CMPD-43, ranging from 0 to 10  $\mu$ M, with a treatment duration of 6 hours [Figure 4.3a]. The assay was conducted using three distinct treatment strategies: LP9 cells only, MC-38 cells only, and both LP9 and MC-38 cells treated with CMPD-43. The number of adhered cells per field was normalized to the control group averages.

A significant reduction in cell adhesion was observed at CMPD-43 concentrations of 5  $\mu$ M and 10  $\mu$ M across all setups [Figure 4.3b]. Additionally, adhesion significantly decreased at concentrations of 1  $\mu$ M and 2  $\mu$ M when MC-38 cells were treated with CMPD-43. These findings suggest that a concentration of 10  $\mu$ M is effective for future experiments aimed at inhibiting Prl-1 in LP9 cells with CMPD-43. Furthermore, the results indicate that MC-38 cancer cells are more responsive to CMPD-43 than LP9 normal cells, consistent with previous literature.<sup>154, 165</sup>

#### **4.4.2 MC-38 ex vivo adhesion assay onto murine peritoneum and omentum explants**

To evaluate the effect of CMPD-43 on adhesion of MC-38 to murine peritoneal tissues, an ex vivo adhesion assay was used [Figure 4.4b]. In this experiment, only the

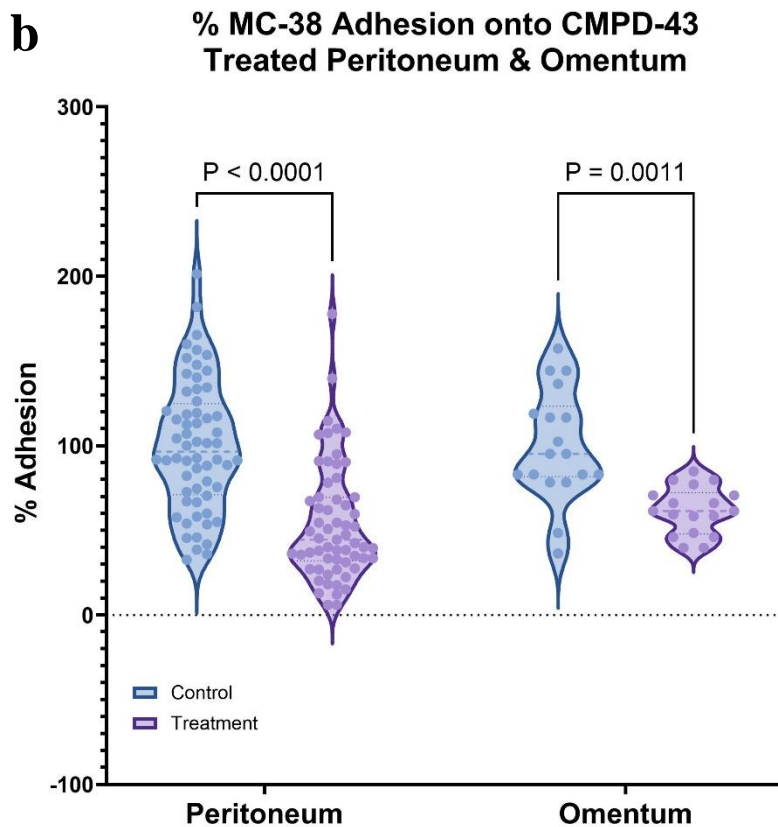
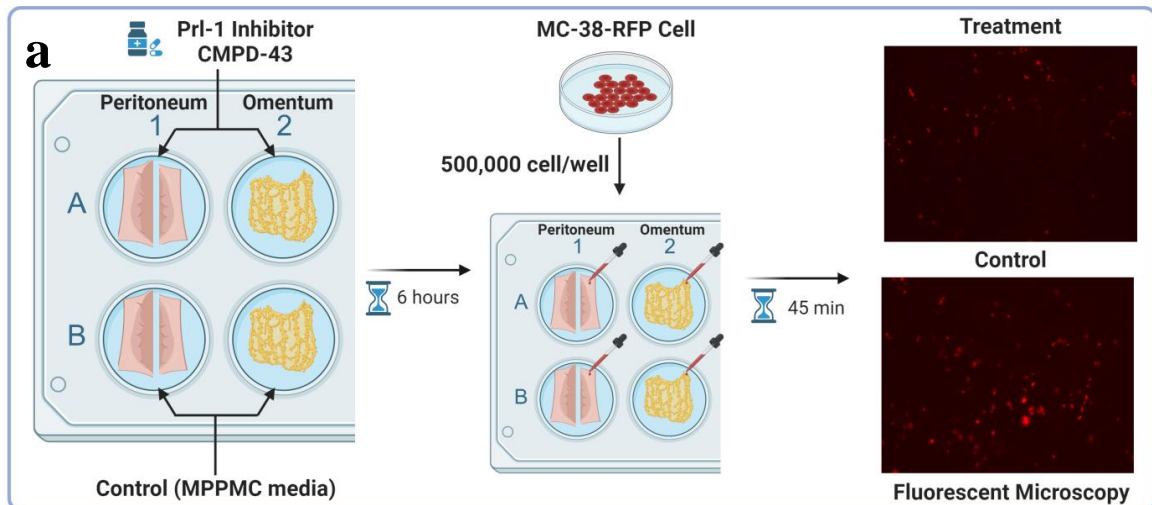


**Figure 4.4 a)** Workflow of an ex vivo adhesion assay; Aged male mice were sacrificed via isoflurane; Peritoneum and omentum tissue explants were collected and pinned in silicone coated dishes; they were then treated with 10  $\mu$ M CMPD-43 for 6 hours; MC-38-RFP cells ( $5 \times 10^5$ ) were added to each well, followed by a 45-minute incubation period; Adhesion was terminated by PBS wash, 3 min 3 times. **b)** Violin plots of % MC-38 adhesion onto CMPD-43 treated peritoneum and omentum. Percentages are normalized on average adhesion of the controls.

tissue explants were treated as the focus of this project is inhibition of host MC-expressed Prl-1. Figure 4.4b illustrates the percentage of MC-38 cell adhesion (non-treated) onto peritoneum and omentum tissues treated with CMPD-43. A noticeable reduction in MC-38 adhesion was observed to both peritoneal and omental tissues post-treatment ( $p < 0.0001$  and  $p = 0.0011$  respectively). This observation supports the hypothesis that Prl-1 is crucial in mediating cancer cell adhesion to the surface of peritoneal organ mesothelial cells.

#### **4.4.3 Prl-1 function assays regarding the Prl1-RhoA-Ncad pathway**

Given that Prl-1 has been confirmed to promote cancer cell adhesion to mesothelial cells, it is crucial to explore the signaling pathways in a molecular level through which this effect is mediated. The first pathway examined in this study is the Prl1-RhoA-Ncad pathway. Prl-1 competitively binds to the SH3 domain of p115 RhoGAP [Figure 4.1], stopping it from binding and deactivating RhoA.<sup>155</sup> As a result, Prl-1 competitively activates RhoA which subsequently promotes N-cad mediated cell-cell adhesion. Initial control experiments were performed to confirm a role for N-cad in mediating CRC to mesothelium adhesion. It is hypothesized that if N-cad functionally mediates MC-38 : LP9 adhesion, thus inhibiting N-cad with a function-blocking antibody should significantly decrease the adhesion. An *in vitro* adhesion assay was conducted with MC-38 cells adhering to LP9 cells treated with the N-cad blocking antibody GC-4 [Figure 4.5a]. The results demonstrated a significant reduction in adhesion of MC-38 cells upon blocking N-cad, indicating the involvement of N-cad in the adhesion between cancer cells and mesothelial cells. Notably, the most significant reduction in adhesion occurred when N-



### MC-38 Adhesion onto LP9 with N-cad Function Blocked

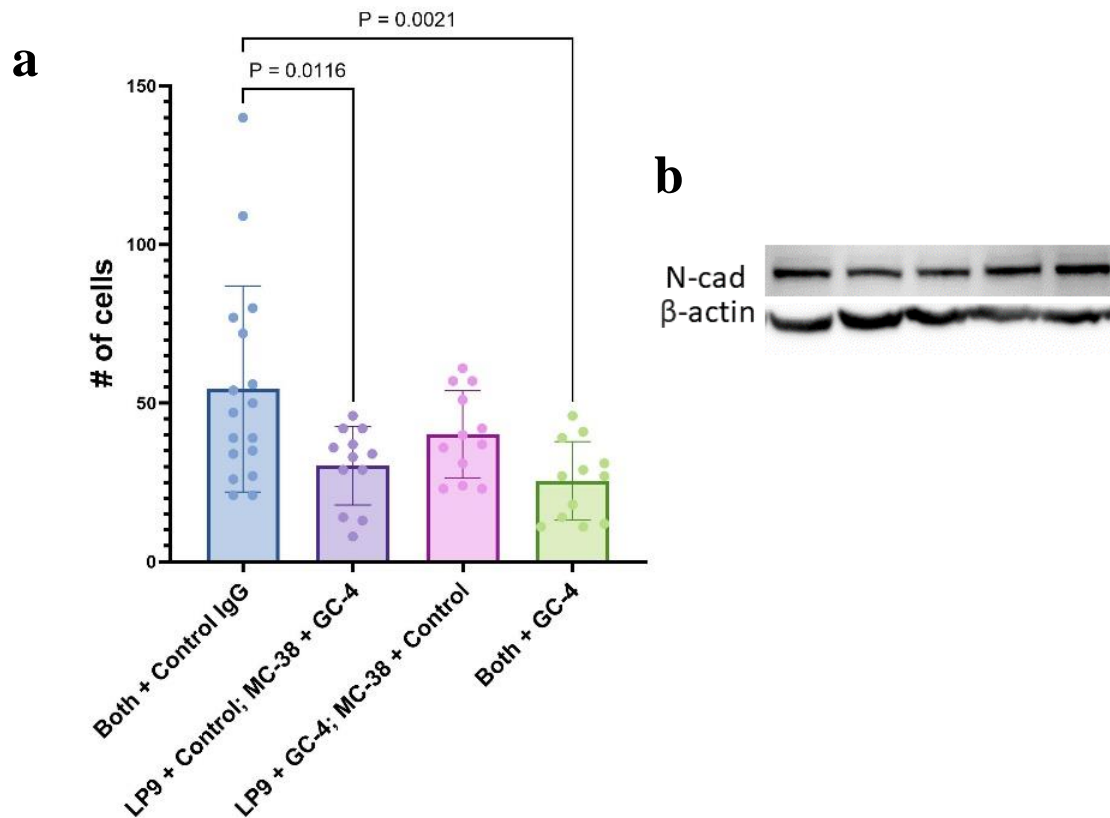


**Figure 4.5 a)** MC-38 adhesion onto LP9 with N-cad function blocking antibody (GC-4, 120  $\mu\text{g/mL}$ , 1 hour incubation); MC-38-RFP cells ( $5 \times 10^5$ ) were added to each well, followed by a 45-minute incubation period; Adhesion was terminated by PBS wash, 3 min 3 times; Treatment combinations includes: 1) Both cells treated with Control IgG; 2) LP9 treated with control IgG + MC-38 treated with GC-4; 3) MC-38 treated with Control IgG + LP9 treated with Anti-N-Cad; 4) Both cells treated with GC-4; **b)** Western blots for CMPD-43 treated LP9 cell lysates against N-cad. LP9 cells were grown to confluence before being treated with 10  $\mu\text{M}$  CMPD-43 in complete media at various time points: 0, 3h, 6h, 12h, and 24h. At the 6-hour mark, treatments were stopped with two washes of PBS, followed by the replacement of complete media. Equal amounts of protein (30 $\mu\text{g}$  per lane) were separated by electrophoresis on 9% SDS-polyacrylamide gels and transferred onto methanol-activated polyvinylidene fluoride (PVDF) membranes. Membranes were blocked with 5% milk in TBST (150mM NaCl, 25mM Tris, 0.05% Tween 20) for one hour at room temperature to prevent non-specific binding. Primary antibodies against N-cad (1:500 in 5% BSA) and incubated with the membranes overnight at 4°C. After thorough washing, membranes were incubated with horseradish peroxidase-conjugated secondary antibodies at a 1: 2000 dilution for one hour at room temperature. The resulting signals were visualized using chemiluminescence with the ChemiDoc™ Imaging system.

cad was blocked in both cancer and LP9 cells. This result aligns with the understanding that N-cadherin-mediated cell-cell adhesion requires the formation of extracellular N-cadherin dimers from both participating cells. Control experiment showed that the expression of N-cad after treatments was not affected [Figure 4.5b]. The RhoA activity assay [Figure 4.6a] further confirmed that inhibiting Prl-1 activity in LP9 cells significantly reduced the levels of active RhoA, providing strong evidence that Prl-1 facilitates cell-cell adhesion, at least in part, via the Prl1-RhoA-Ncad pathway. RhoA activation is known to stabilize  $\beta$ -catenin, leading to the accumulation of  $\alpha$ -catenin at the intracellular domain of N-cad.<sup>160</sup> The activation of RhoA aids in stabilizing the N-cad-catenin complex's attachment to the actin cytoskeleton, thereby reinforcing cell-cell contacts. The data indicate that Prl-1 does not affect N-cadherin expression, corroborated by the western blot results.

#### **4.4.4 The effect of Prl-1 inhibition on the level of active FAK, p130cas, and ERK1/2**

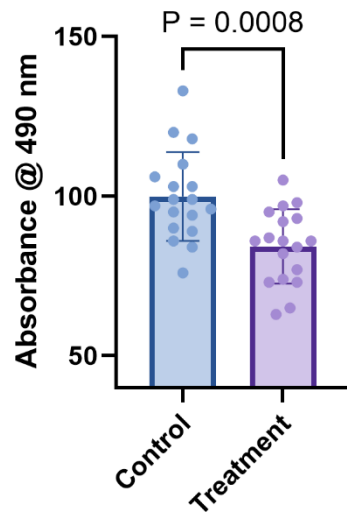
Prl-1 activates the Src/FAK/p130cas kinase cascade, providing a potential mechanism for enhanced cell adhesion, migration, anchorage-independent growth, cell transformation, growth factor stimulation, and cytokine receptor engagement [Figure 4.1].<sup>161, 163</sup> To assess the effects of Prl-1 inhibition on the signaling proteins FAK and p130cas, cell lysates were collected from CMPD-43-treated LP9 cells at various time points, ranging from 0 to 24 hours. The treatment duration was limited to the first 6 hours to align with the protein function assays. Figure 4.6b presents the western blot analyses for FAK, phosphorylated FAK (p-FAK), p130cas, and phosphorylated p130cas (p-p130cas). The phospho-specific antibodies targeted phosphorylation sites Y410 on p130cas and

Y397 on FAK, which are critical for their activation and proper localization during focal adhesions.<sup>163, 166, 167</sup> The results showed a biphasic effect on FAK and p130cas phosphorylation, with a decrease in the phosphorylated levels of these proteins at the 3-6 hour time point [Figure 4.6b], and subsequent increase in the 6-24 h time frame. Meanwhile, the total level of both proteins remains largely consistent throughout the 24-hour period. This is consistent with the hypothesis that Prl-1 activation would enhance the phosphorylation and activation of p130cas and FAK, and thus inhibiting Prl-1 should reduce the phosphorylated (active) form of both proteins without affecting their total expression levels. The data suggest that Prl-1 inhibition significantly reduces the active forms of FAK and p130cas, which could potentially alter cell:matrix adhesion. Although FAK and p130cas do not directly regulate cell:cell adhesion, altered cell:matrix adhesion between mesothelial cells to ECM could also destabilize the ECM structure at the cancerous:mesothelial junction [Figure 4.1]. As a result, inhibiting Prl-1 could deactivate FAK and p130cas, destabilizing the cancer cell:matrix:mesothelial cell complex.

The Erk1/2-MMPs pathway was investigated by measuring the total and phosphorylated ERK1/2 levels using western blots. Interestingly, data have revealed that p-ERK1/2 (active) levels were significantly higher at the 6h time point than all others with a consistent level of total ERK1/2 [Figure 4.6b]. This is inconsistent with the hypothesis that inhibiting Prl-1 would reduce the level of p-ERK1/2. Such dramatic and sudden change in p-ERK1/2 reveals interesting insight into the complexity of Prl-1 involved cellular network and awaits future investigations.

### RhoA Activity Change in LP9 Cells Treated with CMPD-43

**a**



**b**

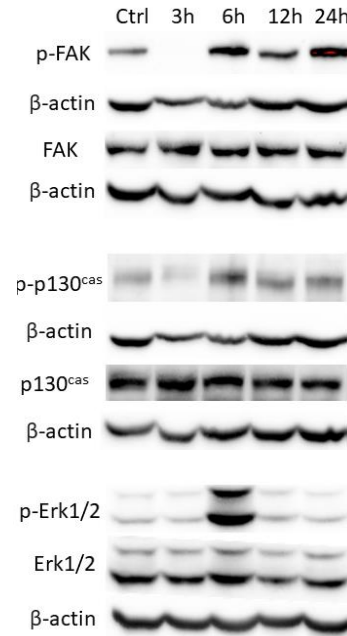


**Figure 4.6** a) RhoA activity in LP9 cells treated with/without CMPD-43; LP9 cells were cultured to confluence and treated with 10  $\mu$ M CMPD-43 in complete media for 6 hours. Treatments were terminated by washing the cells twice with PBS. The RhoA G-LISA Activation Assay Kit was used for RhoA activity. Lysates were standardized to equivalent protein concentrations before being frozen and stored. Cell lysates were combined with binding buffer and loaded into 96-well binding strips, shaken at 200 rpm for 30 minutes at 4°C. This was followed by incubation with Antigen presenting buffer (2 minutes at room temperature), then with anti-RhoA primary antibody diluted 1/250 (200 rpm shaking for 45 minutes at room temperature), and finally with secondary HRP-labeled antibody diluted 1/62.5 (200 rpm shaking for 45 minutes at room temperature). The HRP detection reagent was added (50  $\mu$ L each well, 15 min at 37 °C), and the reaction was terminated with the HRP Stop Buffer. Absorbance was measured at 490 nm. b) Western blots for CMPD-43 treated LP9 cell lysates against FAK, p-FAK, p130cas, p-p130cas, and N-cad. LP9 cells were grown to confluence before being treated with 10  $\mu$ M CMPD-43 in complete media at various time points: 0, 3h, 6h, 12h, and 24h. At the 6-hour mark, treatments were stopped with two washes of PBS, followed by the replacement of complete media. Equal amounts of protein (30 $\mu$ g per lane) were separated by electrophoresis on 9% SDS-polyacrylamide gels and transferred onto methanol-activated polyvinylidene fluoride (PVDF) membranes. Membranes were blocked with 5% milk in TBST (150mM NaCl, 25mM Tris, 0.05% Tween 20) for one hour at room temperature to prevent non-specific binding. Primary antibodies against N-cad, p130cas, phospho-p130cas (p-p130cas), FAK, and phospho-FAK (p-FAK) were diluted to 1:500 in 5% BSA/TBST and incubated with the membranes overnight at 4°C. After thorough washing, membranes were incubated with horseradish peroxidase-conjugated secondary antibodies at a 1: 2000 dilution for one hour at room temperature. The resulting signals were visualized using chemiluminescence with the ChemiDoc™ Imaging system.

#### **4.4.5 Limitations and Future directions**

The very next step could be to perform protein function assays for the remaining USP36-Snail2-Ncad pathway, as suggested. It is hypothesized that inhibiting Prl-1 would regulate the USP36-Snail2-Ncad pathway and cause a reduction in USP36 and Snail2 levels following CMPD-43 treatment, resulting in a decrease in N-cad expression levels. A deubiquitination assay could be used to confirm if inhibiting Prl-1 in LP9 cells reduces Snail2 levels via polyubiquitination. However, N-cad western blot results [Figure 4.5b] showed no change in N-cad expression upon CMPD-43 treatment, suggesting that USP36-Snail2-Ncad is not a key pathway regulating cell:cell adhesion in this system.

One of the concerns regarding this project is the level of influence is not going to be as large as other tumor studies where their oncogenic targets are usually over-expressed. Due to the nature of this study, all treatments are performed on non-cancerous cells and tissues where everything tends to stay homeostatic. Unlike cancer cells, not many proteins in LP9 cells are greatly over- or under-expressed. As a result, inhibiting a protein in LP9 cells may not result in changes as big as if the protein is overexpressed in some cancer cell, making the effects less significant. The reduction in adhesion and RhoA activity after LP9 was treated with CMPD-43 are all significant but small. The N-cad level didn't change too much after CMPD-43 treatments. It could be simple that the USP36-Snail2-Ncad pathway is irrelevant in this experiment. However, it could also be that the changes are just small and the cells' other pathways also expressing N-cad self-rescued the total N-cad level. In future studies, more sensitive analytical methods such as isotope-labelled quantitative mass spectrometry could be used to examine such small changes. On the other hand, this project

also calls for attention that some proteins could have a significant effect on cancer metastatic success without being greatly over expressed as in some cancer cells.

The complexity of tumor metastatic microenvironment of CRC patients can be much higher than in a murine model. Utilizing patient-derived xenografts (PDX) or organoid models can provide more relevant biological contexts to study the effects of Prl-1 inhibitors. Inhibiting Prl-1 in normal or cancerous samples using these models can more accurately reflect the heterogeneity of human tumors and their microenvironments, offering a better predictive platform for clinical outcomes.

While *in vitro* and *ex vivo* studies provide valuable insights, *in vivo* studies using animal models are crucial to confirm the therapeutic potential and safety of CMPD-43 and other Prl-1 inhibitors. These studies can help assess the drug's pharmacokinetics, pharmacodynamics, toxicity, and efficacy in a whole-organism context, which is essential before considering clinical trials. By continuing to investigate the molecular underpinnings of Prl-1's role in cancer, more effective treatments for patients suffering from Prl-1 driven malignancies could be advanced. It is also important to identify biomarkers associated with Prl-1 activity, to help in patient stratification and monitoring therapeutic responses. Such targets may be found from the proteomics data in Chapter 3 (host) or from cancer cell proteomics analysis. Given the complexity of cancer signaling networks, combination therapies involving Prl-1 inhibitors and other targeted treatments (e.g., chemotherapeutics, immunotherapies) might offer enhanced efficacy. Exploring synergistic effects and potential drug interactions in a murine model with CMPD-43 and standard of care therapeutics may further aid the development of more effective treatment regimens. The

question here will be: will a combination of Prl-1 inhibition with standard of care treatment reduce primary tumor size as well as preventing the tumor from forming metastasis?

#### **4.5 Conclusion**

This analysis underscores the pivotal role of both host and tumor Prl-1 in the metastatic process of colorectal cancer, particularly in mediating cancer cell adhesion to mesothelial-linked structures. The study confirms that Prl-1 is an important player in several signaling pathways, including the Prl1-RhoA-Ncad pathway and Src-p130cas and FAK pathway, which are integral to cell proliferation, migration, and adhesion. The utilization of CMPD-43, a Prl-1 inhibitor, has demonstrated significant efficacy in reducing cancer cell adhesion, highlighting its potential as a therapeutic agent. The findings also suggest that the disruption of Prl-1 activity can lead to a decrease in key signaling molecules and pathways, such as FAK and p130cas, thereby potentially preventing cancer cell migration and metastasis.

It is hypothesized that metastatic cancer cells may target membrane-bound Prl-1 expressed by the host's healthy tissues to facilitate recruitment and initiate metastasis. The findings highlight the potential therapeutic value of Prl-1 inhibitors in preventing colorectal cancer metastasis. In patients diagnosed with early-stage colorectal cancer, a Prl-1 inhibitory drug could significantly impede intraperitoneal metastasis, thereby maintaining the disease at an early, more treatable stage. The implications of these results are profound, as they suggest that targeting Prl-1 could offer a strategic advantage in the treatment of colorectal cancer, particularly in preventing metastasis to peritoneal surfaces. Future research should focus on further elucidating the specific mechanisms by which Prl-1

contributes to cancer progression and exploring the therapeutic potential of Prl-1 inhibitors in pre-clinical models and in clinical settings. By continuing to investigate the molecular underpinnings of Prl-1's role in cancer, patients suffering from CRC and malignancies may have more effective treatments for primary or recurrent diseases.



## CHAPTER 5.

### PROJECT SUMMARY

#### 5.1 Introduction

This study seeks to deepen our understanding of how gender and age differences influence peritoneal metastasis in colorectal cancer (CRC) through the use of proteomic approaches. The study identified and investigated potential therapeutic targets that are specialized for different gender and age groups. Colorectal cancer (CRC) remains one of the leading causes of cancer-related mortality worldwide, with a significant proportion of these deaths attributed to peritoneal metastasis.<sup>1, 2</sup> Despite the critical role of metastasis in CRC prognosis, much of the existing research has focused primarily on the cancer cells themselves, rather than the host environment in which these cells metastasize. This study diverges from traditional approaches by shifting the focus to the proteomic differences in healthy tissues, specifically non-cancerous mesothelial cells, across different gender and age groups. The novel aspect of this research lies in its investigation of how these differences influence the metastatic process, particularly in the context of peritoneal metastasis. By examining the proteomic profiles of mesothelial cells in healthy mice, this study seeks to uncover the underlying biological mechanisms that predispose certain groups—most notably older males—to higher rates of metastasis. This focus on the host environment, rather than solely on the cancer cells, offers new insights that could lead to more personalized and effective therapeutic strategies [Figure 5.1].

## Project Summary

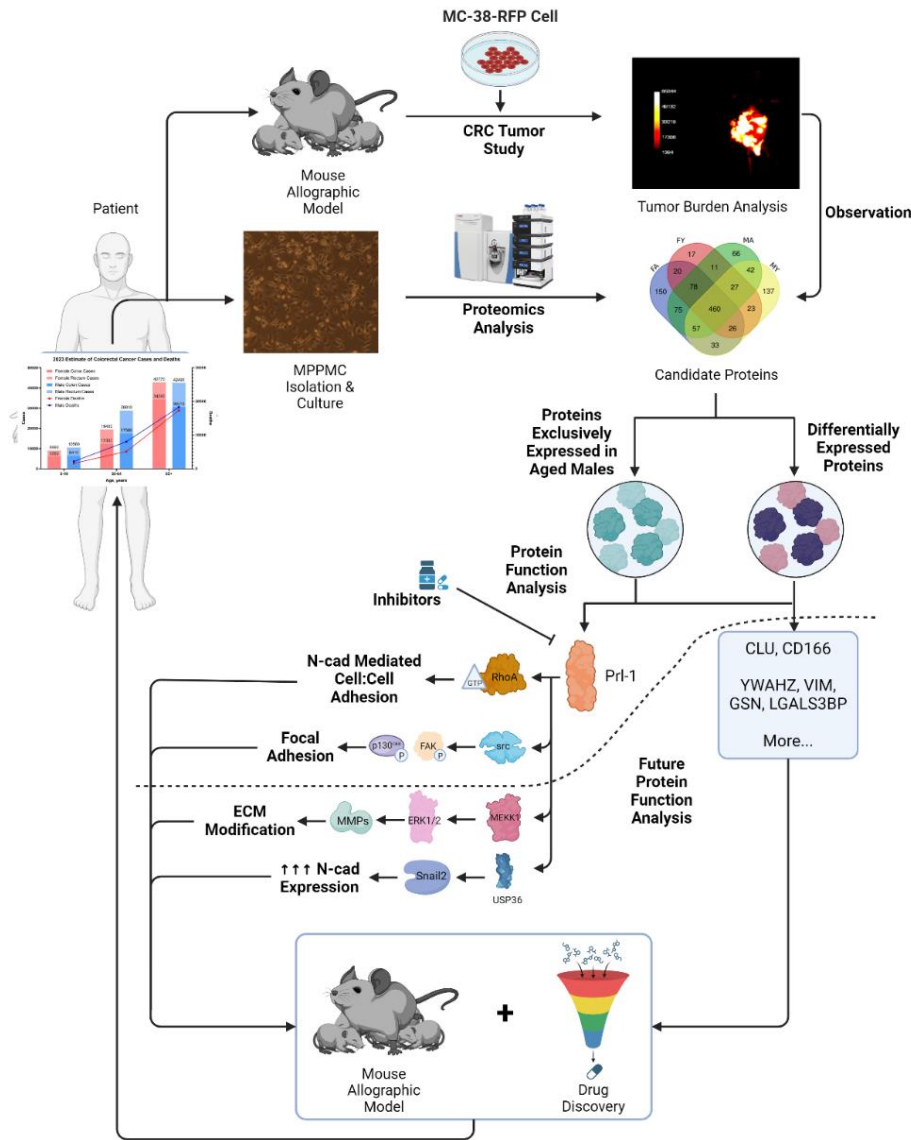


**Figure 5.1 Graphical Abstract.** This project starts with statistical data of colorectal cancer (CRC) patients from different gender and age groups. Using murine models, the study progressed in 2 ways; one is using mouse allograft model to study CRC intra-peritoneal metastasis; the other in the proteomics analysis of isolated tumor naïve murine primary peritoneal mesothelial cells (MPPMCs). The observation from the tumor study, namely that, aged males present the highest tumor burden, was used as a guideline in analyzing the proteomics. Protein candidates potentially contributing to the gender/age differences in CRC metastatic success were identified, followed by protein function analysis. The characterized proteins can then be investigated in animal models and drug discovery for more personalized of CRC metastasis in the aged host.

## **5.2 Gender and Age Effect on CRC Intraperitoneal Metastasis Success**

Cancer predominantly impacts older individuals, with age being one of the most significant risk factors for both the disease and its metastatic spread. Additionally, the biological sex of the individual plays a critical role in determining the likelihood of metastasis and survival outcomes. Men, in particular, are more susceptible to cancer-related mortality. In the case of colorectal cancer (CRC), incidence and mortality rates are notably higher in men, underscoring the serious mortality risks faced by male CRC patients, highlighting that fundamental biological differences between sexes significantly influence cancer progression.

This study begins by exploring the impact of gender and age on the success of CRC metastasis within the peritoneal cavity, using a murine model. The findings reveal that aged male mice exhibit the highest tumor burden, particularly in adipose organs formed by the folding of visceral peritoneum. This observation is consistent with epidemiological data, which indicate higher CRC incidence and mortality rates in males, especially those over the age of 65. The study also highlights the gender-specific differences in tumor burden are more pronounced in aged mice, particularly in the omentum and peritoneal adipose. These results underscore the significant influence of biological sex and age on CRC metastatic patterns and suggest that these factors should be considered when developing therapeutic strategies. They also highlight the necessity of discovering new targets specifically for aged males who carried the highest risk of CRC metastasis.

### **5.3 MPPMC Proteomics Revealed Protein Targets Potentially Mediating CRC**

#### **Intraperitoneal Metastasis Success in Aged Males**

Building on the findings regarding the gender and age effects, the study delves into the proteomic profiles of murine primary peritoneal mesothelial cells (MPPMCs) to identify potential mediators of CRC metastasis. The peritoneum is a large abdominal organ, consisting of an extensive serous membrane that lines the inner walls of the abdominal cavity and the outer surfaces of the visceral organs. Numerous peritoneal diseases, such as peritonitis, primary cancers like mesothelioma, and metastatic cancers including ovarian, pancreatic, and colorectal cancers i.p. metastasis, often begin with interactions involving the peritoneal mesothelial cells. The study developed and finalized an isolation protocol to reproductively isolate MPPMCs *in vitro* culture and utilized mass spectrometry as the gold standard to quantitatively build a proteomic portrait of the mesothelial cells from different gender and age group.

Each cohort, FA, FY, MA, MY, contains a total of 2721, 1982, 2484, 2364 proteins and 899, 662, 816, 805 protein groups respectively. FA, FY, MA, MY, have 379, 58, 202, 423 proteins and 150, 17, 66, 137 protein groups [Figure 3.2 and Table 3.1] unique to their individual group, respectively. By comparing the proteomes of MPPMCs from different gender and age groups, male and female MPPMCs are different in their protein translation and peptide metabolism pathways while the aged and young mesothelial cells have distinct metabolic processes. The study also identified significant differences in protein expression that may contribute to the observed disparities in metastatic success. Our results identified differentially expressed proteins previously associated with peritoneal diseases including

YWHAZ, GSN, VIM, and LGALS3BP. Notably, the proteomic analysis reveals that aged males exhibit a unique protein profile that could be linked to their higher tumor burden. CD166, CLU, and Prl-1 were highlighted from the profile by their metastasis-promoting characteristics. These findings establish baseline proteomic data that not only provide valuable insights into the role of mesothelial cells in maintaining peritoneal homeostasis but also suggest that specific proteins in aged males may facilitate CRC metastasis. This approach introduces a novel area of research, linking these proteomic differences to disease progression and identifying potential targets for future therapeutic intervention. More importantly, the proteomics data has been uploaded into databases which are open to all other researchers who are interested in studying peritoneal diseases, including but not limited to peritonitis, mesothelioma, and metastatic cancer including ovarian, pancreatic and colorectal cancer. While this study focused primarily on the MA cohort, other peritoneal diseases may present different trends according to gender and age, and therefore may find values in examination of these proteomics profiles.

#### **5.4 Comprehensive Analysis of Prl-1 in Colorectal Cancer Metastasis**

One of the key findings of the study is the identification of Prl-1 as a critical factor in CRC metastasis, particularly in aged male mice. Prl-1, a protein tyrosine phosphatase, is shown to play a significant role in promoting cancer cell adhesion and migration. Prl-1 was first identified as a nuclear protein involved in regulating cell growth and is known to affect cell proliferation and differentiation in a tissue-specific manner. The protein undergoes prenylation, which aids in its transport to membrane structures, where it influences cell growth and migration through pathways involving proteins such as

extracellular signal-regulated kinase 1/2 (ERK1/2), the proto-oncogene c-Src (src), and RhoA-GTPase activities.

The study confirms that Prl-1 is involved in several important signaling pathways, including the Prl1-RhoA-Ncad pathway and Src-p130casandFAK pathway, which are integral to cell proliferation, migration, and adhesion. The research further demonstrates that inhibition of Prl-1 using the specific inhibitor CMPD-43 effectively reduces CRC metastasis, making Prl-1 a promising therapeutic target. This comprehensive analysis of Prl-1 provides a deeper understanding of its role in the metastatic process and suggests that targeting this protein could offer a strategic advantage in preventing CRC metastasis, particularly in high-risk groups such as older males.

In the current practice of colorectal cancer (CRC) treatments, commonly used precision therapeutic targets include: EGFR, KRAS, and VEGF etc. EGFR inhibitors like cetuximab and panitumumab are especially effective in tumors without RAS mutations. KRAS mutations are present in around 40% of CRC cases, making it a major therapeutic target. New approaches, including KRAS G12C inhibitors such as KRAZATI, Sotorasib, Adagrasib, and Fruzaqla have recently been approved to treat KRAS-mutated cancers.<sup>168-</sup>  
<sup>171</sup> VEGF/VEGFR could be targeted through VEGF inhibitors like bevacizumab. It interrupts angiogenesis and remains a key strategy, especially in combination with chemotherapy.<sup>170</sup> Other than the pathways proposed in Chapter 4, candidate proteins found from the proteomics data (Chapter 3), PRL-1, CD166, and clusterin, have also been shown to correlate with those known therapeutic targets.

Prl-1, while not traditionally a major therapeutic target, shows potential due to its role in activating the EGFR-PI3K-CaM pathway, promoting cell proliferation and liver regeneration. Given its structural similarity to PRL-3, which is correlated with VEGF expression, PRL-1 keeps emerging as a target worth further investigation.<sup>172, 173</sup> In humans, PRL-1 and PRL-2 share 87% homology in their amino acid sequences, while PRL-1 and PRL-3 are 79% homologous, and PRL-2 and PRL-3 exhibit 76% homology.<sup>146, 174, 175</sup> Like PRL-1, PRL-2 plays a role in cell cycle regulation by promoting the G1 to S phase transition through the downregulation of p21<sup>Cip1/Waf1</sup>.<sup>176</sup> In recent years, several studies have shown that PRL-2 is overexpressed in various cancer cell lines and tumor samples, including pancreatic, breast, and lung cancers. More significantly, PRL-2 has been linked to tumor progression.<sup>146, 177-179</sup> Furthermore, the ectopic overexpression of PRL-2 in hematopoietic cells has been reported to affect malignant progression and metastasis.<sup>146, 180</sup> Prl-2 has been shown to enhance cancer cell migration and metastasis via activating p130cas and ERK.<sup>177</sup> PRL-2 exhibits phosphatase activity on multiple substrates, such as activating VCP/P97 at Y805 and deactivating PTEN at Y336. Overexpression of PRL-2 is believed to activate VCP, supporting lysosomal hemostasis and cancer cell survival.<sup>181</sup> PRL-2 deletion also mitigates p53 deficiency–induced tumor growth by increasing PTEN levels and reducing Akt activity.<sup>182</sup> Although PTEN mutations are rare in colorectal cancer, VCP is a frequently studied target for CRC.<sup>183, 184 185, 186</sup> Interestingly, CMPD-43 has been found to inhibit PRL-2 activity, providing an excellent starting point for further analysis of PRL-2 function.<sup>182</sup> Analyzing the effect of inhibiting Prl-2 in combination with targeting Prl-1 or the other therapeutic targets can be the very next step understanding the complex pro-metastasis activities of the phosphatase of regenerating liver family.

CD166 is another molecule relevant to CRC due to its involvement in cellular adhesion and migration, impacting key pathways regulated by EGFR and KRAS. Researches supported that CD166 enhances EGFR phosphorylation and prolongs the signaling cascade, contributing to a cancer stem cell-like phenotype. Additionally, CD166-positive CRC specimens show a higher frequency of KRAS exon 2 mutations compared to CD166-negative ones, underscoring a potential, albeit unconfirmed, link between CD166 and KRAS-driven pathways in CRC.<sup>170, 187, 188</sup>

Clusterin (CLU) plays a significant role in modulating several oncogenic signaling pathways, including IGF-1/IGFR, EGFR, NF- $\kappa$ B, PI3K/AKT, and TGF- $\beta$ .<sup>189</sup> While many of those pathways can be oncogenic, a significant portion of KRAS mutation positive Non-small cell lung cancer patients are concurrently deficient of CLU.<sup>190</sup> Nevertheless, it has also been shown that heat shock factor 1 upregulated PDL1 (another CRC therapeutic target) expression by inducing clusterin expression and activating STAT3 signaling pathway in Hepatocellular cancer.<sup>165, 191</sup> It indicates that CLU is involved in both tumor-suppressive and tumor-promoting processes depending on the context. Interestingly, clusterin's enhancement of astrocyte proliferation and activation of the Ras/Raf-1/MEK/ERK signaling cascade via EGFR highlights its broader relevance to CRC signaling networks.<sup>192</sup>

While VEGF is widely recognized for its role in CRC treatment, correlations between VEGF and clusterin were observed in other contexts. Intravitreal levels of VEGF and clusterin proportional to severity of diabetic retinopathy.<sup>193</sup> N,N'-Dinitrosopiperazine (DNP) is involved in Nasopharyngeal carcinoma metastasis. DNP promotes NPC metastasis through up-regulating increase CLU, matrix metalloproteinases (MMP) 9 and



vascular endothelial growth factor (VEGF) expression and activity.<sup>194</sup> These findings suggest that clusterin might interact with VEGF-driven processes, indirectly influencing metastasis and tumor progression in CRC as well. The upregulation of both VEGF and clusterin in certain conditions adds to the complexity of their relationship in cancer progression.

Again, Prl-1, CD166, and CLU are all proteins found exclusively from aged male MPPMC proteomics in the tumor naïve host. The identification of proteins closely related to oncogenesis in healthy tissue holds profound importance for the future of cancer research and personalized medicine. These proteins' interaction with metastatic cancer cells carrying those therapeutic targets could represent the early molecular shifts to metastasis, making them crucial targets for preventive strategies, especially given that CRC metastasis could start fast and early in tumor progression even before the carcinoma is clinically detectable.<sup>12</sup> By studying these proteins in their pre-oncogenic tissue, researchers can uncover the subtle changes that occur before metastasis, potentially enabling the development of interventions that halt malignancy at its inception. Additionally, understanding these proteins within healthy tissue offers insights into the delicate balance of cellular processes that maintain normal function and how their dysregulation leads to cancer. As technology advances in proteomics and bioinformatics, the future lies in refining our ability to map these protein networks and their interactions in healthy versus diseased states. Such efforts could lead to more specific drug targets and tailored therapeutic strategies that focus on correcting or mitigating the pre-malignant shifts before they progress into full-blown oncogenesis.

## 5.5 Future Directions

While this study provides significant insights into the role of gender, age, and specific proteins like Prl-1 in CRC metastasis, several limitations should be addressed in future research. One of the main limitations is the use of an *in vitro* culture system that does not fully replicate the complex *in vivo* mesothelial microenvironment. Future studies should incorporate additional factors, such as extracellular matrix components and other cell types like fibroblasts and immune cells, to provide a more comprehensive understanding of the mesothelial environment. Additionally, further research is needed to fully elucidate the mechanisms by which Prl-1 influences signaling pathways involved in CRC metastasis. This could involve more detailed functional assays and *in vivo* studies to validate the therapeutic potential of Prl-1 inhibitors in clinical settings. In addition, a larger *in vivo* cohort with more mice in each could potentially be used. The allograft model used in Chapter 2 exhibits large standard error, which may be reduced by increasing the sample size to at least 30-40 mice per cohort.

The function studies on the Prl1-Erk1/2-MMPs and Prl1-USP36-Snail2-Ncad Pathways are currently ongoing as suggested in order to draw a more comprehensive and connected roadmap for Prl-1 mediated cell:cell adhesion. Other candidate proteins including CD166 and CLU shall also have their function analyzed on the mesothelium. Future research should also explore the therapeutic implications of the identified proteomic differences in MPPMCs, particularly in relation to developing gender- and age-specific treatments. Investigating how these proteins contribute to CRC metastasis in other high-risk populations could lead to more effective and personalized treatment strategies.

Moreover, expanding the study to include other types of cancer that metastasize to the peritoneum could further enhance our understanding of the broader implications of these findings.

Moreover, the peritoneal cavity is not the only site of CRC metastasis, and in many cancers, intra peritoneal, lymph node, and hematologic spread could all happen at the same time.<sup>17, 23</sup> It could be important to also investigate the proteomics profiles specific to each gender and age group. Future researches could perform vertical comparisons between different groups like the current study. They could also conduct horizontal comparisons which focus on candidate proteins shared/differ between healthy tissues for the discovery of new therapeutic targets which could prevent metastasis not only in the peritoneal cavity, but also other parts of the body.

In a recent study, several novel prognostic markers in CRC were identified, including AREG, FLCN, and TYRO3, etc.<sup>195</sup> Their interactions with host tissue, perhaps mesothelial cells, could be a good representation and cut-in point to study cancerous : healthy intracellular interactions. AREG is synthesized as a membrane-anchored precursor protein that can engage in juxtacrine signaling with neighboring cells. Alternatively, after proteolytic processing by cell membrane proteases, AREG is secreted and acts as an autocrine or paracrine factor.<sup>196</sup> AREG is an EGFR ligand associated with a favorable response to anti-EGFR therapy and improved progression-free survival in CRC.<sup>197</sup> AREG activates EGFR signaling in an autocrine manner, promoting mucoepidermoid carcinoma (MEC) cell growth and survival.<sup>198</sup> Additionally, AREG plays a critical role in cell migration, invasion, and EMT through activation of the EGFR/ERK/NF- $\kappa$ B signaling pathway in pancreatic cancer cells.<sup>199</sup> FLCN, a tumor suppressor, also regulates EGFR

signaling by suppressing its activity and enhancing EGF-induced EGFR degradation.<sup>200, 201</sup> PRL-1 is also thought to be an EGFR ligand, but the correlation between these proteins remains unclear. Future research could explore how targeting AREG's dual roles in autocrine and paracrine signaling might optimize therapies, particularly in the context of EGFR inhibitors in CRC and other malignancies. Understanding its interaction with other ligands and potential synergistic effects with PRL-1 could unveil new therapeutic combinations. Investigating the relationship between AREG, FLCN, and PRL-1, especially in the modulation of EGFR mediated pathways, holds promise for new avenues in precision oncology. Future studies could focus on whether they act in concert or opposition in tumor progression and whether manipulating this relationship could yield targeted therapies that enhance treatment efficacy.

Furthermore, circulating small extracellular vesicles (csEV)-mediated TYRO3 activation promotes migration and metastasis via EMT and RhoA stimulation in invasive cancer cells.<sup>202</sup> Moreover, TYRO3 knockdown in gastric cancer (GC) cell lines effectively suppresses the PI3K/AKT/mTOR pathway, inhibiting tumor cell proliferation and migration.<sup>203</sup> The role of TYRO3 in facilitating metastatic processes suggests it could be a viable target for preventing cancer spread. These findings highlight notable parallels with the activity of PRL-1.<sup>160, 172</sup> Future research should delve deeper into csEV-mediated TYRO3 activation mechanisms and its interplay with other pathways like those involving PRL-1. Identifying co-regulatory mechanisms between TYRO3 and PRL-1 could potentially yield biomarkers or targets for combination therapies aimed at halting cancer progression.

## 5.6 Conclusion

In conclusion, this study offers a novel perspective on colorectal cancer metastasis by focusing on the proteomic differences in healthy peritoneal mesothelial cells across different gender and age groups. The research highlights the significant impact of these differences on CRC metastasis, particularly in aged males, and identifies Prl-1 as a key player in the metastatic process. The findings suggest that targeting specific proteins, such as Prl-1, could lead to more effective strategies for preventing CRC metastasis, particularly in high-risk populations. By shifting the focus from the cancer cells themselves to the host environment, this study opens new avenues for personalized medicine and offers the potential for more targeted and effective therapeutic interventions. Identified proteins including but not limited to Prl-1, CD166, and CLU also carry great potential on their relationships with known prognostic signatures of colorectal cancer, which requires future research to uncover. Future research should then build on these findings by exploring the complex interactions within the mesothelial microenvironment and further investigating the therapeutic potential of the identified protein targets.

## BIBLIOGRAPHY

- (1) Siegel, R.; Desantis, C.; Jemal, A. Colorectal cancer statistics, 2014. *CA Cancer J Clin* **2014**, *64* (2), 104-117. DOI: 10.3322/caac.21220.
- (2) Jiang, Y.; Zhao, M.; Tang, W.; Zheng, X. Impacts of systemic treatments on health-related quality of life for patients with metastatic colorectal cancer: a systematic review and network meta-analysis. **2024**, *24* (1), 188.
- (3) *American Cancer Society: Cancer Facts & Statistics*. American Cancer Society, 2024. <https://cancerstatisticscenter.cancer.org/#!/data-analysis/NewCaseEstimates/compare/DeathEstimates> (accessed 2024 June 18).
- (4) Rawla, P.; Sunkara, T.; Barsouk, A. Epidemiology of colorectal cancer: incidence, mortality, survival, and risk factors. *Przegląd gastroenterologiczny* **2019**, *14* (2), 89-103. DOI: 10.5114/pg.2018.81072.
- (5) Alinia, S.; Ahmadi, S.; Mohammadi, Z.; Rastkar Shirvande, F.; Asghari-Jafarabadi, M.; Mahmoudi, L.; Safari, M.; Roshanaei, G. Exploring the impact of stage and tumor site on colorectal cancer survival: Bayesian survival modeling. **2024**, *14* (1), 4270.
- (6) Sandouk, F.; Al Jerf, F.; Al-Halabi, M. H. D. B. Precancerous Lesions in Colorectal Cancer. *Gastroenterol Res Pract* **2013**, *2013*, 457901-457911. DOI: 10.1155/2013/457901.
- (7) Fearon, E. R.; Vogelstein, B. A genetic model for colorectal tumorigenesis. *cell* **1990**, *61* (5), 759-767.
- (8) Bottomley, A.; Aaronson, N. K.; Cancer, E. O. f. R. a. T. o. International perspective on health-related quality-of-life research in cancer clinical trials: the European Organisation for Research and Treatment of Cancer experience. *J Clin Oncol* **2007**, *25* (32), 5082-5086. DOI: 10.1200/JCO.2007.11.3183.
- (9) Brenner, H. P.; Kloor, M. M. D.; Pox, C. P. M. D. Colorectal cancer. *Lancet* **2014**, *383* (9927), 1490-1502. DOI: 10.1016/S0140-6736(13)61649-9.
- (10) Choi, Y.; Kim, N. Sex Difference of Colon Adenoma Pathway and Colorectal Carcinogenesis. *World J Mens Health* **2024**, *42* (2), 256-282. DOI: 10.5534/wjmh.230085.
- (11) Baran, B.; Ozupek, N. M.; Tetik, N. Y.; Acar, E.; Bekcioglu, O.; Baskin, Y. Difference Between Left-Sided and Right-Sided Colorectal Cancer: A Focused Review of Literature. *Gastroenterology Res* **2018**, *11* (4), 264-273. DOI: 10.14740/gr1062w.

- (12) Hu, Z.; Ding, J.; Ma, Z.; Sun, R.; Seoane, J. A.; Scott Shaffer, J.; Suarez, C. J.; Berghoff, A. S.; Cremolini, C.; Falcone, A.; et al. Quantitative evidence for early metastatic seeding in colorectal cancer. *Nature genetics* **2019**, *51* (7), 1113-1122. DOI: 10.1038/s41588-019-0423-x.
- (13) Martin, J.; Petrillo, A.; Smyth, E. C.; Shaida, N.; Khwaja, S.; Cheow, H. K.; Duckworth, A.; Heister, P.; Praseedom, R.; Jah, A.; et al. Colorectal liver metastases: Current management and future perspectives. *World J Clin Oncol* **2020**, *11* (10), 761-808. DOI: 10.5306/wjco.v11.i10.761.
- (14) Paget, S. THE DISTRIBUTION OF SECONDARY GROWTHS IN CANCER OF THE BREAST. *The Lancet (British edition)* **1889**, *133* (3421), 571-573. DOI: 10.1016/S0140-6736(00)49915-0.
- (15) Zhou, H.; Liu, Z.; Wang, Y.; Wen, X.; Amador, E. H.; Yuan, L.; Ran, X.; Xiong, L.; Ran, Y.; Chen, W.; et al. Colorectal liver metastasis: molecular mechanism and interventional therapy. *Signal Transduct Target Ther* **2022**, *7* (1), 70-70. DOI: 10.1038/s41392-022-00922-2.
- (16) Zhang, C.; Zhang, L.; Xu, T.; Xue, R.; Yu, L.; Zhu, Y.; Wu, Y.; Zhang, Q.; Li, D.; Shen, S.; et al. Mapping the spreading routes of lymphatic metastases in human colorectal cancer. *Nat Commun* **2020**, *11* (1), 1993-1993. DOI: 10.1038/s41467-020-15886-6.
- (17) Xia, W.; Geng, Y.; Hu, W. Peritoneal Metastasis: A Dilemma and Challenge in the Treatment of Metastatic Colorectal Cancer. *Cancers (Basel)* **2023**, *15* (23). DOI: 10.3390/cancers15235641.
- (18) Chiappetta, M.; Salvatore, L.; Congedo, M. T.; Bensi, M.; De Luca, V.; Petracca Ciavarella, L.; Camarda, F.; Evangelista, J.; Valentini, V.; Tortora, G.; et al. Management of single pulmonary metastases from colorectal cancer: State of the art. *World journal of gastrointestinal oncology* **2022**, *14* (4), 820-832. DOI: 10.4251/wjgo.v14.i4.820.
- (19) Benson, A. B.; Venook, A. P.; Al-Hawary, M. M.; Cederquist, L.; Chen, Y.-J.; Ciombor, K. K.; Cohen, S.; Cooper, H. S.; Deming, D.; Engstrom, P. F.; et al. NCCN Guidelines Insights: Colon Cancer, Version 2.2018. *Journal of the National Comprehensive Cancer Network* **2018**, *16* (4), 359-369. DOI: 10.6004/jnccn.2018.0021.
- (20) Verwaal, V. J.; Bruin, S.; Boot, H.; van Slooten, G.; van Tinteren, H. 8-Year Follow-up of Randomized Trial: Cytoreduction and Hyperthermic Intraperitoneal Chemotherapy Versus Systemic Chemotherapy in Patients with Peritoneal Carcinomatosis of Colorectal Cancer. *Ann Surg Oncol* **2008**, *15* (9), 2426-2432. DOI: 10.1245/s10434-008-9966-2.
- (21) Jayne, D. G.; Fook, S.; Loi, C.; Seow-Choen, F. Peritoneal carcinomatosis from colorectal cancer. *Br J Surg* **2002**, *89* (12), 1545-1550. DOI: 10.1046/j.1365-2168.2002.02274.x.

- (22) Nagtegaal, N. H. a. C. J. H. a. J. H. W. a. I. D. Metastatic pattern in colorectal cancer is strongly influenced by histological subtype. *Annals of Oncology* **2014**, 25 (3), 651-657. DOI: <https://doi.org/10.1093/annonc/mdt591>.
- (23) Ceelen, W. P. D.; Bracke, M. E. P. Peritoneal minimal residual disease in colorectal cancer: mechanisms, prevention, and treatment. *Lancet Oncol* **2009**, 10 (1), 72-79. DOI: 10.1016/S1470-2045(08)70335-8.
- (24) Sleeman, J.; Steeg, P. S. Cancer metastasis as a therapeutic target: Stopping Cancer in its Tracks: Metastasis as a Therapeutic Target. *European journal of cancer (1990)* **2010**, 46 (7), 1177-1180.
- (25) Pandya, P.; Orgaz, J. L.; Sanz-Moreno, V. Actomyosin contractility and collective migration: may the force be with you. *Curr Opin Cell Biol* **2017**, 48, 87-96. DOI: 10.1016/j.ceb.2017.06.006.
- (26) Lim, S. H. S.; Becker, T. M.; Chua, W.; Ng, W. L.; de Souza, P.; Spring, K. J. Circulating tumour cells and the epithelial mesenchymal transition in colorectal cancer. *Journal of clinical pathology* **2014**, 67 (10), 848-853. DOI: 10.1136/jclinpath-2014-202499.
- (27) Sugarbaker, P. H. Observations concerning cancer spread within the peritoneal cavity and concepts supporting an ordered pathophysiology. *Peritoneal carcinomatosis: principles of management* **1996**, 79-100.
- (28) Pretzsch, E.; Bösch, F.; Neumann, J.; Ganschow, P.; Bazhin, A.; Guba, M.; Werner, J.; Angele, M. Mechanisms of Metastasis in Colorectal Cancer and Metastatic Organotropism: Hematogenous versus Peritoneal Spread. *Journal of oncology* **2019**, 2019, 1-13. DOI: 10.1155/2019/7407190.
- (29) Sluiter, N.; de Cuba, E.; Kwakman, R.; Kazemier, G.; Meijer, G.; te Velde, E. A. Adhesion molecules in peritoneal dissemination: function, prognostic relevance and therapeutic options. *Clinical & experimental metastasis* **2016**, 33 (5), 401-416. DOI: 10.1007/s10585-016-9791-0.
- (30) Lemoine, L.; Sugarbaker, P.; Van der Speeten, K. Pathophysiology of colorectal peritoneal carcinomatosis: Role of the peritoneum. *World J Gastroenterol* **2016**, 22 (34), 7692-7707. DOI: 10.3748/wjg.v22.i34.7692.
- (31) Marcuello, M.; Mayol, X.; Felipe-Fumero, E.; Costa, J.; López-Hierro, L.; Salvans, S.; Alonso, S.; Pascual, M.; Grande, L.; Pera, M. Modulation of the colon cancer cell phenotype by pro-inflammatory macrophages: A preclinical model of surgery-associated inflammation and tumor recurrence. *PLoS One* **2018**, 13 (2), e0192958-e0192958. DOI: 10.1371/journal.pone.0192958.
- (32) de Cuba, E. M. V.; Kwakman, R.; van Egmond, M.; Bosch, L. J. W.; Bonjer, H. J.; Meijer, G. A.; te Velde, E. A. Understanding molecular mechanisms in peritoneal



dissemination of colorectal cancer: Future possibilities for personalised treatment by use of biomarkers. *Virchows Arch* **2012**, *461* (3), 231-243. DOI: 10.1007/s00428-012-1287-y.

(33) Sugarbaker, P. Peritoneal Metastases from Gastrointestinal Cancer. *Current Oncology Reports* **2018**, *20* (8), 1--15.

(34) Mauri, G.; Sartore-Bianchi, A.; Russo, A. G.; Marsoni, S.; Bardelli, A.; Siena, S. Early-onset colorectal cancer in young individuals. *Mol Oncol* **2019**, *13* (2), 109-131. DOI: 10.1002/1878-0261.12417.

(35) Sommariva, A.; Tonello, M.; Coccolini, F.; De Manzoni, G.; Delrio, P.; Pizzolato, E.; Gelmini, R.; Serra, F.; Rreka, E.; Pasqual, E. M.; et al. Colorectal Cancer with Peritoneal Metastases: The Impact of the Results of PROPHYLOCHIP, COLOPEC, and PRODIGE 7 Trials on Peritoneal Disease Management. *Cancers (Basel)* **2022**, *15* (1), 165. DOI: 10.3390/cancers15010165.

(36) UK, C. R. *Having a colostomy*. 2022. <https://www.cancerresearchuk.org/about-cancer/bowel-cancer/treatment/treatment-colon/surgery-colon/having-a-colostomy#:~:text=A%20colostomy%20is%20an%20operation,stoma%20to%20collect%20your%20poo>. (accessed).

(37) Sun, V.; Grant, M.; McMullen, C. K.; Altschuler, A.; Mohler, M. J.; Hornbrook, M. C.; Herrinton, L. J.; Baldwin, C. M.; Krouse, R. S. Surviving Colorectal Cancer: Long-term, Persistent Ostomy-Specific Concerns and Adaptations. *Journal of wound, ostomy, and continence nursing* **2013**, *40* (1), 61-72. DOI: 10.1097/WON.0b013e3182750143.

(38) Rutherford, C.; Müller, F.; Faiz, N.; King, M. T.; White, K. Patient-reported outcomes and experiences from the perspective of colorectal cancer survivors: meta-synthesis of qualitative studies. **2020**, *4* (1), 27.

(39) Marcellinaro, R.; Spoletini, D.; Grieco, M.; Avella, P.; Cappuccio, M.; Troiano, R.; Lisi, G.; Garbarino, G. M.; Carlini, M. Colorectal Cancer: Current Updates and Future Perspectives. *J Clin Med* **2023**, *13* (1), 40. DOI: 10.3390/jcm13010040.

(40) Conteduca, V.; Sansonno, D.; Russi, S.; Dammacco, F. Precancerous colorectal lesions (Review). *International journal of oncology* **2013**, *43* (4), 973-984. DOI: 10.3892/ijo.2013.2041.

(41) Jasperson, K. W.; Tuohy, T. M.; Neklason, D. W.; Burt, R. W. Hereditary and Familial Colon Cancer. *Gastroenterology* **2010**, *138* (6), 2044-2058. DOI: 10.1053/j.gastro.2010.01.054.

(42) Ashworth, A.; Hewish, M.; Lord, C. J.; Martin, S. A.; Cunningham, D. Mismatch repair deficient colorectal cancer in the era of personalized treatment. *Nat Rev Clin Oncol* **2010**, *7* (4), 197-208. DOI: 10.1038/nrclinonc.2010.18.

- (43) van Kessel, A. G.; Hoenselaar, E.; Voorendt, M.; Kuiper, R. P.; Lee, T. Y. H.; Hendriks-Cornelissen, S. J. B.; Yuen, S. T.; van Krieken, J. H. J. M.; Leung, S. Y.; Hoogerbrugge, N.; et al. Heritable somatic methylation and inactivation of MSH2 in families with Lynch syndrome due to deletion of the 3' exons of TACSTD1. *Nat Genet* **2009**, *41* (1), 112-117. DOI: 10.1038/ng.283.
- (44) Fessler, E.; Medema, J. P. Colorectal Cancer Subtypes: Developmental Origin and Microenvironmental Regulation. *Trends Cancer* **2016**, *2* (9), 505-518. DOI: 10.1016/j.trecan.2016.07.008.
- (45) De Palma, F. D. E.; D'Argenio, V.; Pol, J.; Kroemer, G.; Maiuri, M. C.; Salvatore, F. The Molecular Hallmarks of the Serrated Pathway in Colorectal Cancer. *Cancers (Basel)* **2019**, *11* (7), 1017. DOI: 10.3390/cancers11071017.
- (46) Meguid, R. A.; Slidell, M. B.; Wolfgang, C. L.; Chang, D. C.; Ahuja, N. Is there a difference in survival between right- versus left-sided colon cancers? *Annals of surgical oncology* **2008**, *15* (9), 2388-2394. DOI: 10.1245/s10434-008-0015-y.
- (47) *SEER\*Explorer: An interactive website for SEER cancer statistics [Internet]*. Surveillance Research Program, National Cancer Institute, [https://seer.cancer.gov/statistics-network/explorer/application.html?site=1&data\\_type=1&graph\\_type=2&compareBy=sex&chk\\_sex\\_3=3&chk\\_sex\\_2=2&rate\\_type=2&race=1&age\\_range=1&hdn\\_stage=101&advopt\\_precision=1&advopt\\_show\\_ci=on&hdn\\_view=0&advopt\\_show\\_apc=on&advopt\\_display=2#resultsRegion0](https://seer.cancer.gov/statistics-network/explorer/application.html?site=1&data_type=1&graph_type=2&compareBy=sex&chk_sex_3=3&chk_sex_2=2&rate_type=2&race=1&age_range=1&hdn_stage=101&advopt_precision=1&advopt_show_ci=on&hdn_view=0&advopt_show_apc=on&advopt_display=2#resultsRegion0) (accessed).
- (48) Nawa, T.; Kato, J.; Kawamoto, H.; Okada, H.; Yamamoto, H.; Kohno, H.; Endo, H.; Shiratori, Y. Differences between right- and left-sided colon cancer in patient characteristics, cancer morphology and histology. *J Gastroenterol Hepatol* **2008**, *23* (3), 418-423. DOI: 10.1111/j.1440-1746.2007.04923.x.
- (49) Reif de Paula, T.; Simon, H. L.; Profeta da Luz, M. M.; Keller, D. S. Right sided colorectal cancer increases with age and screening should be tailored to reflect this: a national cancer database study. *Tech Coloproctol* **2021**, *25* (1), 81-89. DOI: 10.1007/s10151-020-02329-z.
- (50) Kasi, P. M.; Shahjehan, F.; Cochuyt, J. J.; Li, Z.; Colibaseanu, D. T.; Merchea, A. Rising Proportion of Young Individuals With Rectal and Colon Cancer. *Clin Colorectal Cancer* **2019**, *18* (1), e87-e95. DOI: 10.1016/j.clcc.2018.10.002.
- (51) Holowatyj, A. N.; Wen, W.; Gibbs, T.; Seagle, H. M.; Keller, S. R.; Edwards, D. R. V.; Washington, M. K.; Eng, C.; Perea, J.; Zheng, W.; et al. Racial/Ethnic and Sex Differences in Somatic Cancer Gene Mutations among Patients with Early-Onset Colorectal Cancer. *Cancer Discov* **2023**, *13* (3), 570-579. DOI: 10.1158/2159-8290.CD-22-0764.

- (52) Carethers, J. M. Racial and ethnic disparities in colorectal cancer incidence and mortality. *Adv Cancer Res* **2021**, *151*, 197-229. DOI: 10.1016/bs.acr.2021.02.007.
- (53) Loughran, E. A.; Leonard, A. K.; Hilliard, T. S.; Phan, R. C.; Yemc, M. G.; Harper, E.; Sheedy, E.; Klymenko, Y.; Asem, M.; Liu, Y.; et al. Aging Increases Susceptibility to Ovarian Cancer Metastasis in Murine Allograft Models and Alters Immune Composition of Peritoneal Adipose Tissue. *Neoplasia* **2018**, *20* (6), 621-631. DOI: 10.1016/j.neo.2018.03.007.
- (54) Perotti, V.; Fabiano, S.; Contiero, P.; Michiara, M.; Musolino, A.; Boschetti, L.; Cascone, G.; Castelli, M.; Tagliabue, G.; Cancer Registries Working Group. Influence of Sex and Age on Site of Onset, Morphology, and Site of Metastasis in Colorectal Cancer: A Population-Based Study on Data from Four Italian Cancer Registries. *Cancers (Basel)* **2023**, *15* (3). DOI: 10.3390/cancers15030803.
- (55) Barzi, A.; Lenz, A. M.; Labonte, M. J.; Lenz, H. J. Molecular pathways: Estrogen pathway in colorectal cancer. *Clin Cancer Res* **2013**, *19* (21), 5842-5848. DOI: 10.1158/1078-0432.CCR-13-0325.
- (56) Maingi, J. W.; Tang, S.; Liu, S.; Ngenya, W.; Bao, E. Targeting estrogen receptors in colorectal cancer. *Mol Biol Rep* **2020**, *47* (5), 4087-4091. DOI: 10.1007/s11033-020-05414-6.
- (57) Pretzsch, E.; Nieß, H.; Bösch, F.; Westphalen, C. B.; Jacob, S.; Neumann, J.; Werner, J.; Heinemann, V.; Angele, M. K. Age and metastasis – How age influences metastatic spread in cancer. Colorectal cancer as a model. *Cancer Epidemiol* **2022**, *77*, 102112-102112. DOI: 10.1016/j.canep.2022.102112.
- (58) Jafari, M. D.; Jafari, F.; Halabi, W. J.; Nguyen, V. Q.; Pigazzi, A.; Carmichael, J. C.; Mills, S. D.; Stamos, M. J. Colorectal Cancer Resections in the Aging US Population A Trend Toward Decreasing Rates and Improved Outcomes. *JAMA surgery* **2014**, *149* (6), 557-564. DOI: 10.1001/jamasurg.2013.4930.
- (59) Dong, M.; Cioffi, G.; Wang, J.; Waite, K. A.; Ostrom, Q. T.; Kruchko, C.; Lathia, J. D.; Rubin, J. B.; Berens, M. E.; Connor, J.; et al. Sex Differences in Cancer Incidence and Survival: A Pan-Cancer Analysis. *Cancer Epidemiol Biomarkers Prev* **2020**, *29* (7), 1389-1397. DOI: 10.1158/1055-9965.EPI-20-0036.
- (60) Majek, O.; Gondos, A.; Jansen, L.; Emrich, K.; Holleczer, B.; Katalinic, A.; Nennecke, A.; Eberle, A.; Brenner, H.; Group, G. C. S. W. Sex differences in colorectal cancer survival: population-based analysis of 164,996 colorectal cancer patients in Germany. *PLoS One* **2013**, *8* (7), e68077. DOI: 10.1371/journal.pone.0068077.
- (61) Dekker, E.; Tanis, P.; Vleugels, J.; Kasi, P.; Wallace, M. Colorectal cancer [Internet].
- (62) Abancens, M.; Bustos, V.; Harvey, H.; McBryan, J.; Harvey, B. J. Sexual Dimorphism in Colon Cancer. *Front Oncol* **2020**, *10*, 607909-607909. DOI: 10.3389/fonc.2020.607909.

- (63) Hong, S.; Won, Y.-J.; Park, Y. R.; Jung, K.-W.; Kong, H.-J.; Lee, E. S. Cancer Statistics in Korea: Incidence, Mortality, Survival, and Prevalence in 2017. *Cancer Res Treat* **2020**, *52* (2), 335-350. DOI: 10.4143/crt.2020.206.
- (64) Li, C. H.; Prokopec, S. D.; Sun, R. X.; Yousif, F.; Schmitz, N.; Boutros, P. C.; Translation, P. T. S. a. C.; Consortium, P. Sex differences in oncogenic mutational processes. *Nat Commun* **2020**, *11* (1), 4330. DOI: 10.1038/s41467-020-17359-2.
- (65) Zervoudakis, A.; Strickler, H. D.; Park, Y.; Xue, X.; Hollenbeck, A.; Schatzkin, A.; Gunter, M. J. Reproductive history and risk of colorectal cancer in postmenopausal women. *J Natl Cancer Inst* **2011**, *103* (10), 826-834. DOI: 10.1093/jnci/djr101.
- (66) Amitay, E. L.; Niedermaier, T.; Alwers, E.; Chang-Claude, J.; Hoffmeister, M.; Brenner, H. Reproductive Factors and Colorectal Cancer Risk: A Population-Based Case-Control Study. *JNCI Cancer Spectr* **2022**, *6* (4). DOI: 10.1093/jncics/pkac042.
- (67) White, A.; Ironmonger, L.; Steele, R. J. C.; Ormiston-Smith, N.; Crawford, C.; Seims, A. A review of sex-related differences in colorectal cancer incidence, screening uptake, routes to diagnosis, cancer stage and survival in the UK. *BMC Cancer* **2018**, *18* (1), 906-906. DOI: 10.1186/s12885-018-4786-7.
- (68) Wong, M. C. S.; Ching, J. Y. L.; Chan, V. C. W.; Lam, T. Y. T.; Luk, A. K. C.; Wong, S. H.; Ng, S. C.; Ng, S. S. M.; Wu, J. C. Y.; Chan, F. K. L.; et al. Colorectal Cancer Screening Based on Age and Gender: A Cost-Effectiveness Analysis. *Medicine (Baltimore)* **2016**, *95* (10), e2739-e2739. DOI: 10.1097/MD.0000000000002739.
- (69) Yang, Y.; Wang, G.; He, J.; Ren, S.; Wu, F.; Zhang, J.; Wang, F. Gender differences in colorectal cancer survival: A meta-analysis. *Int J Cancer* **2017**, *141* (10), 1942-1949. DOI: 10.1002/ijc.30827.
- (70) Park, H. C.; Shin, A.; Kim, B. W.; Jung, K. W.; Won, Y. J.; Oh, J. H.; Jeong, S. Y.; Yu, C. S.; Lee, B. H. Data on the characteristics and the survival of korean patients with colorectal cancer from the Korea central cancer registry. *Ann Coloproctol* **2013**, *29* (4), 144-149. DOI: 10.3393/ac.2013.29.4.144.
- (71) Kim, S.-E.; Paik, H. Y.; Yoon, H.; Lee, J. E.; Kim, N.; Sung, M.-K. Sex- and gender-specific disparities in colorectal cancer risk. *World Journal of Gastroenterology* **2015**, *21* (17), 5167-5175. DOI: 10.3748/wjg.v21.i17.5167.
- (72) Rubin, J. B.; Lagas, J. S.; Broestl, L.; Sponagel, J.; Rockwell, N.; Rhee, G.; Rosen, S. F.; Chen, S.; Klein, R. S.; Imoukhuede, P.; et al. Sex differences in cancer mechanisms. *Biol Sex Differ* **2020**, *11* (1), 17-17. DOI: 10.1186/s13293-020-00291-x.
- (73) Hendifar, A.; Yang, D.; Lenz, F.; Lurje, G.; Pohl, A.; Lenz, C.; Ning, Y.; Zhang, W.; Lenz, H.-J. Gender Disparities in Metastatic Colorectal Cancer Survival. *Clin Cancer Res* **2009**, *15* (20), 6391-6397. DOI: 10.1158/1078-0432.CCR-09-0877.

- (74) Matarrese, P.; Mattia, G.; Pagano, M. T.; Pontecorvi, G.; Ortona, E.; Malorni, W.; Care, A. The Sex-Related Interplay between TME and Cancer: On the Critical Role of Estrogen, MicroRNAs and Autophagy. *Cancers* **2021**, *13* (13), 3287. DOI: 10.3390/cancers13133287.
- (75) Young, V. J.; Brown, J. K.; Saunders, P. T. K.; Horne, A. W. The role of the peritoneum in the pathogenesis of endometriosis. *Hum Reprod Update* **2013**, *19* (5), 558-569. DOI: 10.1093/humupd/dmt024.
- (76) Yung, S.; Chan, T.-M. Peritoneal mesothelial cells and the extracellular matrix. *Nephrology (Carlton, Vic.)* **2001**, *6* (6), 250-258. DOI: 10.1046/j.1440-1797.2001.00081.x.
- (77) Nagy, J. A.; Jackman, R. W. Anatomy and Physiology of the Peritoneal Membrane. *Seminars in dialysis* **1998**, *11* (1), 49-56. DOI: 10.1111/j.1525-139X.1998.tb00210.x.
- (78) Liu, Y.; Metzinger, M. N.; Lewellen, K. A.; Cripps, S. N.; Carey, K. D.; Harper, E. I.; Shi, Z.; Tarwater, L.; Grisoli, A.; Lee, E.; et al. Obesity Contributes to Ovarian Cancer Metastatic Success through Increased Lipogenesis, Enhanced Vascularity, and Decreased Infiltration of M1 Macrophages. *Cancer Res* **2015**, *75* (23), 5046-5057. DOI: 10.1158/0008-5472.CAN-15-0706.
- (79) Sodek, K. L.; Murphy, K. J.; Brown, T. J.; Ringuette, M. J. Cell–cell and cell–matrix dynamics in intraperitoneal cancer metastasis. *Cancer Metastasis Rev* **2012**, *31* (1-2), 397-414. DOI: 10.1007/s10555-012-9351-2.
- (80) Witz, C. Composition of the extracellular matrix of the peritoneum. *Journal of the Society for Gynecologic Investigation* **2001**, *8* (5), 299-304. DOI: 10.1016/S1071-5576(01)00122-8.
- (81) Albanese, A. M.; Albanese, E. F.; Miño, J. H.; Gómez, E.; Gómez, M.; Zandomeni, M.; Merlo, A. B. Peritoneal surface area: measurements of 40 structures covered by peritoneum: correlation between total peritoneal surface area and the surface calculated by formulas. *Surg Radiol Anat* **2009**, *31* (5), 369-377. DOI: 10.1007/s00276-008-0456-9.
- (82) Patel, R. R.; Planche, K. Applied peritoneal anatomy. *Clin Radiol* **2013**, *68* (5), 509-520. DOI: 10.1016/j.crad.2012.06.135.
- (83) Lengyel, E. Ovarian Cancer Development and Metastasis. *Am J Pathol* **2010**, *177* (3), 1053-1064. DOI: 10.2353/ajpath.2010.100105.
- (84) Frantz, C.; Stewart, K. M.; Weaver, V. M. The extracellular matrix at a glance. *J Cell Sci* **2010**, *123* (24), 4195-4200. DOI: 10.1242/jcs.023820.
- (85) Haar, J. L.; Ackerman, G. A. A phase and electron microscopic study of vasculogenesis and erythropoiesis in the yolk sac of the mouse. *Anat Rec* **1971**, *170* (2), 199-223. DOI: 10.1002/ar.1091700206.

- (86) Yung, S.; Chan, T. M. Pathophysiology of the Peritoneal Membrane during Peritoneal Dialysis: The Role of Hyaluronan. *J Biomed Biotechnol* **2011**, *2011* (1), 180594. DOI: 10.1155/2011/180594.
- (87) Yung, S.; Li, F. K.; Chan, T. M. Peritoneal Mesothelial Cell Culture and Biology. *Peritoneal dialysis international* **2006**, *26* (2), 162-193. DOI: 10.1177/089686080602600207.
- (88) Riera, M.; McCulloch, P.; Pazmany, L.; Jagoe, T. Optimal method for isolation of human peritoneal mesothelial cells from clinical samples of omentum. *J Tissue Viability* **2006**, *16* (4), 22-24.
- (89) Stylianou, E.; Jenner, L. A.; Davies, M.; Coles, G. A.; Williams, J. D. Isolation, culture and characterization of human peritoneal mesothelial cells. *Kidney Int* **1990**, *37* (6), 1563-1570. DOI: 10.1038/ki.1990.150.
- (90) Zhou, Q.; Yu, X. Isolation and Propagation of Rat Peritoneal Mesothelial Cells. *Methods Mol Biol* **2016**, *1397*, 25-34. DOI: 10.1007/978-1-4939-3353-2\_3.
- (91) Hudson, L. G.; Zeineldin, R.; Stack, M. S. Phenotypic plasticity of neoplastic ovarian epithelium: unique cadherin profiles in tumor progression. *Clin Exp Metastasis* **2008**, *25* (6), 643-655. DOI: 10.1007/s10585-008-9171-5.
- (92) Andrews, P. M.; Porter, K. R. The ultrastructural morphology and possible functional significance of mesothelial microvilli. *Anat Rec* **1973**, *177* (3), 409-426. DOI: 10.1002/ar.1091770307.
- (93) Dobbie, J. W.; Zaki, M.; Wilson, L. Ultrastructural Studies on the Peritoneum with Special Reference to Chronic Ambulatory Peritoneal Dialysis. *Scottish medical journal* **1981**, *26* (3), 213-223. DOI: 10.1177/003693308102600305.
- (94) Mikula-Pietrasik, J.; Sosińska, P.; Maksin, K.; Kucińska, M. G.; Piotrowska, H.; Murias, M.; Woźniak, A.; Szpurek, D.; Książek, K. Colorectal cancer-promoting activity of the senescent peritoneal mesothelium. *Oncotarget* **2015**, *6* (30), 29178-29195. DOI: 10.18632/oncotarget.4932.
- (95) Heldin, P.; Kolliopoulos, C.; Lin, C.-Y.; Heldin, C.-H. Involvement of hyaluronan and CD44 in cancer and viral infections. *Cell Signal* **2020**, *65*, 109427-109427. DOI: 10.1016/j.cellsig.2019.109427.
- (96) Heath, R. M.; Jayne, D. G.; O'Leary, R.; Morrison, E. E.; Guillou, P. J. Tumour-induced apoptosis in human mesothelial cells: a mechanism of peritoneal invasion by Fas Ligand Fas interaction. *Br J Cancer* **2004**, *90* (7), 1437-1442. DOI: 10.1038/sj.bjc.6601635.
- (97) Lee, I. K. M. D.; VanSaun, M. N. P.; Shim, J. H. M. D.; Matrisian, L. M. P.; Gorden, D. L. M. D. Increased metastases are associated with inflammation and matrix

- metalloproteinase-9 activity at incision sites in a murine model of peritoneal dissemination of colorectal cancer. *J Surg Res* **2013**, *180* (2), 252-259. DOI: 10.1016/j.jss.2012.04.074.
- (98) Kataoka, H.; Tanaka, H.; Nagaike, K.; Uchiyama, S.; Itoh, H. Role of Cancer Cell-Stroma Interaction in Invasive Growth of Cancer Cells. *Hum Cell* **2003**, *16* (1), 1-14. DOI: 10.1111/j.1749-0774.2003.tb00123.x.
- (99) Kim, T.-D.; Song, K.-S.; Li, G.; Choi, H.; Park, H.-D.; Lim, K.; Hwang, B.-D.; Yoon, W.-H. Activity and expression of urokinase-type plasminogen activator and matrix metalloproteinases in human colorectal cancer. *BMC Cancer* **2006**, *6* (1), 211-211. DOI: 10.1186/1471-2407-6-211.
- (100) Nataraj, N. B.; Marrocco, I.; Yarden, Y. Roles for growth factors and mutations in metastatic dissemination. *Biochem Soc Trans* **2021**, *49* (3), 1409-1423. DOI: 10.1042/BST20210048.
- (101) Flurkey K, M. C. J., Harrison DE. Chapter 20 - Mouse Models in Aging Research. In: Smith AL., editor. *The Mouse in Biomedical Research* (Second Edition). Burlington: Academic Press 2007. p. 637-72.
- (102) Majek, O.; Gondos, A.; Jansen, L.; Emrich, K.; Holleczech, B.; Katalinic, A.; Nennecke, A.; Eberle, A.; Brenner, H. Sex differences in colorectal cancer survival: population-based analysis of 164,996 colorectal cancer patients in Germany. *PLoS One* **2013**, *8* (7), e68077-e68077. DOI: 10.1371/journal.pone.0068077.
- (103) Gupta, O. T.; Gupta, R. K. Visceral Adipose Tissue Mesothelial Cells: Living on the Edge or Just Taking Up Space? *Trends Endocrinol Metab* **2015**, *26* (10), 515-523. DOI: 10.1016/j.tem.2015.07.003.
- (104) Young, V. J.; Brown, J. K.; Saunders, P. T. K.; Horne, A. W. The role of the peritoneum in the pathogenesis of endometriosis. *Human reproduction update* **2013**, *19* (5), 558-569. DOI: 10.1093/humupd/dmt024.
- (105) Kenny, H. A.; Krausz, T.; Yamada, S. D.; Lengyel, E. Use of a novel 3D culture model to elucidate the role of mesothelial cells, fibroblasts and extra-cellular matrices on adhesion and invasion of ovarian cancer cells to the omentum. *Int J Cancer* **2007**, *121* (7), 1463-1472. DOI: 10.1002/ijc.22874.
- (106) Harper, E. I.; Hilliard, T. S.; Sheedy, E. F.; Carey, P.; Wilkinson, P.; Siroky, M. D.; Yang, J.; Agadi, E.; Leonard, A. K.; Low, E.; et al. Another wrinkle with age: Aged collagen and intra-peritoneal metastasis of ovarian cancer. *Aging and cancer* **2022**, *3* (2), 116-129. DOI: 10.1002/aac2.12049.
- (107) Zougman, A.; Selby, P. J.; Banks, R. E. Suspension trapping (STrap) sample preparation method for bottom-up proteomics analysis. *Proteomics* **2014**, *14* (9), 1006-1000. DOI: 10.1002/pmic.201300553.

- (108) Bruney, L.; Liu, Y.; Grisoli, A.; Ravosa, M. J.; Stack, M. S. Integrin-linked kinase activity modulates the pro-metastatic behavior of ovarian cancer cells. *Oncotarget* **2016**, *7* (16), 21968-21981. DOI: 10.18632/oncotarget.7880.
- (109) Yang, J.; Kasberg, W. C.; Celo, A.; Liang, Z.; Quispe, K.; Stack, M. S. Post-translational modification of the membrane type 1 matrix metalloproteinase (MT1-MMP) cytoplasmic tail impacts ovarian cancer multicellular aggregate dynamics. *J Biol Chem* **2017**, *292* (32), 13111-13121. DOI: 10.1074/jbc.M117.800904.
- (110) Sterck, L. *Calculate and draw custom Venn diagrams*. VIB-UGENT CENTER FOR PLANT SYSTEMS BIOLOGY, <https://bioinformatics.psb.ugent.be/webtools/Venn/> (accessed 2022 07/16).
- (111) Ge, S. X.; Jung, D.; Yao, R. ShinyGO: a graphical gene-set enrichment tool for animals and plants. *Bioinformatics* **2019**, *36* (8), 2628-2629. DOI: 10.1093/bioinformatics/btz931 (accessed 11/17/2022).
- (112) Lex, A.; Gehlenborg, N.; Strobel, H.; Vuilleumot, R.; Pfister, H. UpSet: Visualization of Intersecting Sets. *IEEE Trans Vis Comput Graph* **2014**, *20* (12), 1983-1992. DOI: 10.1109/TVCG.2014.2346248.
- (113) Creaney, J.; Dick, I. M.; Leon, J. S.; Robinson, B. W. A Proteomic Analysis of the Malignant Mesothelioma Secretome Using iTRAQ. *Cancer Genomics Proteomics* **2017**, *14* (2), 103-117. DOI: 10.21873/cgp.20023.
- (114) Boehm, M.; Herzog, R.; Klinglmüller, F.; Lichtenauer, A. M.; Wagner, A.; Unterwurzacher, M.; Beelen, R. H. J.; Alper, S. L.; Aufricht, C.; Kratochwill, K. The Peritoneal Surface Proteome in a Model of Chronic Peritoneal Dialysis Reveals Mechanisms of Membrane Damage and Preservation. *Front Physiol* **2019**, *10*, 472. DOI: 10.3389/fphys.2019.00472.
- (115) Shi, J.; Ye, J.; Fei, H.; Jiang, S.-H.; Wu, Z.-Y.; Chen, Y.-P.; Zhang, L.-W.; Yang, X.-M. YWHAZ promotes ovarian cancer metastasis by modulating glycolysis. *Oncol Rep* **2018**, *41* (2), 1101-1112. DOI: 10.3892/or.2018.6920.
- (116) Du, G.; Yu, X.; Chen, Y.; Cai, W. MiR-1-3p Suppresses Colorectal Cancer Cell Proliferation and Metastasis by Inhibiting YWHAZ-Mediated Epithelial-Mesenchymal Transition. *Front Oncol* **2021**, *11*, 634596-634596. DOI: 10.3389/fonc.2021.634596.
- (117) Chen, M.; Hu, W.; Xiong, C.-L.; Qu, Z.; Yin, C.-Q.; Wang, Y.-H.; Luo, C.-L.; Guan, Q.; Yuan, C.-H.; Wang, F.-B. miR-22 targets YWHAZ to inhibit metastasis of hepatocellular carcinoma and its down-regulation predicts a poor survival. *Oncotarget* **2016**, *7* (49), 80751-80764. DOI: 10.18632/oncotarget.13037.
- (118) Bucki, R.; Levental, I.; Kulakowska, A.; Janmey, P. A. Plasma gelsolin: function, prognostic value, and potential therapeutic use. *Curr Protein Pept Sci* **2008**, *9* (6), 541-551. DOI: 10.2174/138920308786733912.



- (119) Bruschi, M.; Candiano, G.; Santucci, L.; D'Ambrosio, C.; Scaloni, A.; Bonsano, M.; Ghiggeri, G. M.; Verrina, E. Combinatorial Peptide Ligand Library and two dimensional electrophoresis: New frontiers in the study of peritoneal dialysis effluent in pediatric patients. *Journal of proteomics* **2015**, *116*, 68-80. DOI: 10.1016/j.jprot.2015.01.003.
- (120) Li, W.-X.; Yang, M.-X.; Hong, X.-Q.; Dong, T.-G.; Yi, T.; Lin, S.-L.; Qin, X.-Y.; Niu, W.-X. Overexpression of gelsolin reduces the proliferation and invasion of colon carcinoma cells. *Mol Med Rep* **2016**, *14* (4), 3059-3065. DOI: 10.3892/mmr.2016.5652.
- (121) Karamagkiolas, S.; Giotakis, I.; Kyrodimos, E.; Giotakis, E. I.; Kataki, A.; Karagianni, F.; Lazaris, A. M. Expression of vimentin (VIM) and metastasis-associated 1 (MTA1) protein in laryngeal squamous cell carcinoma are associated with prognostic outcome of patients. *Am J Otolaryngol* **2019**, *40* (4), 487-493. DOI: 10.1016/j.amjoto.2019.04.002.
- (122) Bogdanovic, A.; Despotovic, J.; Galun, D.; Bidzic, N.; Nikolic, A.; Rosic, J.; Krivokapic, Z. Prognostic Significance of CDH1 , FN1 and VIM for Early Recurrence in Patients with Colorectal Liver Metastasis After Liver Resection. *Cancer Manag Res* **2021**, *13*, 163-171. DOI: 10.2147/CMAR.S287974.
- (123) Liu, C.-Y.; Lin, H.-H.; Tang, M.-J.; Wang, Y.-K. Vimentin contributes to epithelial-mesenchymal transition cancer cell mechanics by mediating cytoskeletal organization and focal adhesion maturation. *Oncotarget* **2015**, *6* (18), 15966-15983. DOI: 10.18632/oncotarget.3862.
- (124) Zambelli, D.; Zuntini, M.; Nardi, F.; Manara, M. C.; Serra, M.; Landuzzi, L.; Lollini, P. L.; Ferrari, S.; Alberghini, M.; Llombart-Bosch, A.; et al. Biological indicators of prognosis in Ewing's sarcoma: An emerging role for lectin galactoside-binding soluble 3 binding protein (LGALS3BP). *Int J Cancer* **2010**, *126* (1), 41-52. DOI: 10.1002/ijc.24670.
- (125) Iacobelli, S.; Arnò, E.; D'Orazio, A.; Coletti, G. Detection of antigens recognized by a novel monoclonal antibody in tissue and serum from patients with breast cancer. *Cancer Res* **1986**, *46* (6), 3005-3010.
- (126) Gleissner, C. A.; Erbel, C.; Linden, F.; Domschke, G.; Akhavanpoor, M.; Helmes, C. M.; Doesch, A. O.; Kleber, M. E.; Katus, H. A.; Maerz, W. Galectin-3 binding protein, coronary artery disease and cardiovascular mortality: Insights from the LURIC study. *Atherosclerosis* **2017**, *260*, 121-129. DOI: 10.1016/j.atherosclerosis.2017.03.031.
- (127) Dorrington, M. G.; Bradfield, C. J.; Lack, J. B.; Lin, B.; Liang, J. J.; Starr, T.; Ernst, O.; Gross, J. L.; Sun, J.; Miller, A. H.; et al. Type I IFNs facilitate innate immune control of the opportunistic bacteria *Burkholderia cenocepacia* in the macrophage cytosol. *PLoS Pathog* **2021**, *17* (3), e1009395. DOI: 10.1371/journal.ppat.1009395.
- (128) Xu, G.; Xia, Z.; Deng, F.; Liu, L.; Wang, Q.; Yu, Y.; Wang, F.; Zhu, C.; Liu, W.; Cheng, Z.; et al. Inducible LGALS3BP/90K activates antiviral innate immune responses

by targeting TRAF6 and TRAF3 complex. *PLoS pathogens* **2019**, *15* (8), e1008002-e1008002. DOI: 10.1371/journal.ppat.1008002.

(129) Loimaranta, V.; Hepojoki, J.; Laaksoaho, O.; Pulliainen, A. T. Galectin-3-binding protein: A multitask glycoprotein with innate immunity functions in viral and bacterial infections. *J Leukoc Biol* **2018**, *104* (4), 777-786. DOI: 10.1002/JLB.3VMR0118-036R.

(130) Piccolo, E.; Tinari, N.; D'Addario, D.; Rossi, C.; Iacobelli, V.; La Sorda, R.; Lattanzio, R.; D'Egidio, M.; Di Risio, A.; Piantelli, M.; et al. Prognostic relevance of LGALS3BP in human colorectal carcinoma. *J Transl Med* **2015**, *13* (1), 248-248. DOI: 10.1186/s12967-015-0606-x.

(131) Ferragut, F.; Vachetta, V. S.; Troncoso, M. F.; Rabinovich, G. A.; Elola, M. T. ALCAM/CD166: A pleiotropic mediator of cell adhesion, stemness and cancer progression. *Cytokine & growth factor reviews* **2021**, *61*, 27-37. DOI: 10.1016/j.cytogfr.2021.07.001.

(132) von Lersner, A.; Driesen, L.; Zijlstra, A. Modulation of cell adhesion and migration through regulation of the immunoglobulin superfamily member ALCAM/CD166. *Clinical & experimental metastasis* **2019**, *36* (2), 87-95. DOI: 10.1007/s10585-019-09957-2.

(133) Zhang, J.; Ghosh, J.; Mohamad, S. F.; Zhang, C.; Huang, X.; Capitano, M. L.; Gunawan, A. M.; Cooper, S.; Guo, B.; Cai, Q.; et al. CD166 Engagement Augments Mouse and Human Hematopoietic Progenitor Function via Activation of Stemness and Cell Cycle Pathways. *Stem Cells* **2019**, *37* (10), 1319-1330. DOI: 10.1002/stem.3053.

(134) Kim, D. K.; Ham, M. H.; Lee, S. Y.; Shin, M. J.; Kim, Y. E.; Song, P.; Suh, D.-S.; Kim, J. H. CD166 promotes the cancer stem-like properties of primary epithelial ovarian cancer cells. *BMB Reports* **2020**, *53* (12), 622-627. DOI: 10.5483/BMBRep.2020.53.12.102.

(135) Cardeñes, B.; Clares, I.; Bezos, T.; Toribio, V.; López-Martín, S.; Rocha, A.; Peinado, H.; Yáñez-Mó, M.; Cabañas, C. ALCAM/CD166 Is Involved in the Binding and Uptake of Cancer-Derived Extracellular Vesicles. *Int J Mol Sci* **2022**, *23* (10). DOI: 10.3390/ijms23105753.

(136) Peng, M.; Deng, J.; Zhou, S.; Tao, T.; Su, Q.; Yang, X.; Yang, X. The role of Clusterin in cancer metastasis. *Cancer Manag Res* **2019**, *11*, 2405-2414. DOI: 10.2147/CMAR.S196273.

(137) Oh, S. B.; Kim, M. S.; Park, S.; Son, H.; Kim, S. Y.; Kim, M. S.; Jo, D. G.; Tak, E.; Lee, J. Y. Clusterin contributes to early stage of Alzheimer's disease pathogenesis. *Brain Pathol* **2019**, *29* (2), 217-231. DOI: 10.1111/bpa.12660.

(138) Guitart, K.; Loers, G.; Buck, F.; Bork, U.; Schachner, M.; Kleene, R. Improvement of neuronal cell survival by astrocyte-derived exosomes under hypoxic and ischemic conditions depends on prion protein. *Glia* **2016**, *64* (6), 896-910. DOI: 10.1002/glia.22963.

- (139) Chou, T.-Y.; Chen, W.-C.; Lee, A.-C.; Hung, S.-M.; Shih, N.-Y.; Chen, M.-Y. Clusterin silencing in human lung adenocarcinoma cells induces a mesenchymal-to-epithelial transition through modulating the ERK/Slug pathway. *Cell Signal* **2009**, *21* (5), 704-711. DOI: 10.1016/j.cellsig.2009.01.008.
- (140) Téllez, T.; Martín-García, D.; Redondo, M.; García-Aranda, M. Clusterin Expression in Colorectal Carcinomas. *International journal of molecular sciences* **2023**, *24* (19), 14641. DOI: 10.3390/ijms241914641.
- (141) Fu, Y.; Du, Q.; Cui, T.; Lu, Y.; Niu, G. A pan-cancer analysis reveals role of clusterin ( CLU ) in carcinogenesis and prognosis of human tumors. *Front Genet* **2023**, *13*, 1056184-1056184. DOI: 10.3389/fgene.2022.1056184.
- (142) Castro-Sánchez, P.; Ramírez-Munoz, R.; Martín-Cófreces, N. B.; Aguilar-Sopeña, O.; Alegre-Gomez, S.; Hernández-Pérez, S.; Reyes, R.; Zeng, Q.; Cabañas, C.; Sánchez-Madrid, F.; et al. Phosphatase of Regenerating Liver-1 (PRL-1) Regulates Actin Dynamics During Immunological Synapse Assembly and T Cell Effector Function. *Front Immunol* **2018**, *9*, 2655-2655. DOI: 10.3389/fimmu.2018.02655.
- (143) Flores-Perez, A.; Marchat, L. A.; Rodriguez-Cuevas, S.; Pina Bautista, V.; Fuentes-Mera, L.; Romero-Zamora, D.; Maciel-Dominguez, A.; Hernandez de la Cruz, O.; Fonseca-Sanchez, M.; Ruiz-Garcia, E.; et al. Suppression of cell migration is promoted by miR-944 through targeting of SIAH1 and PTP4A1 in breast cancer cells. *BMC Cancer* **2016**, *16* (1), 379-379. DOI: 10.1186/s12885-016-2470-3.
- (144) Diamond, R. H.; Cressman, D. E.; Laz, T. M.; Abrams, C. S.; Taub, R. PRL-1, a unique nuclear protein tyrosine phosphatase, affects cell growth. *Mol Cell Biol* **1994**, *14* (6), 3752-3762. DOI: 10.1128/MCB.14.6.3752.
- (145) Diamond, R. H.; Peters, C.; Jung, S. P.; Greenbaum, L. E.; Haber, B. A.; Silberg, D. G.; Traber, P. G.; Taub, R. Expression of PRL-1 nuclear PTPase is associated with proliferation in liver but with differentiation in intestine. *Am J Physiol* **1996**, *271* (1), G121-G129. DOI: 10.1152/ajpgi.1996.271.1.G121.
- (146) Rios, P.; Li, X.; Köhn, M. Molecular mechanisms of the PRL phosphatases. *FEBS J* **2013**, *280* (2), 505-524. DOI: 10.1111/j.1742-4658.2012.08565.x.
- (147) Wang, J.; Kirby, C. E.; Herbst, R. The Tyrosine Phosphatase PRL-1 Localizes to the Endoplasmic Reticulum and the Mitotic Spindle and Is Required for Normal Mitosis. *J Biol Chem* **2002**, *277* (48), 46659-46668. DOI: 10.1074/jbc.M206407200.
- (148) Peng, Y.; Genin, A.; Spinner, N. B.; Diamond, R. H.; Taub, R. The gene encoding human nuclear protein tyrosine phosphatase, PRL-1 - Cloning, chromosomal localization, and identification of an intron enhancer. *J Biol Chem* **1998**, *273* (27), 17286-17295. DOI: 10.1074/jbc.273.27.17286.

- (149) Dumauval, C. M.; Sandusky, G. E.; Soo, H. W.; Werner, S. R.; Crowell, P. L.; Randall, S. K. Tissue-specific alterations of PRL-1 and PRL-2 expression in cancer. *Am J Transl Res* **2012**, *4* (1), 83-101.
- (150) Huang, L.; Chen, S.; Fan, H.; Ji, D.; Chen, C.; Sheng, W. GINS2 promotes EMT in pancreatic cancer via specifically stimulating ERK/MAPK signaling. *Cancer Gene Ther* **2021**, *28* (7-8), 839-849. DOI: 10.1038/s41417-020-0206-7.
- (151) Carroni, M.; De March, M.; Medagli, B.; Krastanova, I.; Taylor, I. A.; Amenitsch, H.; Araki, H.; Pisani, F. M.; Patwardhan, A.; Onesti, S. New insights into the GINS complex explain the controversy between existing structural models. *Sci Rep* **2017**, *7*, 40188. DOI: 10.1038/srep40188.
- (152) Kubota, Y.; Takase, Y.; Komori, Y.; Hashimoto, Y.; Arata, T.; Kamimura, Y.; Araki, H.; Takisawa, H. A novel ring-like complex of *Xenopus* proteins essential for the initiation of DNA replication. *Genes Dev* **2003**, *17* (9), 1141-1152. DOI: 10.1101/gad.1070003.
- (153) Hu, H.; Ye, L.; Liu, Z. GINS2 regulates the proliferation and apoptosis of colon cancer cells through PTP4A1. *Mol Med Rep* **2022**, *25* (4). DOI: 10.3892/mmr.2022.12633.
- (154) Bai, Y.; Yu, Z.-H.; Liu, S.; Zhang, L.; Zhang, R.-Y.; Zeng, L.-F.; Zhang, S.; Zhang, Z.-Y. Novel Anticancer Agents Based on Targeting the Trimer Interface of the PRL Phosphatase. *Cancer Res* **2016**, *76* (16), 4805-4815. DOI: 10.1158/0008-5472.CAN-15-2323.
- (155) Bai, Y.; Luo, Y.; Liu, S.; Zhang, L.; Shen, K.; Dong, Y.; Walls, C. D.; Quilliam, L. A.; Wells, C. D.; Cao, Y.; et al. PRL-1 protein promotes ERK1/2 and RhoA protein activation through a non-canonical interaction with the Src homology 3 domain of p115 Rho GTPase-activating protein. *J Biol Chem* **2011**, *286* (49), 42316-42324. DOI: 10.1074/jbc.M111.286302.
- (156) Zhang, J. X.; Mai, S. J.; Huang, X. X.; Wang, F. W.; Liao, Y. J.; Lin, M. C.; Kung, H. F.; Zeng, Y. X.; Xie, D. MiR-29c mediates epithelial-to-mesenchymal transition in human colorectal carcinoma metastasis via PTP4A and GNA13 regulation of beta-catenin signaling. *Annals of oncology* **2014**, *25* (11), 2196-2204. DOI: 10.1093/annonc/mdl439.
- (157) Liu, B.; Si, W.; Wei, B.; Zhang, X.; Chen, P. PTP4A1 promotes oral squamous cell carcinoma (OSCC) metastasis through altered mitochondrial metabolic reprogramming. *Cell death discovery* **2023**, *9* (1), 360-360. DOI: 10.1038/s41420-023-01657-x.
- (158) Liu, L.-Z.; He, Y.-Z.; Dong, P.-P.; Ma, L.-J.; Wang, Z.-C.; Liu, X.-Y.; Duan, M.; Yang, L.-X.; Shi, J.-Y.; Zhou, J.; et al. Protein tyrosine phosphatase PTP4A1 promotes proliferation and epithelial-mesenchymal transition in intrahepatic cholangiocarcinoma via the PI3K/AKT pathway. *Oncotarget* **2016**, *7* (46), 75210-75220. DOI: 10.18632/oncotarget.12116.

- (159) Fiordalisi, J. J.; Keller, P. J.; Cox, A. D. PRL tyrosine phosphatases regulate rho family GTPases to promote invasion and motility. *Cancer Res* **2006**, *66* (6), 3153-3161. DOI: 10.1158/0008-5472.CAN-05-3116.
- (160) Mrozik, K. M.; Blaschuk, O. W.; Cheong, C. M.; Zannettino, A. C. W.; Vandyke, K. N-cadherin in cancer metastasis, its emerging role in haematological malignancies and potential as a therapeutic target in cancer. *BMC Cancer* **2018**, *18* (1), 939. DOI: 10.1186/s12885-018-4845-0.
- (161) Luo, Y.; Liang, F.; Zhang, Z. Y. PRL1 promotes cell migration and invasion by increasing MMP2 and MMP9 expression through Src and ERK1/2 pathways. *Biochemistry* **2009**, *48* (8), 1838-1846. DOI: 10.1021/bi8020789.
- (162) Qiu, W.; Cai, X.; Xu, K.; Song, S.; Xiao, Z.; Hou, Y.; Qi, X.; Liu, F.; Chen, Y.; Yang, H.; et al. PRL1 Promotes Glioblastoma Invasion and Tumorigenesis. *Front Oncol* **2021**, *11*, 795633. DOI: 10.3389/fonc.2021.795633.
- (163) Westhoff, M. A.; Serrels, B.; Fincham, V. J.; Frame, M. C.; Carragher, N. O. Src-Mediated Phosphorylation of Focal Adhesion Kinase Couples Actin and Adhesion Dynamics to Survival Signaling. *Mol Cell Biol* **2004**, *24* (18), 8113-8133. DOI: 10.1128/MCB.24.18.8113-8133.2004.
- (164) Sharma, A.; Mayer, B. J. Phosphorylation of p130Cas initiates Rac activation and membrane ruffling. *BMC Cell Biol* **2008**, *9* (1), 50-50. DOI: 10.1186/1471-2121-9-50.
- (165) Chen, H.; Bai, Y.; Kobayashi, M.; Xiao, S.; Cai, W.; Barajas, S.; Chen, S.; Miao, J.; Meke, F. N.; Vemula, S.; et al. PRL2 phosphatase enhances oncogenic FLT3 signaling via dephosphorylation of the E3 ubiquitin ligase CBL at tyrosine 371. *Blood* **2023**, *141* (3), 244-259. DOI: 10.1182/blood.2022016580.
- (166) Goldmann, W. H. Vinculin-p130Cas interaction is critical for focal adhesion dynamics and mechano-transduction. *Cell Biol Int* **2014**, *38* (3), 283-286. DOI: 10.1002/cbin.10204.
- (167) Goldmann, W. H. Mechanotransduction and focal adhesions. *Cell Biol Int* **2012**, *36* (7), 649-652. DOI: 10.1042/CBI20120184.
- (168) Administration, U. S. F. a. D. *FDA approves trifluridine and tipiracil with bevacizumab for previously treated metastatic colorectal cancer*. 08/02/2023. <https://www.fda.gov/drugs/drug-approvals-and-databases/fda-approves-trifluridine-and-tipiracil-bevacizumab-previously-treated-metastatic-colorectal-cancer> (accessed 2024 8/15).
- (169) Santarpia, M.; Ciappina, G.; Spagnolo, C. C.; Squeri, A.; Passalacqua, M. I.; Aguilar, A.; Gonzalez-Cao, M.; Giovannetti, E.; Silvestris, N.; Rosell, R. Targeted therapies for KRAS-mutant non-small cell lung cancer: from preclinical studies to clinical development-

a narrative review. *Translational lung cancer research* **2023**, *12* (2), 346-368. DOI: 10.21037/tlcr-22-639.

(170) Kim, S. H.; Kim, J. Y.; Park, S. Y.; Jeong, W. T.; Kim, J. M.; Bae, S. H.; Kim, G. J. Activation of the EGFR-PI3K-CaM pathway by PRL-1-overexpressing placenta-derived mesenchymal stem cells ameliorates liver cirrhosis via ER stress-dependent calcium. *Stem Cell Res Ther* **2021**, *12* (1), 551-551. DOI: 10.1186/s13287-021-02616-y.

(171) Wu, X.; Song, W.; Cheng, C.; Liu, Z.; Li, X.; Cui, Y.; Gao, Y.; Li, D. Small molecular inhibitors for KRAS-mutant cancers. *Frontiers in immunology* **2023**, *14*, 1223433-1223433. DOI: 10.3389/fimmu.2023.1223433.

(172) Yu, I. S.; Kopetz, S. The Emergence of Targetable Pathways in Colorectal Cancer. *Clin Adv Hematol Oncol* **2021**, *19* (12), 774-783.

(173) Radke, I.; Goette, M.; Kersting, C.; Mattsson, B.; Kiesel, L.; Wuelfing, P. Expression and prognostic impact of the protein tyrosine phosphatases PRL-1, PRL-2, and PRL-3 in breast cancer. *Br J Cancer* **2006**, *95* (3), 347-354. DOI: 10.1038/sj.bjc.6603261.

(174) Wei, M.; Korotkov, K. V.; Blackburn, J. S. Targeting phosphatases of regenerating liver (PRLs) in cancer. *Pharmacol Ther* **2018**, *190*, 128-138. DOI: 10.1016/j.pharmthera.2018.05.014.

(175) Stephens, B. J.; Han, H.; Gokhale, V.; Von Hoff, D. D. PRL phosphatases as potential molecular targets in cancer. *Mol Cancer Ther* **2005**, *4* (11), 1653-1661. DOI: 10.1158/1535-7163.MCT-05-0248.

(176) Werner, S. R.; Lee, P. A.; DeCamp, M. W.; Crowell, D. N.; Randall, S. K.; Crowell, P. L. Enhanced cell cycle progression and down regulation of p21(Cip1/Waf1) by PRL tyrosine phosphatases. *Cancer Lett* **2003**, *202* (2), 201-211. DOI: 10.1016/s0304-3835(03)00517-2.

(177) Wang, Y.; Lazo, J. S. Metastasis-associated phosphatase PRL-2 regulates tumor cell migration and invasion. *Oncogene* **2012**, *31* (7), 818-827. DOI: 10.1038/onc.2011.281.

(178) Hardy, S.; Wong, N. N.; Muller, W. J.; Park, M.; Tremblay, M. L. Overexpression of the protein tyrosine phosphatase PRL-2 correlates with breast tumor formation and progression. *Cancer Res* **2010**, *70* (21), 8959-8967. DOI: 10.1158/0008-5472.CAN-10-2041.

(179) Stephens, B.; Han, H.; Hostetter, G.; Demeure, M. J.; Von Hoff, D. D. Small interfering RNA-mediated knockdown of PRL phosphatases results in altered Akt phosphorylation and reduced clonogenicity of pancreatic cancer cells. *Mol Cancer Ther* **2008**, *7* (1), 202-210. DOI: 10.1158/1535-7163.MCT-07-0542.

- (180) Akiyama, S.; Dhavan, D.; Yi, T. PRL-2 increases Epo and IL-3 responses in hematopoietic cells. *Blood Cells Mol Dis* **2010**, *44* (4), 209-214. DOI: 10.1016/j.bcmd.2010.02.013.
- (181) Bai, Y.; Yu, G.; Zhou, H.-M.; Amarasinghe, O.; Zhou, Y.; Zhu, P.; Li, Q.; Zhang, L.; Nguele Meke, F.; Miao, Y.; et al. PTP4A2 promotes lysophagy by dephosphorylation of VCP/p97 at Tyr805. *Autophagy* **2023**, *19* (5), 1562-1581. DOI: 10.1080/15548627.2022.2140558.
- (182) Nguele Meke, F.; Bai, Y.; Ruiz-Avila, D.; Carlock, C.; Ayub, J.; Miao, J.; Hu, Y.; Li, Q.; Zhang, Z.-Y. Inhibition of PRL2 Upregulates PTEN and Attenuates Tumor Growth in Tp53-deficient Sarcoma and Lymphoma Mouse Models. *Cancer Res Commun* **2024**, *4* (1), 5-17. DOI: 10.1158/2767-9764.CRC-23-0308.
- (183) Xia, J.; Ma, N.; Shi, Q.; Liu, Q.-C.; Zhang, W.; Cao, H.-J.; Wang, Y.-K.; Zheng, Q.-W.; Ni, Q.-Z.; Xu, S.; et al. XAF1 promotes colorectal cancer metastasis via VCP-RNF114-JUP axis. *J Cell Biol* **2024**, *223* (2), 1. DOI: 10.1083/jcb.202303015.
- (184) Wang, F. a. Q. Q. a. Q. B. a. W. Y. a. H. Y. a. L. Q. a. S. X. a. W. X. a. Y. S. a. P. G. a. C. Targeting VCP potentiates immune checkpoint therapy for colorectal cancer. *Cell Reports* **2023**, *42*, 113318. DOI: 10.1016/j.celrep.2023.113318.
- (185) Serebriiskii, I. G.; Pavlov, V.; Tricarico, R.; Andrianov, G.; Nicolas, E.; Parker, M. I.; Newberg, J.; Frampton, G.; Meyer, J. E.; Golemis, E. A. Comprehensive characterization of PTEN mutational profile in a series of 34,129 colorectal cancers. *Nat Commun* **2022**, *13* (1), 1618-1618. DOI: 10.1038/s41467-022-29227-2.
- (186) Serebriiskii, I. G.; Pavlov, V. A.; Andrianov, G. V.; Litwin, S.; Basicckes, S.; Newberg, J. Y.; Frampton, G. M.; Meyer, J. E.; Golemis, E. A. Source, co-occurrence, and prognostic value of PTEN mutations or loss in colorectal cancer. *Npj genomic medicine* **2023**, *8* (1), 40-40. DOI: 10.1038/s41525-023-00384-7.
- (187) Chen, X.; Liang, R.; Lin, H.; Chen, K.; Chen, L.; Tian, G.; Zhu, X. CD166 promotes cancer stem cell-like phenotype via the EGFR/ERK1/2 pathway in the nasopharyngeal carcinoma cell line CNE-2R. *Life Sci* **2021**, *267*, 118983. DOI: 10.1016/j.lfs.2020.118983.
- (188) Jia, G.; Wang, X.; Yan, M.; Chen, W.; Zhang, P. CD166-mediated epidermal growth factor receptor phosphorylation promotes the growth of oral squamous cell carcinoma. *Oral Oncol* **2016**, *59*, 1-11. DOI: 10.1016/j.oraloncology.2016.05.010.
- (189) Kadam, R.; Teni, T. Clusterin in cancer: Dual role as a tumor suppressor gene and an oncogene. *Biomedical Research Journal* **2016**, *3* (2), 130-156. DOI: 10.4103/2349-3666.240609.
- (190) Chen, Z.; Fan, Z.; Dou, X.; Zhou, Q.; Zeng, G.; Liu, L.; Chen, W.; Lan, R.; Liu, W.; Ru, G.; et al. Inactivation of tumor suppressor gene Clusterin leads to hyperactivation of

TAK1-NF- $\kappa$ B signaling axis in lung cancer cells and denotes a therapeutic opportunity. *Theranostics* **2020**, *10* (25), 11520-11534. DOI: 10.7150/thno.44829.

(191) Cheng, H.; Wang, S.; Huang, A.; Ma, J.; Gao, D.; Li, M.; Chen, H.; Guo, K. HSF1 is involved in immunotherapeutic response through regulating APOJ/STAT3-mediated PD-L1 expression in hepatocellular carcinoma. *Cancer Biol Ther* **2023**, *24* (1), 1-9. DOI: 10.1080/15384047.2022.2156242.

(192) Shim, Y.-J.; Shin, Y.-J.; Jeong, S.-Y.; Kang, S.-W.; Kim, B.-M.; Park, I.-S.; Min, B.-H. Epidermal growth factor receptor is involved in clusterin-induced astrocyte proliferation. *Neuroreport* **2009**, *20* (4), 435-439. DOI: 10.1097/WNR.0b013e3283262df8.

(193) Li, Y.; Jin, M.; Yin, X.; Zhou, B.; Ni, H. Effects of leptin treatment immediately after neonatal seizures on serum clusterin and VEGF levels and brain oxidative stress-related proteins and neurobehavioral phenotypes. *Epilepsy Behav* **2023**, *138*, 109016. DOI: 10.1016/j.yebeh.2022.109016.

(194) Li, Y.; Lu, J.; Zhou, S.; Wang, W.; Tan, G.; Zhang, Z.; Dong, Z.; Kang, T.; Tang, F. Clusterin induced by N,N'-Dinitrosopiperazine is involved in nasopharyngeal carcinoma metastasis. *Oncotarget* **2016**, *7* (5), 5548-5563. DOI: 10.18632/oncotarget.6750.

(195) Nunes, L.; Li, F.; Wu, M.; Luo, T.; Hammarström, K.; Torell, E.; Ljuslinder, I.; Mezheyski, A.; Edqvist, P.-H.; Löfgren-Burström, A.; et al. Prognostic genome and transcriptome signatures in colorectal cancers. *Nature (London)* **2024**. DOI: 10.1038/s41586-024-07769-3.

(196) Berasain, C.; Avila, M. A. Amphiregulin. *Semin Cell Dev Biol* **2014**, *28*, 31-41. DOI: 10.1016/j.semcdb.2014.01.005.

(197) Uysal, D.; Thaqi, B.; Fierek, A.; Jurgowski, D.; Popovic, Z. V.; Siegel, F.; Michel, M. S.; Nuhn, P.; Worst, T. S.; Erben, P.; et al. Prognostic significance of EGFR, AREG and EREG amplification and gene expression in muscle invasive bladder cancer. *Frontiers in oncology* **2024**, *14*, 1370303. DOI: 10.3389/fonc.2024.1370303.

(198) Chen, Z.; Chen, J.; Gu, Y.; Hu, C.; Li, J. L.; Lin, S.; Shen, H.; Cao, C.; Gao, R.; Li, J.; et al. Aberrantly activated AREG-EGFR signaling is required for the growth and survival of CRTC1-MAML2 fusion-positive mucoepidermoid carcinoma cells. *Oncogene* **2014**, *33* (29), 3869-3877. DOI: 10.1038/onc.2013.348.

(199) Wang, L.; Wang, L.; Zhang, H.; Lu, J.; Zhang, Z.; Wu, H.; Liang, Z. AREG mediates the epithelial-mesenchymal transition in pancreatic cancer cells via the EGFR/ERK/NF- $\kappa$ B signalling pathway. *Oncol Rep* **2020**, *43* (5), 1558-1568. DOI: 10.3892/or.2020.7523.

(200) Laviolette, L. A.; Mermoud, J.; Calvo, I. A.; Olson, N.; Boukhali, M.; Steinlein, O. K.; Roeder, E.; Sattler, E. C.; Huang, D.; Teh, B. T.; et al. Negative regulation of EGFR signalling by the human folliculin tumour suppressor protein. *Nat Commun* **2017**, *8* (1), 15866-15866. DOI: 10.1038/ncomms15866.



(201) Zheng, J.; Duan, B.; Sun, S.; Cui, J.; Du, J.; Zhang, Y. Folliculin Interacts with Rab35 to Regulate EGF-Induced EGFR Degradation. *Front Pharmacol* **2017**, *8*, 688-688. DOI: 10.3389/fphar.2017.00688.

(202) Park, M.; Kim, J. W.; Kim, K. M.; Kang, S.; Kim, W.; Kim, J.-K.; Cho, Y.; Lee, H.; Baek, M. C.; Bae, J.-H.; et al. Circulating small extracellular vesicles activate TYRO3 to drive cancer metastasis and chemoresistance. *Cancer Res* **2021**, *81* (13), 3539-3553. DOI: 10.1158/0008-5472.CAN-20-3320.

(203) Wang, J.; Cheng, Z.; Dai, D.; Li, H.; Shao, X.; Xu, M. Overexpression of TYRO3 indicates poor prognosis and induces gastric cancer progression via AKT-mTOR pathway. *Mol Carcinog* **2023**, *62* (9), 1325-1337. DOI: 10.1002/mc.23566.